

210 80 8 18

14 NSWC TR-80-417

LEVEL II

12

AD A102320

6 SPACE SHUTTLE RANGE SAFETY COMMAND
DESTRUCT SYSTEM ANALYSIS AND VERIFICATION.
PHASE II - ORDNANCE OPTIONS FOR A SPACE SHUTTLE
RANGE SAFETY COMMAND DESTRUCT SYSTEM.

9 Final Rept.

11 MAR 81

12 125

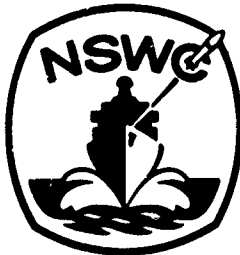
DTIC ELECTE
S AUG 03 1981 D
E

PREPARED FOR THE
NATIONAL AERONAUTICS AND SPACE ADMINISTRATION
GEORGE C. MARSHALL SPACE FLIGHT CENTER, ALABAMA

NASA DEFENSE PURCHASE REQUEST H-13047B
NAVSURFWPCEN TASK NO. WR14ZAN01

Approved for public release, distribution unlimited.

10
W. M. / Finckley
D. L. / Hehto
N. L. / Coleman
A. J. / Grechiod
J. M. / Ward



NAVAL SURFACE WEAPONS CENTER

Dahlgren, Virginia 22448 • Silver Spring, Maryland 20910

FILE COPY

411563

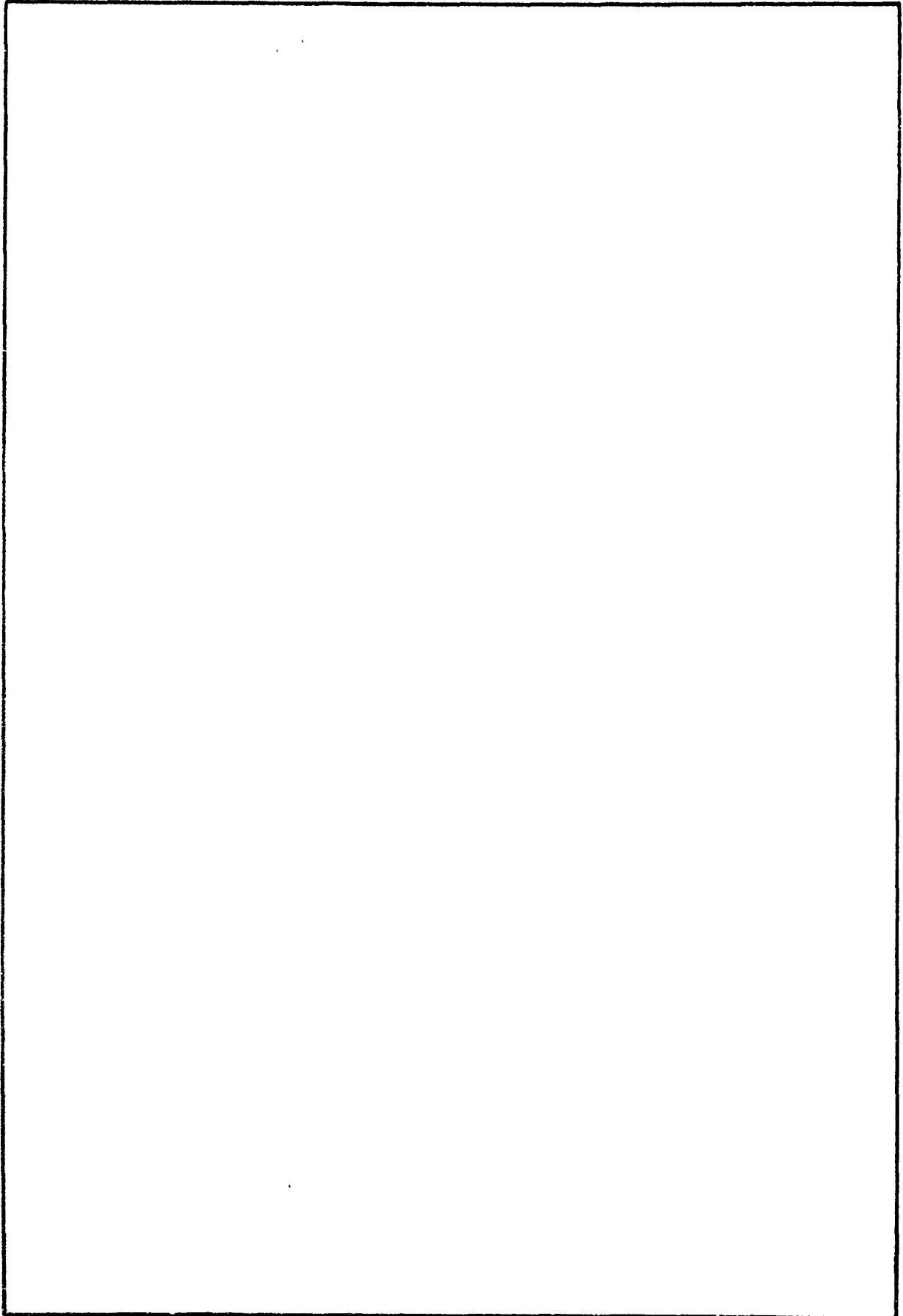
UNCLASSIFIED

SECURITY CLASSIFICATION OF THIS PAGE (When Data Entered)


REPORT DOCUMENTATION PAGE		READ INSTRUCTIONS BEFORE COMPLETING FORM
1. REPORT NUMBER NSWC TR 80-417 ✓	2. GOVT ACCESSION NO. AD-A102320	3. RECIPIENT'S CATALOG NUMBER
4. TITLE (and Subtitle) PHASE II - SPACE SHUTTLE RANGE SAFETY COMMAND DESTRUCT SYSTEM ANALYSIS AND VERIFICATION	5. TYPE OF REPORT & PERIOD COVERED Final	
	6. PERFORMING ORG. REPORT NUMBER	
7. AUTHOR(s) W. M. Hinckley, D. L. Lehto, N. L. Coleburn, A. J. Gorechlad, J. M. Ward, and J. Petes	8. CONTRACT OR GRANT NUMBER(s)	
9. PERFORMING ORGANIZATION NAME AND ADDRESS Naval Surface Weapons Center White Oak Laboratory Silver Spring, MD 20910	10. PROGRAM ELEMENT, PROJECT, TASK AREA & WORK UNIT NUMBERS NASA 0,0,R15KA	
11. CONTROLLING OFFICE NAME AND ADDRESS	12. REPORT DATE March 1981	
	13. NUMBER OF PAGES 129	
14. MONITORING AGENCY NAME & ADDRESS (if different from Controlling Office)	15. SECURITY CLASS. (of this report) UNCLASSIFIED	
	15a. DECLASSIFICATION/DOWNGRADING SCHEDULE	
16. DISTRIBUTION STATEMENT (of this Report) Approved for public release; distribution unlimited.		
17. DISTRIBUTION STATEMENT (of the abstract entered in Block 20, if different from Report)		
18. SUPPLEMENTARY NOTES Ext. ... Tank (ET)		
19. KEY WORDS (Continue on reverse side if necessary and identify by block number) space shuttle solid rocket booster finite elements fragments destruct system structural response flight dynamics detonation linear shaped charge explosion debris external tank aerodynamic drag hydrogen-oxygen-air orbiter stress analysis blast		
20. ABSTRACT (Continue on reverse side if necessary and identify by block number) ET mounted command destruct system ordnance options were analyzed and judged on the basis of performance, cost, weight, development time, safety and ease of installation. A system using LSC's installed in the cable tray on the ET LOX/LH ₂ tanks was recommended.		

UNCLASSIFIED

SECURITY CLASSIFICATION OF THIS PAGE (When Data Entered)



UNCLASSIFIED

Accession For	
NTIS GRA&I	<input checked="" type="checkbox"/>
DTIC TAB	<input type="checkbox"/>
Unannounced	<input type="checkbox"/>
Justification	
By _____	
Distribution/	
Availability Codes	
Dist	Avail and/or Special
	

FOREWORD

This report is submitted to the National Aeronautics and Space Administration (NASA), George C. Marshall Space Flight Center, Alabama, in fulfillment of the NASA-Defense Purchase Request H-13047B dated 15 May 1975 and as modified by Amendment 3 on 8 March 1976. The initial purchase request called for a study of the then current Space Shuttle Range Safety Command Destruct System. The results of that Phase I study, indicating marginal performance of the system, were transmitted to NASA in a letter report dated 2 February 1976.

The current Phase II study analyzes ordnance options for a destruct system that will overcome the shortcomings of the earlier system and will assure catastrophic breakup of the external liquid propellant tanks of the Space Shuttle. The new analysis, reported herein, indicates the feasibility of a destruct system utilizing linear-shaped charges mounted in the operational instrumentation trays on the external tank to accomplish the objective.

A current Phase III study under a new amendment to the purchase request is developing the break-up model of the Space Shuttle cluster at various times into flight.

The work described in this report represents the cooperative effort of many persons here at the White Oak Laboratory, Marshall Space Flight Center, and various NASA contractor facilities. To name all to whom we, the authors of this report, are indebted would be impossible since much of the necessary information and the proffered help came from "staff." So, to these staffs - many thanks. The fact that we had easy access to these staffs at Marshall Space Flight Center, Martin Marietta Aerospace, Michoud, Louisiana, Rockwell International, Downey, California, and other places, is due to the efforts of Jack Roach, Code EL-42, MSFC. His managerial and technical direction and guidance of the task, executed so cooperatively and patiently, are greatly appreciated. The final touch to this report, its typing, represents the dedicated efforts of Monica Lloyd, Valarie Williams, and Wanda Ohm who strived mightily, and succeeded, against great odds, e.g., short deadline, poorly legible manuscripts, and the press of other tasks. Thanks!

N.L. COLEBURN
W.M. HINCKLEY
D.L. LEHTO

T.P. LIDDIARD
R.E. PHINNEY
J. PETES, Team Leader



J. F. PROCTOR
By direction

CONTENTS

<u>Chapter</u>		<u>Page</u>
1	BACKGROUND.....	1-1
	INTRODUCTION.....	1-1
	OBJECTIVES.....	1-2
	ASSUMPTIONS.....	1-2
	SCOPE OF WORK.....	1-2
	DISCUSSION.....	1-3
	SUMMARY.....	1-5
2	EXECUTIVE SUMMARY.....	2-1
	OBJECTIVES AND ANALYSES.....	2-1
	CONCLUSIONS.....	2-3
3	STRUCTURAL DAMAGE AND BLAST CONSIDERATIONS.....	3-1
	STRUCTURAL ANALYSIS.....	3-1
	INTRODUCTION.....	3-1
	EXPLOSIVE CHARGE CENTRALLY LOCATED IN INTERTANK.....	3-2
	EXPLOSIVE CHARGE CENTRALLY LOCATED IN LH ₂ TANK.....	3-7
	LINE SOURCE NEAR WALL OF LOX OR LH ₂ TANK.....	3-10
	SUMMARY.....	3-12
	MIXING AND BLAST YIELDS.....	3-13
	ON LAUNCH PAD.....	3-13
	CONFINED MIXING.....	3-14
	DUMPING TO OUTSIDE OF ET.....	3-14
4	EXPLOSIVE SYSTEM OPTIONS - DEVICES INSIDE INTERTANK.....	4-1
	BARE CHARGES.....	4-1
	SINGLE LARGE CHARGE.....	4-1
	SMALL CHARGE NEAR WALL.....	4-1
	FOCUSED-BLAST CHARGES.....	4-1
	CASED CHARGE.....	4-2
	CONTINUOUS ROD CHARGE.....	4-2
	CONICALLY AND HEMISPHERICALLY-LINED SHAPED CHARGES.....	4-2
	CONICALLY LINED (TANDEM).....	4-2
	HEMISPHERICALLY LINED.....	4-2
	EXPLOSIVE COMPOSITIONS.....	4-10
	LINEAR-SHAPED CHARGE DESTRUCT CONFIGURATIONS.....	4-12
	EXPLOSIVE PENETRATOR.....	4-14
	INTRODUCTION.....	4-14

CONTENTS - Continued

<u>Chapter</u>		<u>Page</u>
4	CHARGE SIZE REQUIRED.....	4-16
	VELOCITY LOSS CAUSED BY PUNCHING TANK.....	4-16
	DRAG SLOWDOWN.....	4-16
	STABILITY.....	4-17
	TYPICAL DESIGN.....	4-17
	CONCLUSIONS.....	4-18
	OTHER SYSTEMS.....	4-18
	DISCUSSION AND COMPARISONS OF IT-SITED DESTRUCT SYSTEMS.....	4-18
5	EXPLOSIVE SYSTEM OPTIONS: DEVICES OUTSIDE INTERTANK.....	5-1
	INTRODUCTION.....	5-1
	HYBRID (HEMISPHERICALLY LINED SHAPED CHARGES) SYSTEM.....	5-1
	LINEAR-SHAPED CHARGES.....	5-1
	HYBRID SYSTEM.....	5-1
	LOX TANK DESTRUCT CHARGE.....	5-2
	ET CROSS-BEAM CHARGE FOR LH ₂ TANK DESTRUCT.....	5-4
	LINEAR-SHAPED CHARGES ON ET.....	5-10
	TARGET CONSIDERATIONS.....	5-10
	TEST CONSIDERATIONS.....	5-14
	TEST ARRANGEMENTS.....	5-14
	RESULTS.....	5-16
	DISCUSSION.....	5-18
	BRACKET FAILURE ANALYSIS.....	5-20
	SUMMARY AND CONCLUSIONS.....	5-26
	COMPARISON OF SYSTEMS WITH DEVICES OUTSIDE INTERTANK.....	5-27
	HYBRID SYSTEM.....	5-27
	LSC'S IN OPERATIONAL INSTRUMENTATION CABLE TRAYS.....	5-27
	CONCLUSIONS.....	5-27
Appendix A	BASIC BARE-CHARGE BLAST DATA.....	A-1
	CHARGE AT SEA LEVEL.....	A-1
	CHARGE IN VACUUM.....	A-4
Appendix B	EFFECTS OF HIGH-EXPLOSIVE CHARGE IN LIQUID HYDROGEN.....	B-1
	INTRODUCTION.....	B-1
	EQUATION OF STATE OF LH ₂	B-1
	RESULTS OF EXPLOSION CALCULATIONS.....	B-3
Appendix C	FLOW FROM RUPTURED TANKS.....	C-1
	INTRODUCTION.....	C-1
	VEHICLE STANDING ON LAUNCH PAD.....	C-1
	VEHICLE IN FREE FALL.....	C-2
Appendix D	SHOCK STRENGTH SCALING LAWS.....	D-1
	INTRODUCTION.....	D-1
	SPHERICAL WAVES IN A LIQUID.....	D-1
	SHOCK FROM SHAPED CHARGE JETS.....	D-3

ILLUSTRATIONS

<u>Figure</u>		<u>Page</u>
2-1	TWO-ELEMENT DESTRUCT SYSTEM, LSC/CABLE TRAY INSTALLATION - ET TOP VIEW.....	2-2
2-2	DESTRUCT CHARGE OPTIONS IN INTERTANK.....	2-8
2-3	FIVE-ELEMENT DESTRUCT SYSTEM.....	2-11
2-4	THREE-ELEMENT DESTRUCT SYSTEM.....	2-12
3-1	INTERTANK STRUCTURE.....	3-2
3-2	DEFLECTION MODE SHAPE OF ONE INTERTANK BAY.....	3-3
3-3	INTERTANK STRINGER AND SKIN SECTION.....	3-6
3-4	TYPICAL LH ₂ TANK BARREL SECTION.....	3-9
3-5	LH ₂ TANK STRINGER AND SKIN SECTION.....	3-10
3-6	LH ₂ TANK DEFLECTION MODE SHAPE (LOCAL WALL LOADING).....	3-11
3-7	TREND IN MEASURED EQUIVALENT TNT WEIGHT FROM LOX/LH ₂ PROPELLANT EXPLOSIONS COMPARED TO DESIGN RULES.....	3-15
4-1	CONICAL TANDEM-SHAPED CHARGE ARRANGEMENT.....	4-3
4-2	HEMISPHERICALLY LINED SHAPED CHARGE.....	4-4
4-3	LOCATION OF DESTRUCT SHAPED CHARGES AND DAMAGE RADII.....	4-6
4-4	JET PENETRATION INTO LH ₂ TANK.....	4-7
4-5	METHOD OF OBTAINING INITIAL PEAK PRESSURE GENERATED IN WATER AND LIQUID HYDROGEN BY A COPPER JET FRAGMENT MOVING AT 2000 M/SEC.....	4-9
4-6	500 GT/FT-RDX-LOADED, CU-SHEATHED, LINEAR-SHAPED CHARGE.....	4-13
5-1	HEMISPHERICALLY LINED CHARGE PLACEMENT IN INTERTANK.....	5-3
5-2	HEMISPHERICALLY LINED SHAPED CHARGE FOR ALTERNATIVE ARRANGEMENT A....	5-4
5-3	HEMISPHERICALLY LINED SHAPED CHARGE FOR ALTERNATIVE ARRANGEMENT B....	5-5
5-4	MOUNTING LOCATION OF CHARGE IN INTERTANK.....	5-7
5-5	MOUNTING LOCATION OF CHARGE IN CROSSBEAM.....	5-7
5-6	CHARGE PLACEMENT IN CROSSBEAM.....	5-8
5-7	REGION OF LH ₂ TANK DOME ATTACKED BY DESTRUCT SHAPED CHARGE IN ORBITER CROSSBEAM.....	5-9
5-8	SKIN PAD AND WELDS ON TANK FORWARD AND AFT GORE SECTIONS.....	5-10
5-9	LH ₂ CABLE TRAY GEOMETRY.....	5-11
5-10	LOX CABLE TRAY GEOMETRY.....	5-11
5-11	CABLE TRAY BRACKETS ON LOX TANK.....	5-12
5-12	BEAM CROSS SECTION.....	5-13
5-13	TEST ARRANGEMENT (LH ₂ TANK).....	5-15
5-14	TEST ARRANGEMENT (LO ₂ TANK).....	5-15
5-15	RESULTS OF LINEAR-SHAPED CHARGE (COPPER-LINER, 500-GR/FT, RDX-LOADED) ACTION ON SIMULATED CABLE TRAY/LH ₂ TANK.....	5-17
5-16	RESIDUAL PENETRATION AT 1-INCH INTERVALS.....	5-19
5-17	500-GR/FT TEST RESULT FOR CABLE TRAY APPLICATION.....	5-21
5-18	LIGAMENT REMAINING IN LOX TANK SKIN AFTER LSC CUT.....	5-22
5-19	FLAW PATTERN - LOX TANK BARREL SECTION.....	5-24
5-20	LH ₂ TANK CABLE TRAY BRACKET.....	5-25
5-21	TWO-ELEMENT DESTRUCT SYSTEM, LSC/CABLE TRAY INSTALLATION - ET TOP VIEW.....	5-28
A-1	PRESSURE VS. DISTANCE FOR TNT CHARGE.....	A-2
A-2	REFLECTED IMPULSE FROM TNT SPHERE IN SEA-LEVEL AIR.....	A-3
A-3	REFLECTED IMPULSE FROM TNT CHARGE IN VACUUM.....	A-5

ILLUSTRATIONS — Continued

<u>Figure</u>		<u>Page</u>
B-3	BLAST FROM 1-LB SPHERICAL PENTOLITE CHARGE IN LIQUID PARA-HYDROGEN...	B-3
C-1	SPELLING OF LH ₂ AND LO ₂ FROM ET TANKS OPENED AT BOTTOM WHILE ON LAUNCH PAD.....	C-3
C-2	CRITICAL FLOW MASS FLUX OF HYDROGEN LIQUID/VAPOR MIXTURE.....	C-6
C-3	CRITICAL FLOW MASS FLUX OF NITROGEN LIQUID/VAPOR MIXTURE.....	C-7
C-4	P-V EXPANSION PATHS FOR LH ₂	C-9
C-5	P-V EXPANSION PATHS FOR LO ₂	C-10
C-6	DUMPING OF LH ₂ DURING FREE FALL.....	C-11
C-7	DUMPING OF LO ₂ DURING FREE FALL.....	C-12
C-8	MASS FLUX OF LH ₂ DURING FREE FALL AT FLIGHT TIME OF 100 SECONDS.....	C-13
C-9	MASS FLUX OF LO ₂ DURING FREE FALL AT FLIGHT TIME OF 100 SECONDS.....	C-14

TABLES

<u>Table</u>		<u>Page</u>
1-1	ET FLUID VOLUMES AND PRESSURES.....	1-6
2-1	COMPARISON OF ORDNANCE DEVICES AND SYSTEMS.....	2-4
3-1	CHARGE WEIGHT VS. HOLE SIZE — LOX AND LH ₂ TANK DOMES.....	3-8
3-2	SUMMARY OF IMPULSE REQUIREMENTS TO RUPTURE ET STRUCTURE.....	3-13
3-3	TNT EQUIVALENCE OF ET EXPLOSION.....	3-16
4-1	DESTRUCT CHARGE SPECIFICATIONS.....	4-11
4-2	HNS/TEFLON, 90/10, QUALIFICATION TEST RESULTS (6-LB CHARGE).....	4-11
4-3	LSC DESTRUCT CONFIGURATIONS FOR INTERTANK OPTIONS.....	4-15
5-1	WEIGHTS OF COMPONENTS FOR HEMISPHERICALLY LINED SHAPED CHARGES IN HYBRID SYSTEM.....	5-6
5-2	TEST RESULTS OF RDX-LOADED LINEAR-SHAPED CHARGES (LH ₂ TANK).....	5-16
5-3	TEST RESULTS OF RDX-LOADED LINEAR-SHAPED CHARGES (LOX TANK).....	5-18
5-4	SUMMARY OF RECOMMENDED LINEAR-SHAPED CHARGE SPECIFICATIONS.....	5-26
A-1	EFFECTS OF TNT CHARGE AT STANDOFF DISTANCE OF 2 FEET FROM LH ₂ TANK DOME.....	A-6

CHAPTER 1

BACKGROUND

INTRODUCTION

A number of explosive ordnance system options were analyzed for defeating the structural integrity of the external tank (ET) of the Space Shuttle upon command of the range safety officer. In destructing the ET, rapid dumping and minimum mixing of the LOX and LH₂ contained in the ET were specific objectives. In some of the options studied, the ordnance is contained in the intertank (IT) with the explosive forces directed against the IT walls and the lower LOX tank and upper LH₂ tank domes and walls. In other options, all ordnance material is located outside the ET, with the explosive power directed against the LOX and LH₂ tank walls. In a third option, ordnance is located inside the IT and outside the ET — a so-called hybrid system — with explosive forces directed at the lower portions of the LOX and LH₂ tanks.

The number of options analyzed was large, because many demands for the total system had to be satisfied. Assured destruct at all stages of flight from lift-off to orbiter separation, light weight, commonality of ordnance for LOX and LH₂ tank destruct, safety and reliability of the ordnance, minimum structural and design changes to the Space Shuttle system, and minimum mixing of the dumped LOX and LH₂ were some of the conditions that had to be considered. The extent to which these conditions could be met provided the criteria by which the different options could be and were evaluated. Analysis and some tests indicated that a system consisting of linear-shaped charges (LSC's) mounted into the operational instrumentation (OI) cable trays outside the ET would best meet the destruct requirements.

The requirement for an ordnance system dedicated to destruct the ET became evident, in part, after the earlier Phase I study of the then current design of the Space Shuttle Command Destruct System indicated that destruct of the ET, and specifically the LH₂ tank of the ET, was not assured for all flight times from lift-off to 100 seconds. In this early system, there was no explosive ordnance system on the ET itself. ET destruct was largely dependent on the blast, thrust, and fragment forces generated by the solid rocket boosters (SRB's) attached to the ET upon command destruct of the SRB's. (Destruct of the LOX tank portion of the ET was to be accomplished by conically shaped charges located in the SRB frustums and directed at the LOX tank.)

In this early study, two destruct models for destroying the LH₂ tank of the ET were investigated. One model considered a clamshell-type longitudinal opening of the SRB's which generated large lateral inboard thrusts on the ET. The other

examined a catastrophic and rapid breakup of the SRB's, creating blast and fragments to impact the ET with destructive force. The two models were considered to be mutually exclusive, i.e., if one model were realized in actuality, the other would not be. The blast model predicted the catastrophic buckling of the LH₂ tank at all time of interest into flight. However, the degree of rupturing (tearing) and the rate of LH₂ dispersal were difficult to quantify. The clamshell model was predicted to have more modest destruct capabilities. Destruct of the LH₂ tank was predicted for late times into flight, i.e., 50 and 100 seconds, but at earlier times, i.e., 0 and 10 seconds, destruct was considered marginal or unlikely.

With no clear indication as to which model of SRB destruct would prevail in actuality and considering the marginal nature of the subsequent LH₂ tank destruct, particularly in the clamshell analysis, it was concluded in the Phase I study that ET destruct via SRB destruct was not assured for all the flight times and conditions of interest.

This Phase II study was initiated to explore and analyze destruct system ordnance alternatives which would assure ET breakup and rapid dumping of the LOX and LH₂. The options to be analyzed would produce explosive forces that directly attacked the ET (both the LOX and LH₂ tanks) without depending on SRB destruct mechanisms. Since there was no dependence on SRB actions or presence, the range of flight time interest could be extended to post-orbiter separation.

OBJECTIVES

The guidelines, assumptions, and objectives of Phase II changed as the study progressed. These changes provided a broader range of options than first considered. The initial set of assumptions and scope of work as specified by NASA were as follows.

ASSUMPTIONS

1. The Triplex Command Destruct System shall be the baselined design.
2. Configurations to be considered:
 - a. Nominal first-stage cluster (2 SRB's plus orbiter/ET).
 - b. First-stage cluster with one SRB inadvertently separated.
 - c. Nominal second-stage cluster (ET/orbiter).
3. The SRB destruct system will not include conically shaped charges mounted in the SRB frustum for the purpose of destructing the ET LOX tank.

SCOPE OF WORK. Part I, based on the assumptions outlined above, analyzes the destruct system ordnance options for installation in the ET intertank region (between the LOX and LH₂ tanks). This analysis should consider such devices as conically shaped charges, pancake charges, bi-directional charges, etc., and will produce the following end products:

1. Determination of the most effective type of charge for ET propellant dispersion (both LOX and LH₂ tanks) in accordance with Eastern Test Range requirements.

2. Definition of the optimum location for the charge installations in the ET intertank which will produce catastrophic failure of both propellant tanks, with the minimum yield resulting from destruct action. Charges must be redundant and redundantly initiated by a confined detonating fuse (CDF).

It must be noted that in this initial statement of work, the ordnance system options were limited to installation in the IT region between the LOX and LH₂ tanks constituting the ET. It soon became apparent that this limitation imposed severe design and operational problems, particularly in terms of the large weight of ordnance items required, and the relatively high degree of LOX-LH₂ mixing anticipated.

To ease these problems, the guidelines were modified to permit destructing the LH₂ tank by means of an externally located shaped charge positioned in the cross beam connecting the aft end of the orbiter to the ET. Also, the requirement for redundancy was dropped.

Once the initial specification to contain all ordnance items in the IT was breached, the next logical step was to permit analysis of options using all the necessary explosive ordnance items outside the IT. In fact, it is this later option which is recommended for ET destruct. The description of the recommended system and the other options studied are described in the following chapters.

DISCUSSION

Some elaboration of the assumptions, scope of work, and objectives as initially stated and as they evolved may be useful in putting the following chapters into proper perspective.

The called for Triplex Command Destruct System consists of three separate explosive ordnance systems, two dedicated to SRB destruct and the third to ET destruct. The two SRB destruct systems are identical, consisting of LSC's mounted outboard and along about 75 percent of each SRB length. The function of this system is twofold: (1) to rupture and destroy the SRB's and thus terminate the forward thrust of the Space Shuttle; and (2) through the SRB hydrodynamic and mechanical destruct effects, e.g., blast, fragments, and lateral thrust of the ruptured SRB, buckle and destroy the LH₂ portion of the ET and thus dump the LH₂. This system works for SRB destruct and, in general, for ET destruct so long as at least one of the SRB's is attached to the ET when the command destruct signal is given. However, as noted earlier and described in detail in Phase I, assured destruct of the ET at early times into flight is marginal and, perhaps, unlikely.

The purpose of the third system is to overcome this marginal situation by providing ordnance to produce directly catastrophic failure of the ET upon command. Dependence on the presence of functioning of the SRB destruct system is not necessary. With a system dedicated solely to ET destruct, times of interest for destruct action can now extend from lift-off to second-stage deployment when only the ET and the orbiter make up the cluster. For command destruct signals initiated when one or both SRB's are part of the cluster, the SRB destruct effects can be considered as bonus effects enhancing the effectiveness of the ET destruct system.

Effective ET destruct is the obvious goal. But what is effective? In the context of the range safety problem the command destruct system is designed to solve,

the Air Force Eastern Test Range Manual (AFETRM-127-1) serves as an official guide. It states:

4.3.1.3.1.2 For liquid propellant stages using nontoxic propellants, the destruct charges must cause penetration of the propellant tanks, both fuel and oxidizer, to the extent necessary for rapid dispersion of the propellants. The intent of this requirement is to ensure the maximum possible amount of propellants are dispersed before vehicle impact with the ground. This will reduce the impact area hazard by reducing the explosive yield.

Penetration of the tanks is given as a specific structural requirement for a destruct system. However, the intent of this penetration (or catastrophic failure as outlined in the initial work statement) can be considered the governing measure of the destruct system's effectiveness. This intent is to reduce the blast and fragment hazards associated with the dispersal, mixing, and potential explosion of the LOX and LH₂ upon rupture of the ET.

While the AFETRM concerns itself primarily with hazards upon impact with the ground, NASA is also concerned about the hazards to the Space Shuttle orbiter and its occupants. Hence, minimum explosive yield due to destruct action at all times of flight is called for in the Scope of Work. The Scope of Work further calls for consideration of such explosive devices for ET destruct as conically shaped charges, pancake charges, bi-directional charges, and others. The specified charges were all considered along with hemispherical and linear-shaped charges, omni-directional bare and cased charges, focused blast and projectile charges, and continuous rod charges.

This multiplicity of charge types permitted many options to be examined - options of charge placement and options of destruct mechanisms. Initial guidelines required all ordnance items to be contained in the IT. This limitation was imposed with the desire to keep ET design changes incurred by the addition of the ET destruct system to a minimum. However, it soon became evident that IT locations imposed severe limitations and compromised performance for all of the options analyzed: ordnance weight was large, and for all but one of the many systems studied, LOX and LH₂ mixing would potentially produce high blast yields. This one exception, an explosive projectile penetrator, had the dubious distinction of requiring the most development time. Later guidelines permitted ordnance to be located outside the IT. This provided more options and, as indicated earlier, the externally mounted LSC's offered the best solution to effective ET destruct.

The several destruct mechanisms provided by the explosive charges were considered in the options. These mechanisms include shock waves in air and liquids, e.g., LOX and LH₂, explosion product gases and debris, fragments from cased charges, and jets of metallic material from shaped charges.

Airblast - the pressure wave of finite amplitude generated in air by an explosion - was a primary damage mechanism. But as the altitude of concern increased with increased time into flight and near vacuum atmospheric conditions were approached, blast became a less effective damage mechanism. This resulted in the need for larger and larger charges to produce the same desired degree of ET damage as could be obtained at sea level with smaller charges. Jets, fragments, and

explosion gases and debris products do not suffer from these shortcomings; hence, they became viable contenders in many of the options as the primary damage mechanisms. In fact, the jet produced by LSC's proved to be the most effective ET destruct mechanism.

The immediate purpose of the ET destruct system is, of course, penetration or catastrophic rupture of the ET, resulting in rapid dumping of the LOX and LH₂, particularly at altitude. The size of the penetrations and ruptures and the rate of dumping are more than just functions of the destruct explosive performance; they are also functions of the pressure across the ET walls and the amount of LOX and LH₂ in the tanks at any particular time into flight. These too are functions of altitude. The range of interest for the destruct charge to operate extends from lift-off to about 450 seconds into flight, from sea level altitude to about 378,000 feet, from atmospheric pressures of 14.7 psi to 9.7×10^{-8} psi or near vacuum conditions. Some of these items of interest for discrete times are shown in Table 1-1.

As indicated in the Scope of Work Statement, blast yield of the mixed LH₂ and LOX is of concern. But the pressure amplitudes at different distances from any given yield are important in terms of hazards to ground installations and Space Shuttle components. These pressure versus distance relationships are strongly dependent on the altitude at which the LOX and LH₂ mixture explodes. At high altitudes, i.e., low atmospheric pressures, the pressure generated by a given yield at a given distance is considerably less than that at lower altitude, such as sea level. All the foregoing altitude dependent phenomena and effects are taken into account in this report.

It is reiterated that the efforts in this study concentrated on ET destruct, i.e., rupturing both the LOX and LH₂ tanks with ordnance items dedicated solely to ET destruct. No dependence on ordnance items on the SRB's or SRB destruct actions is necessary, as was the case in the Phase I study. However, the 's damage effects to the ET resulting from SRB destruct mechanisms are recognized. This bonus will be encountered in the nominal first-stage cluster when both SRB's are attached to the ET and for the first-stage cluster when one SRB is inadvertently separated. The increased severity of rupture in the LH₂ tank, and probably in the LOX tank, may be a mixed blessing. On one hand, there is the probability that the enhanced damage will bring about more mixing of the dumped LOX and LH₂ with a concurrent potentially larger blast yield. On the other hand, the more rapid dumping may bring about greater dispersal of the LH₂ and LOX with a lesser potential blast yield resulting. These situations were not analyzed. It is believed that the analysis of and predictions for the basic ET destruct system are adequate for planning and operational purposes. The "bonus effects" if analyzed in all their complexity would be very time-consuming and would not significantly change the basic results.

SUMMARY

With the foregoing discussion attempting to put the study in time and technology perspectives, and hopefully serving as a catalyst to bring the succeeding chapters into a coherent whole, the objectives of the task are summarized.

TABLE 1-1 ET FLUID VOLUMES AND PRESSURES

	LOX Tank		LH ₂ Tank	
	Ullage	LOX	Ullage	LH ₂
Temp (°F)	-210 to -124	-297	-372 to -180	-423
Total Vol (ft ³)	19,610		53,510	
Vol (ft ³) at 0 sec	600	19,010	2,180	51,330
10	1,010	18,600	3,270	50,240
50	2,540	17,070	7,360	46,150
100	4,520	15,090	12,640	40,870
350	14,750	4,860	40,140	13,370
450	18,640	970	50,600	2,910
Mass (lb) at 0 sec		1.345×10^6		2.258×10^5
10		1.316×10^6		2.210×10^5
50		1.208×10^6		2.030×10^5
100		1.068×10^6		1.798×10^5
350		0.344×10^6		0.588×10^5
450		0.0685×10^6		0.128×10^5
Height (in) at 0 sec		500		1,080
10		475		1,055
50		415		975
100		360		865
350		140		310
450		55		95
Ullage Pressure	20 psia to 25 psig		32 psia to 37 psia	
Pressure at 0 sec	5-25	25-45 at bottom	17-22	20-25 at bottom
across tank 10	6-25	39-58	18-23	23-28
wall (psi) 50	15-25	39-49	27-32	30-35
100	20-25	62-67	32-37	38-43
350	20-25	32-37	32-37	34-39
450	20-25	27-32	32-37	33-38

The basic objective of the Phase II study was to analyze and provide conceptual designs for destruct ordnance options required to produce catastrophic failure of both liquid propellant tanks comprising the ET. Important considerations were:

1. Rapid dumping of the LOX and LH₂ at altitude.
2. Minimum mixing of the LOX and LH₂ to achieve minimum potential blast yield of the mixture.

NSWC TR 80-417

3. Minimum weight of ordnance devices.
4. Commonality of ordnance devices.
5. Location of ordnance devices.

CHAPTER 2

EXECUTIVE SUMMARY

OBJECTIVES AND ANALYSES

More than a dozen explosive systems to destruct the external tank (ET) of the Space Shuttle upon command of a range safety officer were designed in concept and evaluated in this Phase II study. Based on the relative merits of these systems, linear-shaped charges (LSC's) mounted in the Operational Instrumentation (OI) trays of the LH₂ and LOX tanks (Fig. 2-1) are considered to be the most effective way of meeting the objectives.

In the earlier Phase I study it was determined that the Command Destruct System, as then designed, did not assuredly bring about the desired destruction of the ET at all times of interest. In this early system, ET destruct was dependent on the mechanical and hydrodynamic effects generated through the operation of the explosive system used to destruct the attached solid rocket boosters (SRB's).

This Phase II study had as its objectives the analysis of ordnance systems dedicated solely to ET destruct, evaluating the relative merits of each system, and then, suggesting a most feasible system for development, verification, and demonstration. Although catastrophic failure of the liquid propellant tanks was the major objective, other objectives or concerns had to be considered. Effective destruct had to be attained at all times into flight from lift-off to second-stage separation. "Effective" was defined as rapid dispersal of the LOX and LH₂ with minimum mixing so that the potential blast yield of the mixture would be at a minimum. Recognizing the weight restrictions common to space vehicles, it was necessary to strive for small ordnance systems. To avoid unduly severe environments for the ordnance items and to achieve more or less ready placement of the items, location of the ordnance items in and about the ET had to be considered. Costs and development times were also of concern.

In the study, destruct system options were analyzed with all of the foregoing in mind. The first step in the analysis was to ascertain that the ordnance item could cause LH₂ and LOX tank breakup. If this criterion was met, the other considerations were investigated. As it turned out, many of the systems and devices studied were found wanting in many of these characteristics. Some were much too heavy, some quite expensive, others difficult to position for effective operation, and still others required much development and advanced technology. These findings are noted for the systems studied. They, in fact, provided the basis for selecting and suggesting the best system to accomplish the desired objectives.

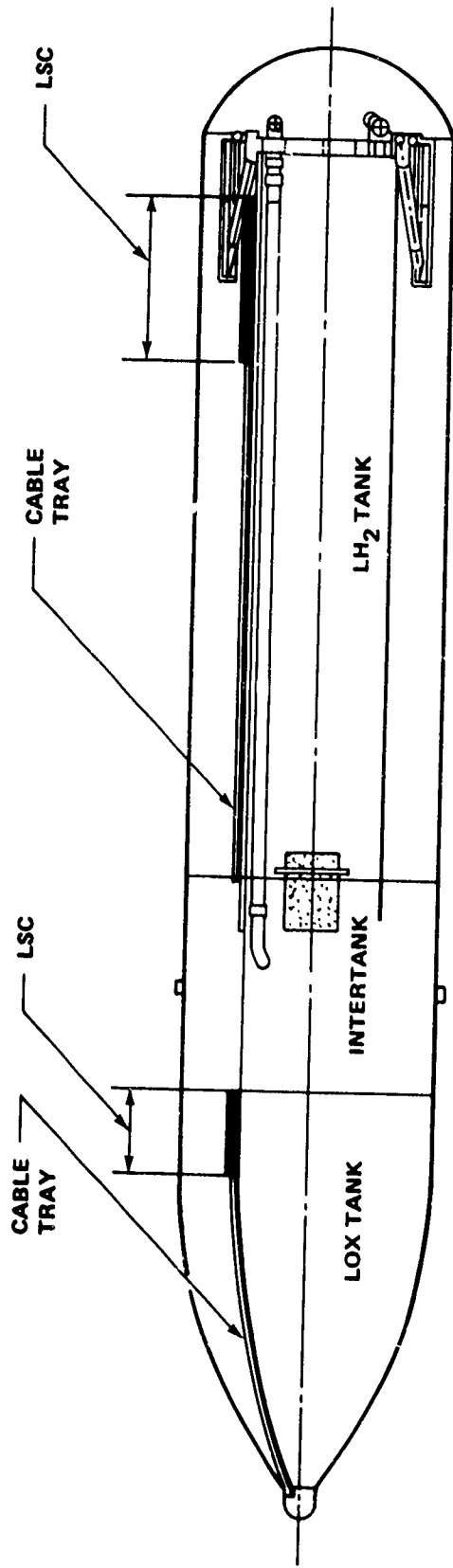


FIGURE 2-1 TWO-ELEMENT DESTRUCT SYSTEM, LSC/CABLE TRAY INSTALLATION - ET TOP VIEW

The options analyzed are described in the succeeding chapters. Table 2-1 lists their most significant features and forms a basis for comparisons. Figures 2-2 through 2-4 depict most of the options analyzed.

CONCLUSIONS

The system using LSC's in the OI trays, mounted on the external skin of the ET, best meets the objectives and concerns. Repeating from the text in Chapter 5, this system effectively destructs the LH₂ and LOX tanks. Large initial ruptures, about 20-feet long, assure rapid dumping of the liquid propellants. Because the rupture areas are separated by a long distance — at the lower ends of both tanks — minimal mixing of the LOX and LH₂ will take place. Hence, minimal potential blast yield of the mixture can be expected. There is commonality of the ordnance items; similar LSC's are used for LH₂ and LOX tank destructs. The LSC's are relatively small in weight, approximately 20 pounds being required for the total package. Only about 4 pounds of this weight are explosive. The cost of the LSC itself should be low, less than \$1,500 per flight. Another attribute of the LSC option is that LSC's have been qualified for space vehicle operations by NASA. Therefore, qualification for the Space Shuttle should be relatively easy. An equally important advantage in using LSC's is that NASA personnel have experience and competence in handling this item. The other explosive items considered, while not novel, may not be as familiar.

In this study, more work was done on this LSC system than on the other systems. Its feasibility was demonstrated by test. Mockups of the OI tray/ET geometries were made. Copper-sheathed, 500-grain/foot LSC's effectively cut the simulated ET skins. Although the brackets supporting the OI trays were not modeled, analysis indicates that the LSC would cut enough of the bracket to violate its structural integrity and thus not inhibit ET destruct. If larger LSC's can be accommodated in the OI trays (and indications are they can), it is recommended that a 750-grain/foot, copper-sheathed LSC be used. This would cut the brackets more effectively.

TABLE 2-1 COMPARISON OF ORDNANCE DEVICES AND SYSTEMS

Ordnance Options	Explosive Device	Total Weights (lb)		Damaged Region	TNT Equivalent* Blast Yield (lb)	Cost† (\$)	Development Effort
		Device	Explosive				
I- In Intertank A-1 Omni-directional Blast\$	One bare spherical TATB or HNS.	450	390	Large holes in LO ₂ and LH ₂ domes and IT walls; sever SRB beam.	54,000-7,500	6,000* - 24,000*	Minimal
2 Omni-directional Blast\$	Two bare spherical TATB or HNS.	50	40	Smaller holes in LO ₂ and LH ₂ domes and IT walls.		150 - 1,100 per charge	Minimal
B- Focused Blast\$	One cylindrical, dual-end initiated.	250	200	Moderate holes in LO ₂ and LH ₂ domes; rupture IT walls.	54,000-7,500	6,000 - 15,000	Moderate
C- Cased Charge\$	One spherical, steel cased.	400	200	Large holes in LO ₂ and LH ₂ domes, and IT walls via blast and fragments; SRB beam severed. Fragment hazard to orbiter.	54,000-7,500	6,000 - 15,000	Minimal
D- Continuous Rod\$	One cylindrical charge cased in an expanding steel rod.	70	20	Moderate holes in LH ₂ and LO ₂ domes; large cut in IT wall. Rod hazard to orbiter.	54,000-7,500	500 - 1,500	Minimal

TABLE 2-1 COMPARISON OF ORDNANCE DEVICES AND SYSTEMS - Continued

Ordnance Options	Explosive Device	Total Weights (lb)		Damaged Region	TNT Equivalent* Blast Yield (lb)	Cost† (\$)	Development Effort
		Device	Explosive				
E-1 Conically Shaped Charges (CSC)	Cylindrical charge with conical cop- per liner to produce jet.	16	10	Jet and shock damage to LO2 tank; jet and blast damage to LH2 tank; blast damage to IT walls.		5,000	Extensive
E-2 Hemispherically Shaped Charge (HSC)	Cylindrical charge with hemispherically copper liner to produce jet.	16	10	Same as for E-1.		4,000	Extensive
F- Linear-Shaped Charge (LSC)	Copper-sheathed linear charge with 90° apex angle; 200 gr/ft RDX explosive.	0.31 per ft	0.03 per ft	Large holes in LO2 and LH2 tank domes; sever IT wall and SRB beam.		10 per ft	Minimal
G- Explosive Penetrator	Explosively loaded and fused projectile shot into LH2 tank.	Projectile 120 Launcher 50	100 Propellant 30	LH2 tank lower walls and dome.		Unknown	Very extensive
H- Intertank Systems	1. LSC in crotch between LH2 tank and IT wall.	12	1.2	Cut LH2 dome.	54,000-7,500	400	Moderate
I- Five Elements	2. LSC in crotch between LO2 tank and IT wall.	12	1.2	Cut LO2 dome.		400	

TABLE 2-1 COMPARISON OF ORDNANCE DEVICES AND SYSTEMS -- Continued

Ordnance Options	Explosive Device	Total Weights (lb)		Damaged Region	TNT Equivalent* Blast Yield (lb)	Cost† (\$)	Development Effort
		Device	Explosive				
H- Intertank Systems (Cont.)	3. Back-to-back LSC's with above.	24	2.4	Sever IT wall.		800	
	4. LSC on SRB beam.	2.4	0.24	Cut SRB beam.		100	
	5. CSC directed at LH ₂ tank.	16	10	Hole in LH ₂ tank.		4,000	
	Total	66	15			5,700	
2- Three Elements	1. CSC directed at LO ₂ tank.	16	10	LO ₂ tank dome and wall.	54,000-7,500	5,000	Extensive
	2. Two HSC's directed at LOX tank and IT wall.	32	20	LH ₂ dome and wall.		4,000	
	Total	48	30			9,000	
Ii- Hybrid System (Ordnance in - and out-side IT)	1. HSC in IT.	16	10	LO ₂ tank dome and wall.	54,000-810	4,000	Extensive
	2. HSC in cross beam.	16	10	Lower LH ₂ tank dome.		4,000	
	Total	32	20			8,000	

TABLE 2-1 COMPARISON OF ORDNANCE DEVICES AND SYSTEMS - Continued

Ordnance Options	Explosive Device	Total Weight (lb)		Damaged Region	TNT Equivalent* Blast Yield (lb)	Cost† (\$)	Development Effort
		Device	Explosive				
III-LSC's outside ET in OI cable trays	1. 750 gr/ft copper-sheathed LSC, 20 ft long.	10	2	Lower LO2 tank wall.	5 1/4,000-810	600	Minimal
	2. 750 gr/ft copper-sheathed LSC, 20 ft long.	10	2	Lower LH2 tank wall.			
	Total	20	4			1,200	

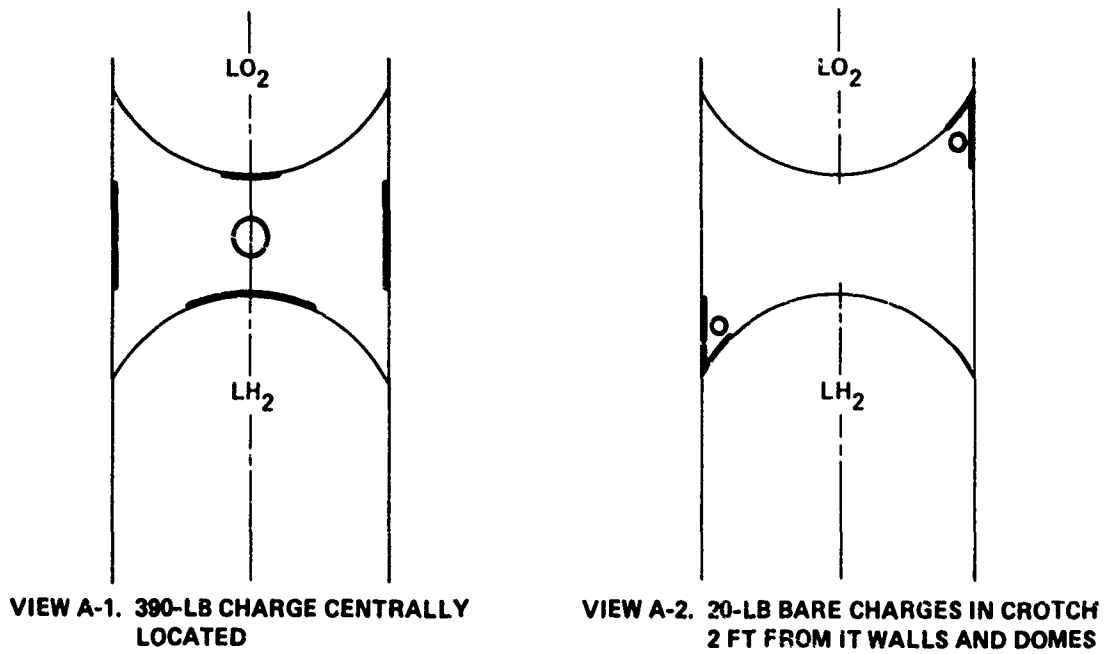
*Blast yields are time of flight dependent.

†Costs are estimates for device material and fabrication and amortized development costs; the latter are very rough estimates.

‡Estimated cost of TATB is \$5 per lb; HNS is \$50 per lb. HNS would probably cost less if bought in large quantities.

§The device constitutes the system.

¶Intertank and hybrid systems use devices tabulated in first part of table.



(HEAVY LINE INDICATES DESTRUCT REGION)

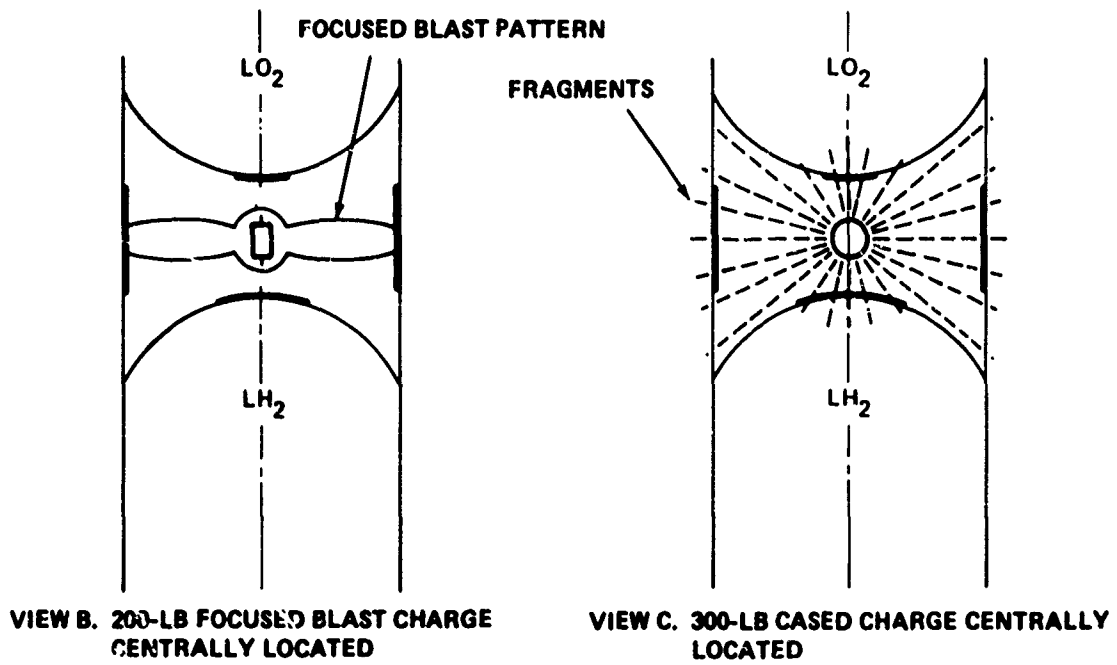
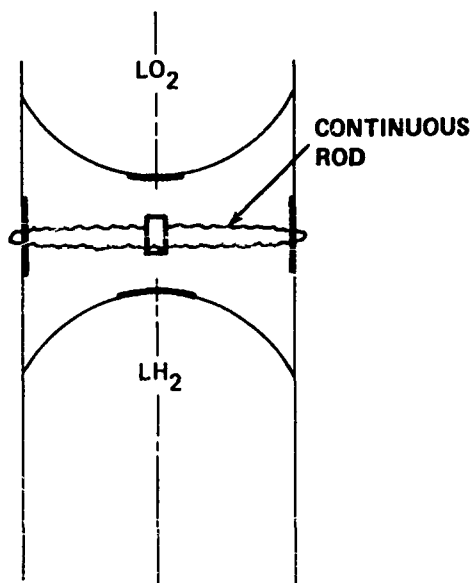
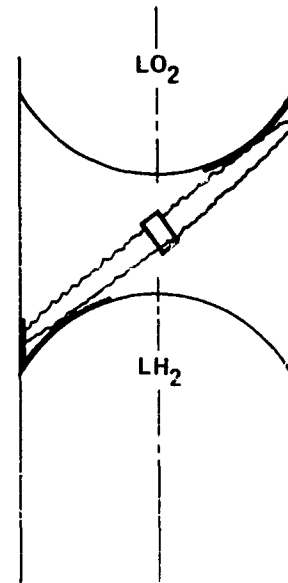


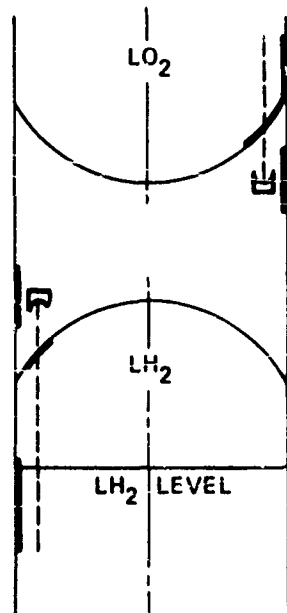
FIGURE 2-2 DESTRUCT CHARGE OPTIONS IN INTERTANK (Sheet 1 of 3)



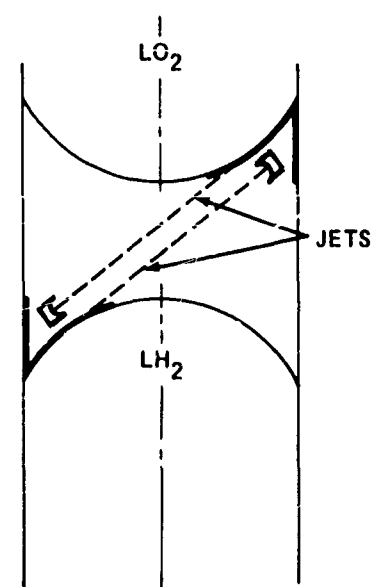
VIEW D-1. 70-LB CONTINUOUS ROD CHARGE CENTRALLY LOCATED



VIEW D-2. CONTINUOUS ROD CHARGE ALTERNATIVE POSITION

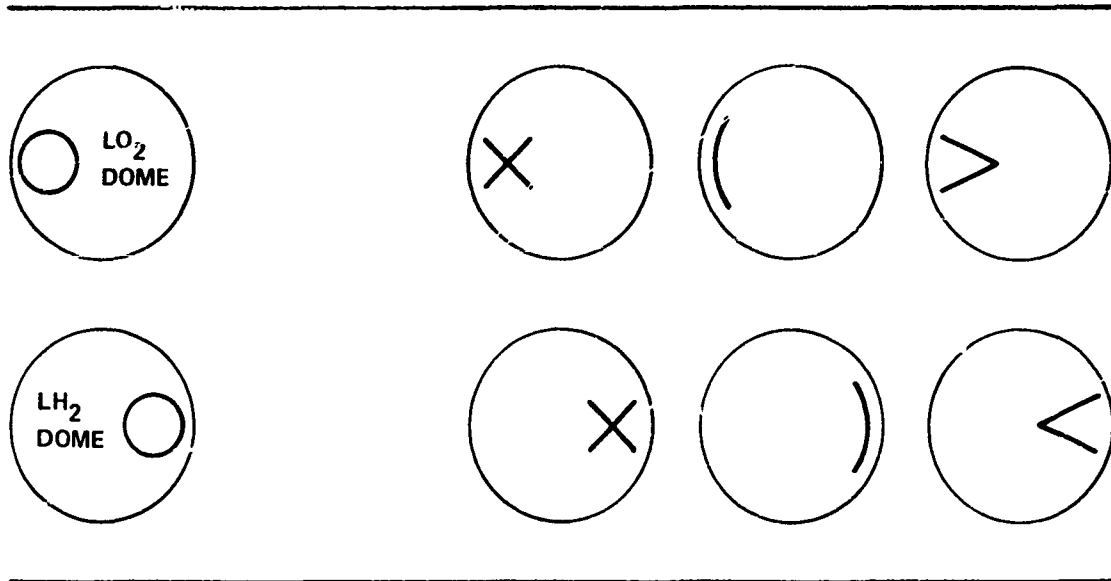


VIEW E-1. CONICALLY OR HEMISPHERICALLY SHAPED CHARGES - JETS ABOUT 4" FROM TANK WALLS

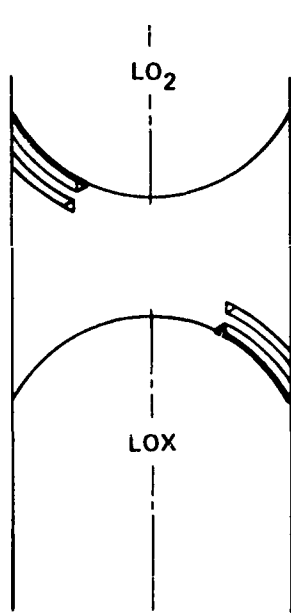


VIEW E-2. CONICALLY OR HEMISPHERICALLY SHAPED CHARGE DIRECTED AT NEAR TANGENCY TO DOMES

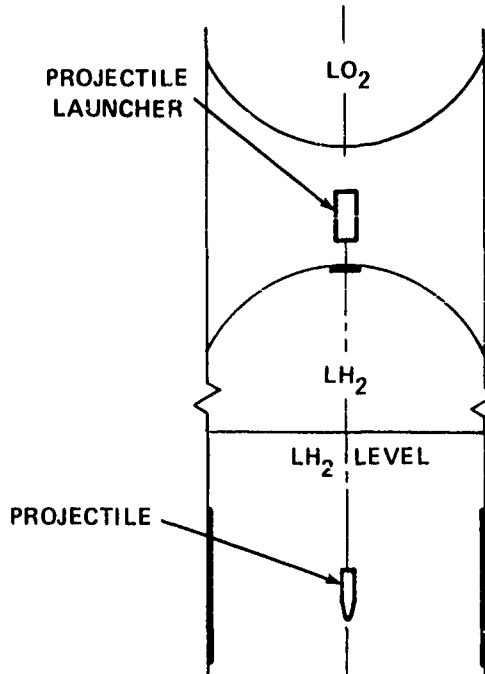
FIGURE 2-2 DESTRUCT CHARGE OPTIONS IN INTERTANK (Sheet 2 of 3)



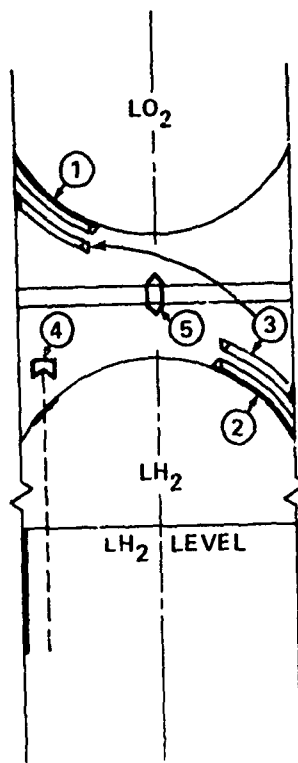
VIEW F-1. ALTERNATIVE POSITIONS OF LSC'S ON LH₂ AND LOX IT DOMES



VIEW F-2. BACK-TO-BACK LSC'S TO CUT DOMES AND TANK WALL

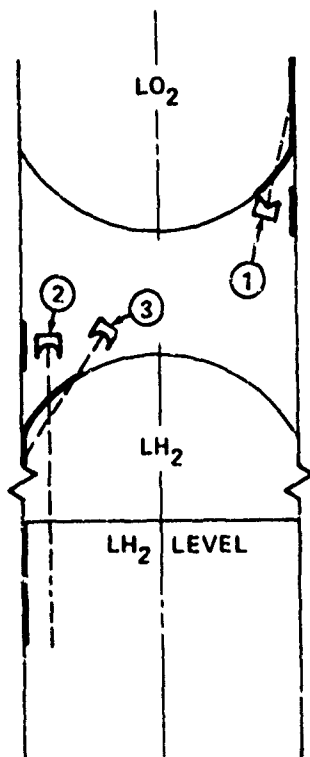


VIEW G. EXPLOSIVE PENETRATOR - CENTRALLY LOCATED FOR LH₂ TANK DESTRUCT



- ① LSC IN CROTCH OF LO_2 TANK TO CUT UP TO 180° ARC
- ② LSC IN CROTCH OF LH_2 TANK TO CUT UP TO 180° ARC IN SECTOR OPPOSITE TO LO_2 CUT
- ③ LSC'S BACK-TO-BACK WITH ① AND ② TO CUT IT WALLS
- ④ CONICALLY SHAPED CHARGE TO RUPTURE LH_2 TANK WALL IN REGION OF LIQUID H_2
- ⑤ LSC TO RUPTURE SRB BEAM

FIGURE 2-3 FIVE-ELEMENT DESTRUCT SYSTEM



- ① CONICALLY SHAPED CHARGE TO DEFEAT LO_2 TANK
- ② HEMISPHERICALLY SHAPED CHARGE TO DEFEAT LH_2 TANK IN PRESENCE OF LIQUID H_2
- ③ HEMISPHERICALLY SHAPED CHARGE TO HOLE LH_2 TANK WHERE ONLY GASEOUS H_2 IS PRESENT

FIGURE 2-4 THREE-ELEMENT DESTRUCT SYSTEM

CHAPTER 3

STRUCTURAL DAMAGE AND BLAST CONSIDERATIONS

STRUCTURAL ANALYSIS

INTRODUCTION. As a prerequisite to establishing charge weight and placement, structural analyses germane to each destruct system concept are given below to identify the momentum transfer required to fail the external tank (ET) under the guidelines of Chapter 1, i.e., rapid dump, minimum mixing, and low system weight. The present objective is to define the primary level of damage to be inflicted upon the ET in order to initiate adequate dispersal of the LOX and LH₂. (Prediction of the propagation of that damage into overall destruction of the ET was left for the follow-on, Phase III study.)

The explosive system options listed in Chapters 4 and 5 group into two categories: those that aim to destroy the ET via pressure loading, e.g., mass charge, and those that initiate damage via direct cutting, e.g., linear-shaped charge (LSC). The requirements of the latter are well defined for optimum geometric arrangements and can be defined by feasibility testing for more complex installations. These tests have been performed for the LSC cable tray installation and are reported in Chapter 5. The systems that depend upon pressure loading can be further categorized into systems which symmetrically load the structure, i.e., centrally located explosive charges, and systems which locally load the structure, i.e., energy sources placed adjacent to a wall of the structure.

The following analyses are attempts to establish damage thresholds for the various components (LOX tank, intertank (IT), and LH₂ tank) subjected to the generalized dynamic pressure loadings given above. The specific analyses are for (1) an explosive charge centrally located in the intertank, (2) an explosive charge centrally located in the LH₂ tank, and (3) a line energy source located near the wall of the LOX or LH₂ tank.

The following assumptions apply to all of the dynamic analyses with the exception of the empirical prediction for holing of the LOX tank and LH₂ tank domes via blast loading:

1. The loading is purely impulsive. The momentum is delivered to the structure in a time interval which is short relative to the response or dissipation time of the structure.

2. The structural material acts as a rigid, perfectly plastic material with no elasticity or work hardening. Since energy dissipation and flow stress are the critical parameters to be matched, reasonable rigid plastic models for the materials of interest can be established.

3. Strain rate effects are negligible for the materials of interest at low temperatures.

4. The initial state of stress has negligible impact on the requirements since the elastic strain energy associated with normal operation is small compared to the energy required to rupture the material.

EXPLOSIVE CHARGE CENTRALLY LOCATED IN INTERTANK. The IT wall is comprised of a cylindrical membrane and longitudinal stringers of 2024-T81 aluminum, stiffened with internal ring frames at approximately 45-inch intervals (Fig. 3-1). The assumed deflection model shape for symmetric internal loading is shown in Figure 3-2. Plastic hinges form in the membrane and stringers at the ring frames and at mid-bay. Energy dissipation is by hoop membrane extension and by hinging.

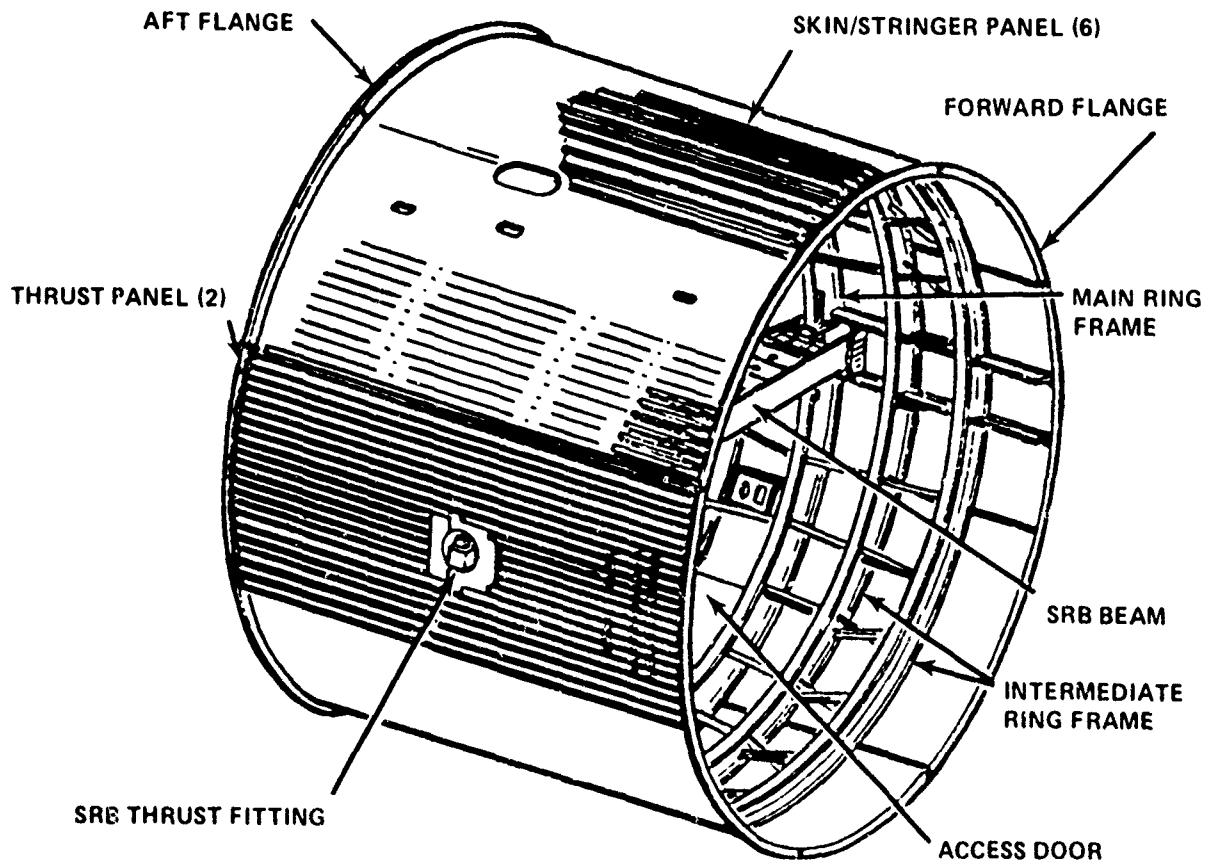


FIGURE 3-1 INTERTANK STRUCTURE

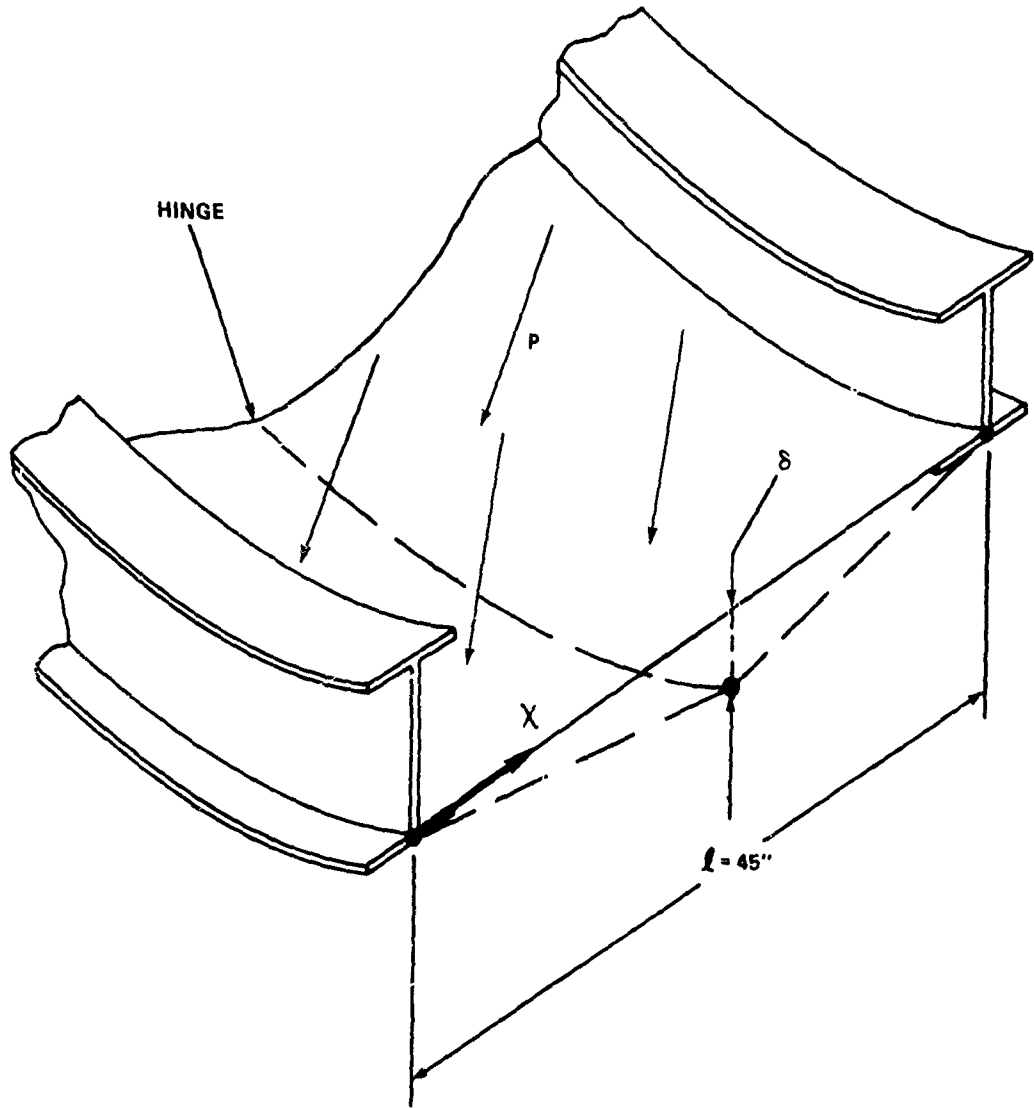


FIGURE 3-2 DEFLECTION MODE SHAPE OF ONE INTERTANK BAY

Fertis presents a one-degree-of-freedom lumped mass analysis for approximating the dynamic behavior of a structural element or component element of a multi-element structure.¹ The derivation of an equivalent single-degree spring-mass system involving the parameters m_e , F_e , and R_e (effective mass, effective load, and effective resistance, respectively) requires the assumption of an appropriate shape for the deflection of the element. The assumed shape establishes an equation that relates the relative deflection of all points, thus permitting the motion of the element to be specified by a single point on the element. The equivalent system is obtained by making the displacement of its mass m_e the same as that of a significant point on the structural element, i.e., midspan.

For impulsive loading only

$$\delta = \frac{I_e^2}{2m_e R_e} \quad (3-1)$$

where

δ = mid-span deflection

I_e = effective impulse

m_e = effective mass

R_e = effective resistance

The effective impulse associated with bursting the IT wall is then given by

$$I_e = \sqrt{2m_e R_e \delta_{cr}} \quad (3-2)$$

where δ_{cr} is the deflection at which the skin will rupture. The effective parameters are determined from the actual parameters m , P , R , and I (mass, load, resistance, and impulse) for this case as follows:

$$m_e = \int_0^{\ell} m\beta^2(x) dx \quad (3-3)$$

For the assumed shape of Figure 3-2 and a bay length of ℓ ,

$$\beta(x) = \frac{2x}{\ell} \quad 0 \leq x \leq \ell/2 \quad (3-4)$$

Therefore, the effective mass is

$$m_e = 2 \int_0^{\ell/2} m(2x/\ell)^2 dx = (1/3)m \quad (3-5)$$

¹Fertis, D.G., Dynamics and Vibration of Structures, (New York: John Wiley & Sons, Inc., 1973).

The equivalent resistance is related to the actual resistance by the same factor as that relating the equivalent and actual loads. For this case, the actual load $q(x)$ is assumed to be uniformly distributed both axially and circumferentially. The effective load is then given by

$$P_e = \int_0^{\ell} q(x)\beta(x)dx = \int_0^{\ell} q\beta(x)dx \quad (3-6)$$

Substituting for $\beta(x)$ yields

$$P_e = 2 \int_0^{\ell/2} q(2x/\ell)dx = 1/2 (q\ell) \quad (3-7)$$

Since $(q\ell)$ is the total actual load P ,

$$P_e = (1/2)P \quad (3-8)$$

and as indicated above

$$R_e = (1/2)R \quad (3-9)$$

Integrating the load-time curves yields

$$I_e = \int_0^t P_e dt = \int_0^t (1/2)P dt = (1/2)I \quad (3-10)$$

Consider the wall section illustrated in Figure 3-3. The section consists of one stringer and the corresponding skin segment. The total mass of the stringer and skin (0.080-in thick) is 5.2 lbm. The resistance is derived from two sources, membrane stretching in the hoop direction and stringer hinging in the radial direction. The former is related to the material flow stress by the following equation for small θ ($\theta = 2.50^\circ = 0.0436$ Rad, Fig. 3-3).

$$R_m = \sigma_0 h \ell \theta = (75,000)(0.080)(45)(0.0436) = 11,800 \text{ lb} \quad (3-11)$$

The latter is related to the fully plastic bending moment capability M_p of the stringer/skin section.

$$R_s = \frac{16M_p}{\ell} = \frac{(16)(22,600)}{(45)} = 8,000 \text{ lb} \quad (3-12)$$

The total resistance R becomes 19,800 lb, the algebraic sum of R_m and R_s .

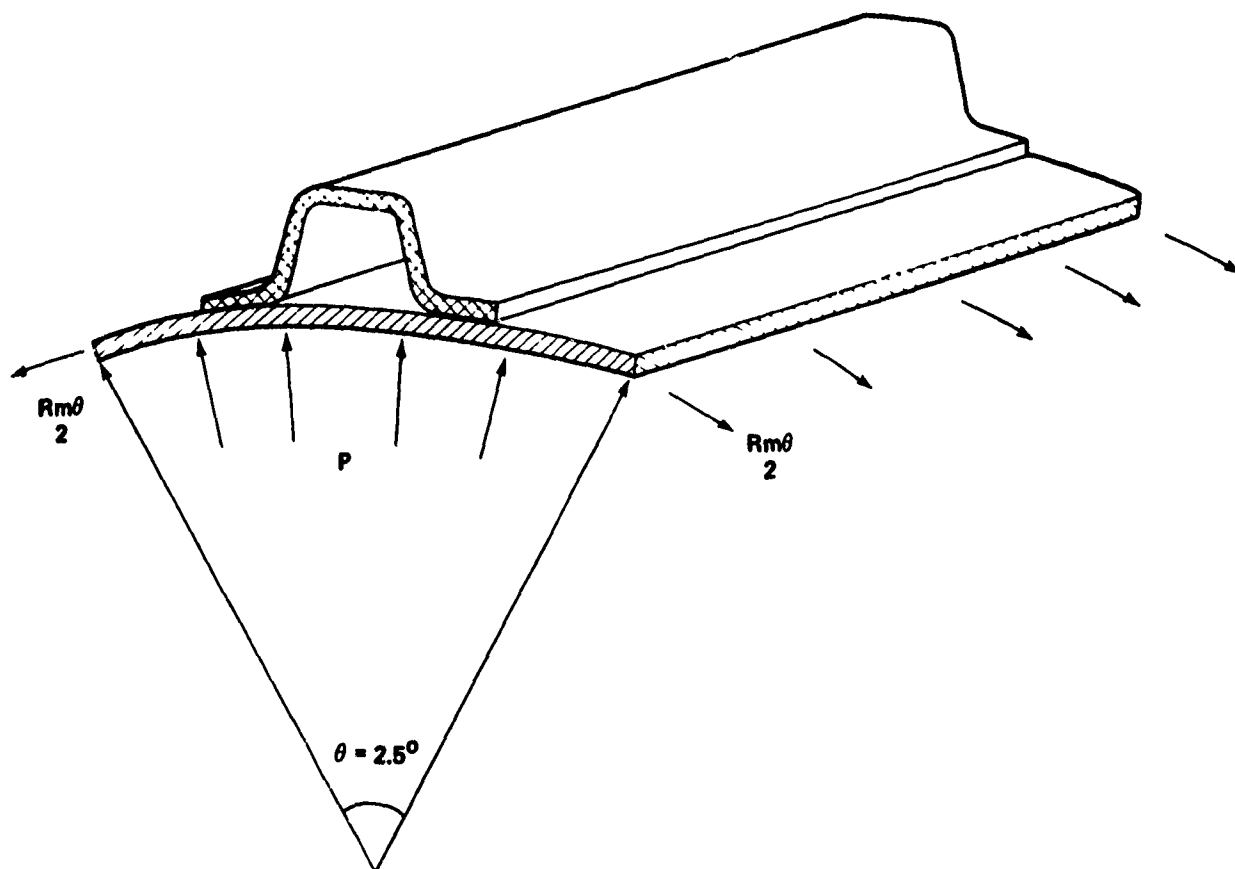


FIGURE 3-3 INTERTANK STRINGER AND SKIN SECTION

The only remaining parameter to be defined is the displacement δ_{cr} . The radial displacement is related to the ultimate strain

$$\delta_{cr} = r_o \epsilon_{ult} \quad (3-13)$$

where r_o is the radius of the cylinder (165.5 in). The skin material has an ultimate strain ϵ_{ult} of about 15 percent. The minimum displacement to produce material failure is therefore

$$\delta_{cr} = 24.8 \text{ in} \quad (3-14)$$

Substituting for the effective parameters in the impulse Equation 3-2 yields

$$I_r = \frac{2}{\ell w} \sqrt{\frac{m R \delta_{cr}}{3g_c}} = \frac{2}{(45)(7.2)} \sqrt{\frac{(5.2)(19,800)(24.8)}{(3)(386)}} = 0.29 \text{ psi-sec} \quad (3-15)$$

where I_r is the minimum reflected impulse per unit area that will rupture the IT wall and w is the width of the 2.5 degree skin segment. The selection of the explosive charge capable of producing the required impulse is addressed in Chapter 4.

An explosive charge capable of destroying the IT wall will also inflict considerable damage upon the adjacent domes of the LOX and LH₂ tanks. An empirical correlation has been developed to predict the size of blast damage holes in steel. This correlation has been extended here via limit analysis to predict the damage to the ET aluminum domes.

Assuming that holing can be correlated with deflection and that deflection is proportional to the square of the reflected impulse divided by the resistance (plastic bending moment M_p) and the mass (Equation 3-1) yields the following ratio for the impulse required to hole an aluminum plate versus a steel plate, then

$$\frac{I_{r\text{al}}}{I_{r\text{st}}} = \sqrt{\frac{m_{\text{al}} M_{p\text{al}}}{m_{\text{st}} M_{p\text{st}}}} \quad (3-16)$$

For plates of the same dimensions, Equation 3-16 can be further simplified to one of ratios of material properties.

$$\frac{I_{r\text{al}}}{I_{r\text{st}}} = \sqrt{\frac{\rho_{\text{al}} \sigma_{\text{al}}}{\rho_{\text{st}} \sigma_{\text{st}}}} = \sqrt{\frac{(0.10)(95,000)}{(0.28)(175,000)}} = 0.45 \quad (3-17)$$

Table 3-1 lists charge weights and the resulting damage expected at sea level (1 atm) in the domes due to a charge centrally located in the IT. The effect of fluid backing in the LOX tank is not considered. Extension of these results to the high altitude environment (vacuum) will be found in Appendix A.

EXPLOSIVE CHARGE CENTRALLY LOCATED IN LH₂ TANK. The LH₂ tank wall consists of four barrel sections joined at major ring frames and stiffened with intermediate ring frames. The skin (predominantly 0.137-in thick 2219-T87 Al) contains integrally machined, T-shaped, longitudinal stiffeners placed at 3.75 degree intervals around the circumference (Fig. 3-4).

Assume that the intermediate frames are not of sufficient strength to influence the deflected mode shape and that the barrels deflect radially as though infinitely long except near the major ring frames. Then the effective values for the parameters used in the single-degree-of-freedom analysis are equal to the actual values since all points on the structure respond with the same displacement. The impulse equation for the skin/stringer segment illustrated in Figure 3-5 becomes

$$I_r = \frac{1}{w} \sqrt{\frac{2}{g_c} \left(\frac{m}{\ell}\right) \left(\frac{R}{\ell}\right)} \delta_{cr} \quad (3-18)$$

TABLE 3-1 CHARGE WEIGHT VS. HOLE SIZE - LOX AND LH₂ TANK DOMES

Charge Weight (TNT) Holing of Steel Plate (1b)	Equivalent Charge Weight (TNT) Holing of Aluminum Plate (1b)	Standoff Distance (ft)	Hole Diameter in 0.11-In-Thick Plate (LH ₂ Tank Dome) (ft)	Hole Diameter in 0.15-In-Thick Plate (LOX Tank Dome) (ft)
1	0.36	2	0.9	0.0*
2	0.73	2	2.4	1.2
5	1.95	2	3.7	2.9
10	3.9	2	4.7	3.9
25	10.3	2	6.1	5.2
50	20.0	2	7.2	6.3
100	39.0	2	8.5	7.4
200	72.0	2	9.8	8.6
300	104.0	2	10.7	9.4

*Holing not predicted.

where $(m/l) = 0.253 \text{ lbm/in}$, and for 2219-T87 Al at -423°F

$$\delta_{cr} = r_o \epsilon_{ult} = 165.5(0.15) = 24.8 \text{ in} \quad (3-19)$$

Since the stringers do not contribute to the resistance for the mode shape chosen here, the resistance per unit length is given by

$$\left(\frac{R}{l}\right) = \sigma_o h \theta = (95,000)(0.137)(0.0654) = 851 \text{ lb/in} \quad (3-20)$$

Substituting the above parameters into the impulse equation yields

$$I_r = \frac{1}{10.8} \sqrt{\frac{2(0.253)(851)(24.8)}{386}} = 0.49 \text{ psi-sec} \quad (3-21)$$

as the minimum reflected impulse per unit area required to rupture the LH₂ tank wall, liquid or vapor filled.

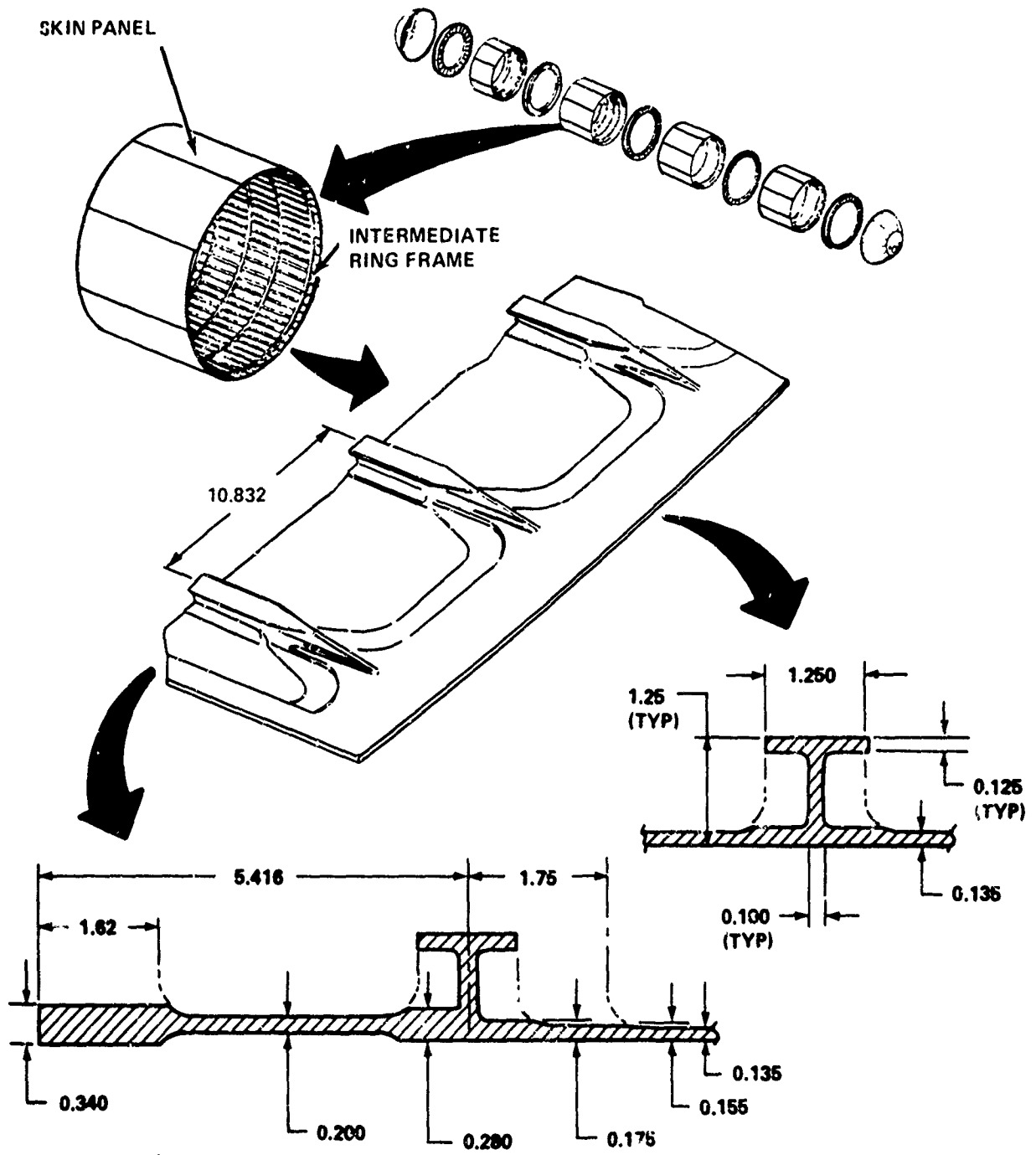
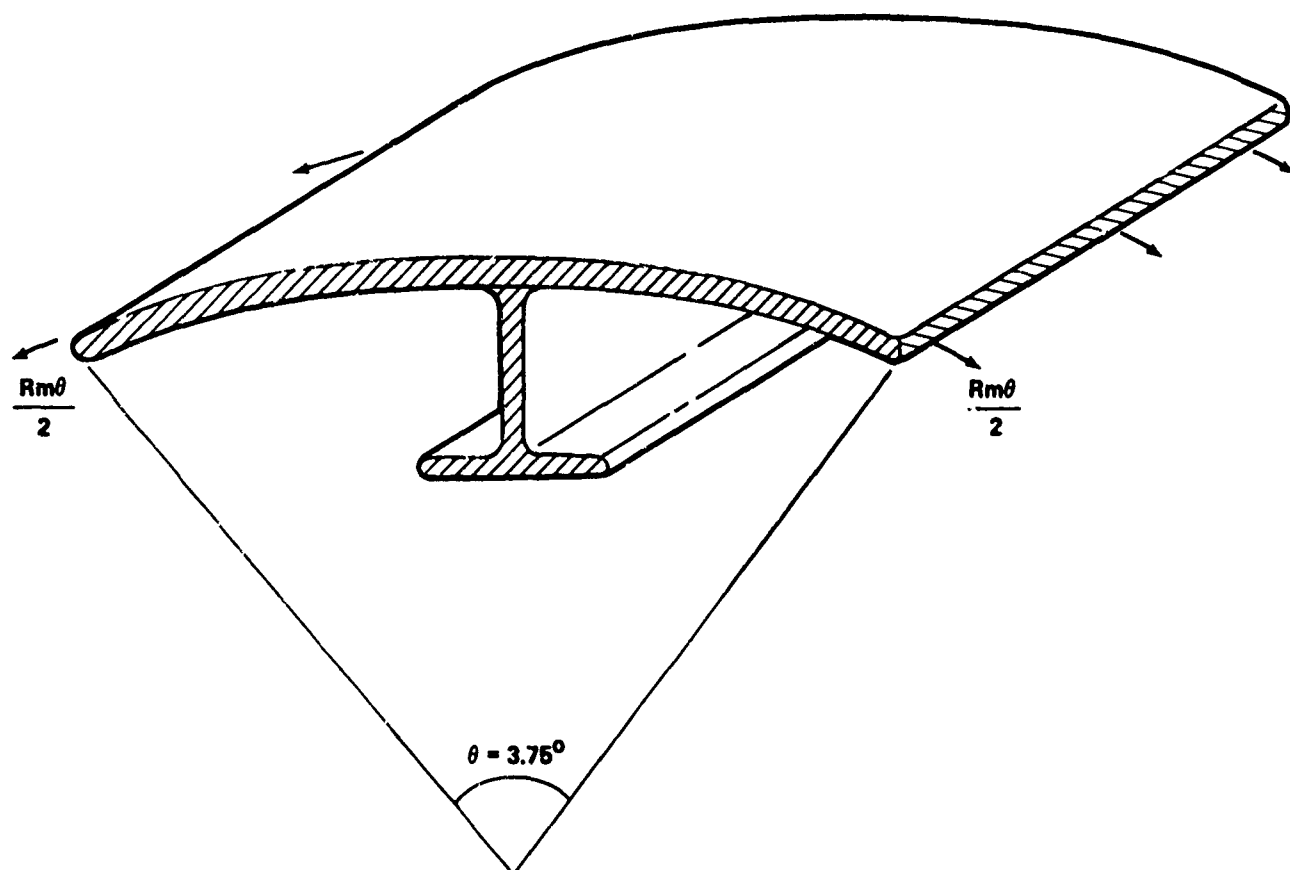


FIGURE 3-4 TYPICAL LH₂ TANK BARREL SECTION

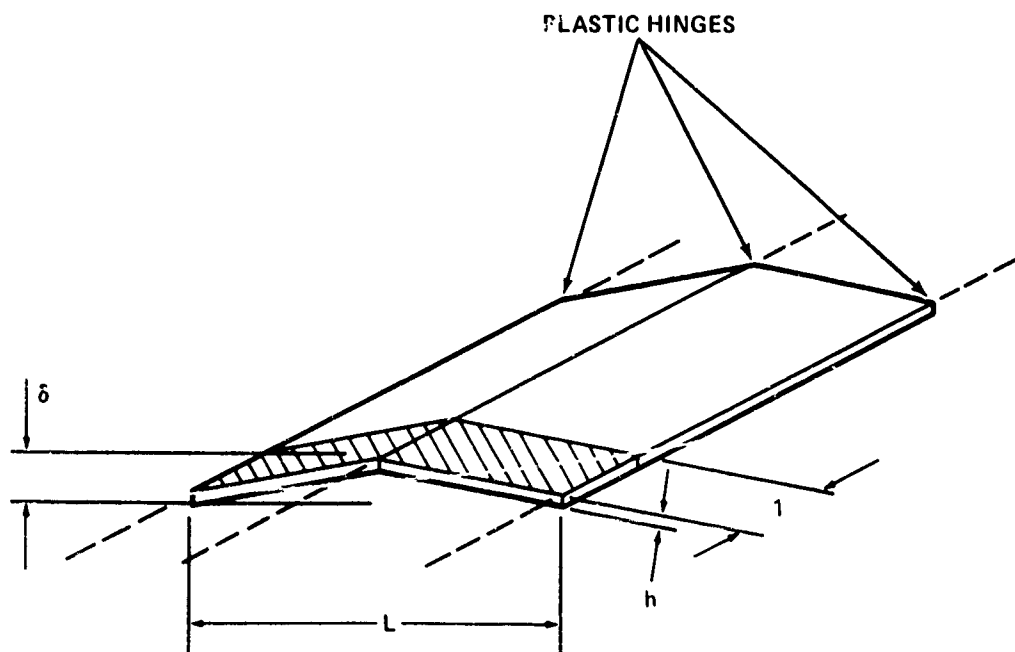
FIGURE 3-5 LH₂ TANK STRINGER AND SKIN SECTION

LINE SOURCE NEAR WALL OF LOX OR LH₂ TANK. The conically or hemispherically shaped charges reviewed in Chapters 4 and 5 are to be installed such that the jets, having penetrated the tanks, will enter the LOX and LH₂ and pass nearly parallel to and in close proximity to the tank walls. For large jet penetration distances, the region of influence is long and narrow. Therefore, an analysis of an infinitely long region is applicable except in the vicinity of the ends. The response of the shell to the shock loading is to form a plastic hinge along the center line of the region and two hinges along the edges of the region. Since the region is infinitely long, a unit-width strip can be analyzed as a beam to obtain the deflections (Fig. 3-6).

Humphreys gives the following relationship for the plastic string response of a beam undergoing a large deflection, δ :³

$$\zeta - 2 < \frac{2\delta}{h} < \zeta - 1 \quad (3-22)$$

³Humphreys, J.S., "Plastic Deformation of Impulsively Loaded Straight Clamped Beams," Journal of Applied Mechanics, Mar 1965, pp. 7-10.

FIGURE 3-6 LH₂ TANK DEFLECTION MODE SHAPE (LOCAL WALL LOADING)

ζ is defined as

$$\zeta = \frac{I_r L}{h^2} \left(\frac{1}{\rho \sigma_o} \right)^{1/2} \quad (3-23)$$

where I_r is the reflected impulse per unit area, ρ is the material density, σ_o is the plastic stress, and L and h are defined in Figure 3-6. Assuming that on the average

$$\frac{2\delta}{h} = \zeta - 1.5 = \frac{I_r L}{h^2} \left(\frac{1}{\rho \sigma_o} \right)^{1/2} - 1.5 \quad (3-24)$$

and rearranging terms yields

$$I_r = \left[\frac{2\delta h}{L} + 1.5 \frac{h^2}{L} \right] [\rho \sigma_o]^{1/2} \quad (3-25)$$

The deflection required to cause rupture can be written in terms of the ultimate strain of the material as follows:

$$\delta_{cr}^2 = [(1 + \epsilon)^2 - 1] (L/2)^2 \quad (3-26)$$

For an ultimate strain of 15 percent (2219-T87 Al at cryogenic temperatures) δ_{cr} becomes

$$\delta_{cr} = 0.568 (L/2) \quad (3-27)$$

Substituting into the equation for I_r gives

$$I_r = \left[0.568h + 1.5h \left(\frac{h}{L} \right) \right] [\rho\sigma_0]^{1/2} \quad (3-28)$$

For this case, L is much greater than h , and the second term can be eliminated with less than a 10-percent error. The impulse per unit area required to rupture the tank wall then becomes

$$I_r = [0.568h] [\rho\sigma_0]^{1/2} \quad (3-29)$$

For 2219-T87 Al at liquid oxygen temperature ($\sigma_0 = 75,000$ psi)

$$I_r = 2.6h \quad (3-30)$$

Since the skin thickness in the region of the LOX tank barrel section to be ruptured is about 0.2 inch, the calculated impulse required to rupture the LOX tank via shock loading is

$$I = 0.5 \text{ psi-sec} \quad (3-31)$$

Experiments performed with jets penetrating water at NSWC/WOL (unpublished) yielded incident impulses in excess of 0.80 psi-sec at a 12-inch radial distance from the jet path. The results for LOX should be very similar. The reflected impulse is on the order of twice the incident impulse, giving a delivered impulse to the structure of about 1.6 psi-sec. Since the jet in the destruct system will pass much closer to the wall (<4 in), and the impulse developed in the LOX should be slightly greater due to its higher density, the delivered impulse will exceed the calculated rupture limit of the barrel section by at least a factor of three. Therefore, rupture of the LOX tank barrel section wall is predicted.

Rupture of the LH₂ tank barrel sections is not demonstrated in the same manner. The impulse required to rupture the LH₂ tank wall at LH₂ temperature ($\sigma_0 = 95,000$ psi) is

$$I_r = 2.8h = (2.8)(0.137) = 0.4 \text{ psi-sec} \quad (3-32)$$

Scaling the delivered impulse by the density ratio between hydrogen and water gives an experimental value for the minimum reflected impulse of 0.11 psi-sec at a 12-inch distance. At about 4 to 8 inches from the jet, the impulse is expected to be higher, but how much is not known. Hence, the feasibility of rupturing the LH₂ tank wall via this method is neither assured nor disproven by the limited experiments cited above. Demonstration tests are required.

SUMMARY. Table 3-2 summarizes the results of this section. Impulses on the order of 0.3 to 0.5 psi-sec are required to rupture the LOX, LH₂, and IT walls.

TABLE 3-2 SUMMARY OF IMPULSE REQUIREMENTS TO RUPTURE ET STRUCTURE

Structure	Minimum Impulse To Initiate Failure (psi-sec)	Charge Placement
LOX Tank Wall	0.5	Adjacent to wall
IT Wall	0.29	On ET axis
LH ₂ Tank Wall	0.49	On ET axis
LH ₂ Tank Wall	0.4	Adjacent to wall
LOX Tank Dome	0.096*	On ET axis 2-ft standoff
LH ₂ Tank Dome	0.056*	On ET axis 2-ft standoff

*≈1-ft diameter hole (see Table 3-1 and Appendix A for requirements for larger holes).

MIXING AND BLAST YIELDS

ON LAUNCH PAD. Any destruct occurring while the vehicle is on or very near the launch pad is likely to cause a large explosion. There is no place to put the spilling propellant. The LOX and LH₂ will mix on the pad and auto-ignition will occur when large quantities are involved. Farber estimates that the critical mass for auto-ignition of LOX/LH₂ is 2,300 pounds.⁴

The primary work on propellant explosions has been summarized by Baker, et al.⁵ The main studies are the PYRO experiments⁶ and the work of Farber, et al (see footnote 4, below). Sutherland argues that the TNT equivalence of LOX/LH₂ should obey a 2/3 power law.⁷ He gives an upper bound of

⁴Farber, E.A., Klement, F.W., and Lonzon, C.F., "Prediction of Explosive Yield and Other Characteristics of Liquid Rocket Propellant Explosions," Final Report, NASA-CR-137372, N74-20580, Contract No. NAS 10-1255, University of Florida, Gainesville, 30 Jun 1973.

⁵Baker, W.E., et al, "Assembly and Analysis of Fragmentation Data for Liquid Propellant Vessels," NASA CR-134538, Contract No. NAS 3-16009, Southwest Research Institute, San Antonio, Texas, Jan 1974.

⁶Willoughby, A.B., Wilton, C., and Mansfield, J., "Liquid Propellant Explosive Hazards. Final Report-Dec. 1968. Vol. I - Technical Documentary Report; Vol II - Test Data; Vol. III - Prediction Methods," AFRPL-TR-68-92, URS-652-35, URS Research Co., Burlingame, California.

⁷Sutherland, L.C., "A Simplified Method for Estimating the Approximate TNT Equivalent from Liquid Propellant Explosions," Paper before 15th Annual Explosives Safety Seminar, San Francisco, 20 Sep 1973.

$$W_{\text{TNT}} = 4 W_p^{2/3} \quad (3-33)$$

where W_{TNT} is the blast-equivalent weight of TNT in pounds and W_p is the weight of LOX/LH₂ propellant in pounds. Figure 3-7 (taken from footnote 7, p. 3-13) indicates that the 2/3 power law works quite well. It has been adopted here.

CONFINED MIXING. Some of the destruct options involve penetration of the tank domes in the IT and penetration of the outer IT wall, with the hope that the LOX and LH₂ will exit without too much mixing.

Although there is normally no LH₂ contacting the top dome of the tank, there will be such contact when the LH₂ boils upon loss of ullage pressure at altitude or when the vehicle tumbles. If both IT domes are penetrated by destruct charges, there is an opportunity for LOX and LH₂ to mix in the confined IT space. The IT volume is large and can easily hold enough propellant to auto-ignite. This IT explosion can further open up the tank domes. This allows massive direct mixing of the LOX and LH₂ in the partial confinement of the remaining tanks. The driving force for the mixing is the vapor pressure of the boiling liquids.

A value sometimes used for the TNT equivalence of a missile destroyed in flight is 1 percent of the propellant weight. Because of the opportunity for considerable mixing in the IT, Equation 3-1 for the confined explosion that can be caused by destruct charges in the IT is used. The "Method 1" column of Table 3-3 shows the calculated TNT yields.

DUMPING TO OUTSIDE OF ET. If the LOX and LH₂ are dumped directly to the outside of the ET, the only driving force for mixing is the turbulent flow in the wake of the vehicle. A long diffusing streamer of LOX/LH₂/air mixture results. Whether auto-ignition of such a streamer would occur is not clear. This low mixing is a strong point of the hybrid (Method 2, Table 3-3) and LSC (Method 3, Table 3-3) destruct methods. The 1-percent rule is used in Table 3-3 to get the TNT equivalence for outside dumping in flight.

Subsequent events such as crushing of the ET by an SRB explosion or aerodynamic breakup could, of course, increase the TNT yield, particularly if the breakup is such as to allow jets of LOX and LH₂ to collide.

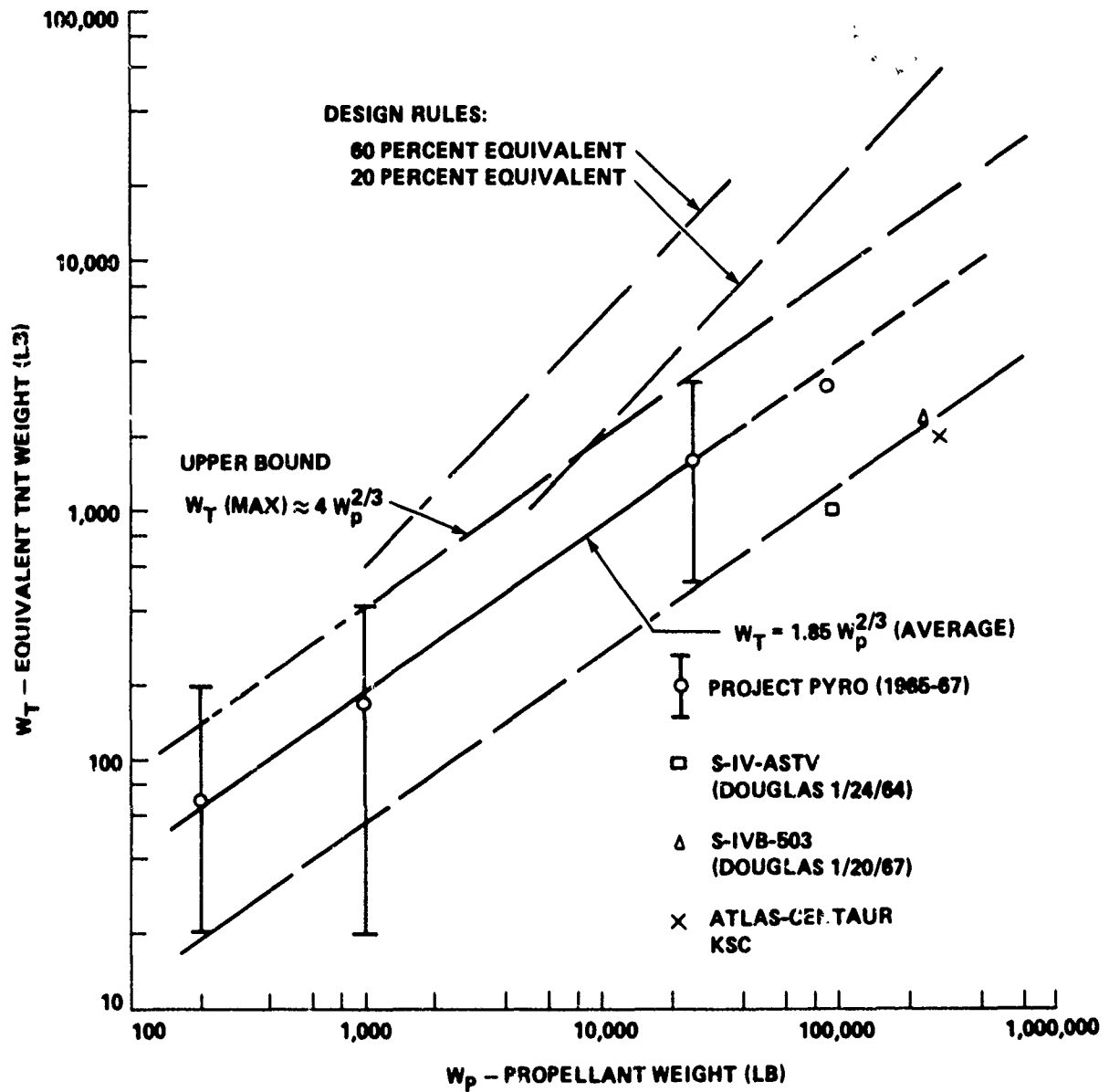
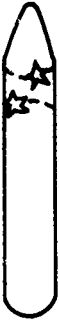




FIGURE 3-7 TREND IN MEASURED EQUIVALENT TNT WEIGHT FROM LOX/LH₂ PROPELLANT EXPLOSIONS COMPARED TO DESIGN RULES

TABLE 3-3 TNT EQUIVALENCE OF ET EXPLOSION

  			
Method 1 Method 2 Method 3			
Time (sec)	Altitude (kft)	TNT Equivalence (lb)	
		Method 1	Methods 2 and 3
0	0.0	54,000*	54,000*
10	0.8	53,000*	15,400 [†]
50	24.0	50,000*	14,100 [†]
100	99.0	46,000*	12,500 [†]
350	390.0	38,000*	9,300 [†]
450	380.0	7,500*	810 [†]

*Upper bound from $W_{TNT} = 4 W_p^{2/3}$. Confinement by missile is taken as equivalent to confinement by ground surface.

[†]Explosion in flight without confinement by missile; TNT equivalent weight is taken as 1 percent of propellant weight.

CHAPTER 4

EXPLOSIVE SYSTEM OPTIONS — DEVICES INSIDE INTERTANK

This section includes systems in which the ordnance is placed into the intertank (IT). This encompasses charges that act by blast or produce gas pressure in the IT, are launched outside the IT before they detonate, or detonate in the IT but depend on fragments or jets of matter (which may leave the IT) to carry out the destruct action.

BARE CHARGES

The destruction of the IT wall and the domes of the tanks by means of an uncased, i.e., nonfragmenting charge is complicated by the fact that the IT is vented to the outside atmosphere. The destruct charge must produce the desired loading in all ambient conditions from sea level to vacuum. At sea level, the damaging effect is the shock wave driven by the explosion products. As the ambient pressure is reduced, this shock becomes less effective, and the damage is done by the collision of the explosion products with the wall.

SINGLE LARGE CHARGE. A charge placed at the center of the IT could take out the solid rocket booster (SRB) beam, the IT walls on all sides, the LH₂ dome, and probably the LO₂ dome. An impulse of about 0.3 psi/sec is needed to break the IT wall. Putting $I_r = 0.3$ psi/sec and $r = 13$ feet into Equation A-4, Appendix A, gives a required charge size (for vacuum IT conditions) of 390 pounds TNT. (For sea-level conditions, 81 pounds would be enough.) This charge would be sufficient for putting a large hole into the LH₂ dome. The charge size needed for the LO₂ dome is unknown, because it is backed by the dense LO₂ which makes it much more blast-resistant than the LH₂ dome presumed to have only ullage gas behind it at destruct time.

SMALL CHARGE NEAR WALL. A 10-pound charge placed 2 feet from the IT wall would just penetrate the IT (Equation A-4, Appendix A). A somewhat larger charge would be needed to make a hole of useful size. A single 20-pound charge placed 2 feet from both the IT wall and the LH₂ tank dome would put holes about 4 or 5 feet in diameter into both IT wall and dome.

FOCUSED-BLAST CHARGES

The blast from a cylindrical charge can be focused in the equatorial plane by detonating the charge simultaneously at both ends. At altitudes around 50 kft, such a charge can give an impulse equal to that of a spherical charge roughly three times as massive. At about 80 kft, however, the focused beam tends to spread out and some of the advantage may be lost. The net effect is that a focused-blast charge in vacuum of about 200 pounds and perhaps as low as 130 pounds TNT would give the same impulse on the IT wall as a 390-pound spherical charge.

CASED CHARGE

A steel-cased charge, i.e., a bomb, of about 300-pound total weight placed near the center of the IT would give sufficient fragment penetration of the domes and IT walls to permit venting, and would also cut the SRB beam. However, the fragments would travel hundreds of feet after leaving the IT and would present a hazard to the orbiter.

CONTINUOUS ROD CHARGE

The fragment energy of a cased charge can be focused into a single expanding ring of metal. Such a device is a developed military item weighing about 70 pounds and containing about 20 pounds of explosive. The device would be near the IT center, and the ring would be aimed at taking out the IT walls. The general blast from such a device at 2-foot standoff from the LH₂ tank dome would make an approximately 3-foot diameter hole in the dome and would cut the SRB beam. The direction of the ring could be tilted to slice the bottom of the LOX tank dome. Again, the fragments of the rod would leave the IT and would be a hazard to the orbiter.

CONICALLY AND HEMISPHERICALLY LINED SHAPED CHARGES

A highly penetrating jet is formed from a metal shell lining a conical or hemispherical cavity within an explosive charge. The jet is propelled with such force and velocity toward the axis of the charge that jet fragments are easily able to penetrate several charge diameters of metal and up to 20 charge diameters within liquids. Both for military and mining operations, shaped charge jets have many important applications. The purpose of this section is to describe the design of shaped charges for destruct action which would dump the LH₂ and LOX tanks.

CONICALLY LINED (TANDEM). The design of a shaped charge containing a copper conical tandem liner is shown in Figure 4-1. The charge arrangement contains 7 pounds of the heat-resistant, plastic-bonded explosive HNS/Teflon, 90/10,* which can be fabricated for a cost of about \$5,000. The jet formed from this charge could penetrate ~4 charge diameters (22 inches) of steel.

HEMISPHERICALLY LINED. A hemispherically-lined shaped charge is shown in Figure 4-2. This charge contains 10 pounds of HNS/Teflon, 90/10, which is easier to fabricate than the tandem-lined charge, at a cost of ~\$4,000. Jet penetration through 3.5-charge diameters (19 inches) of steel is possible with this charge. An entry hole diameter in the steel of ~2 inches could be expected from this charge if it were fired at ~5-charge diameters from the target steel. This hole size would be about twice the hole diameter made by the jet from the conical liner.

* HNS is 2,2¹, 4,4¹, 6,6¹ Hexanitrostilbene.

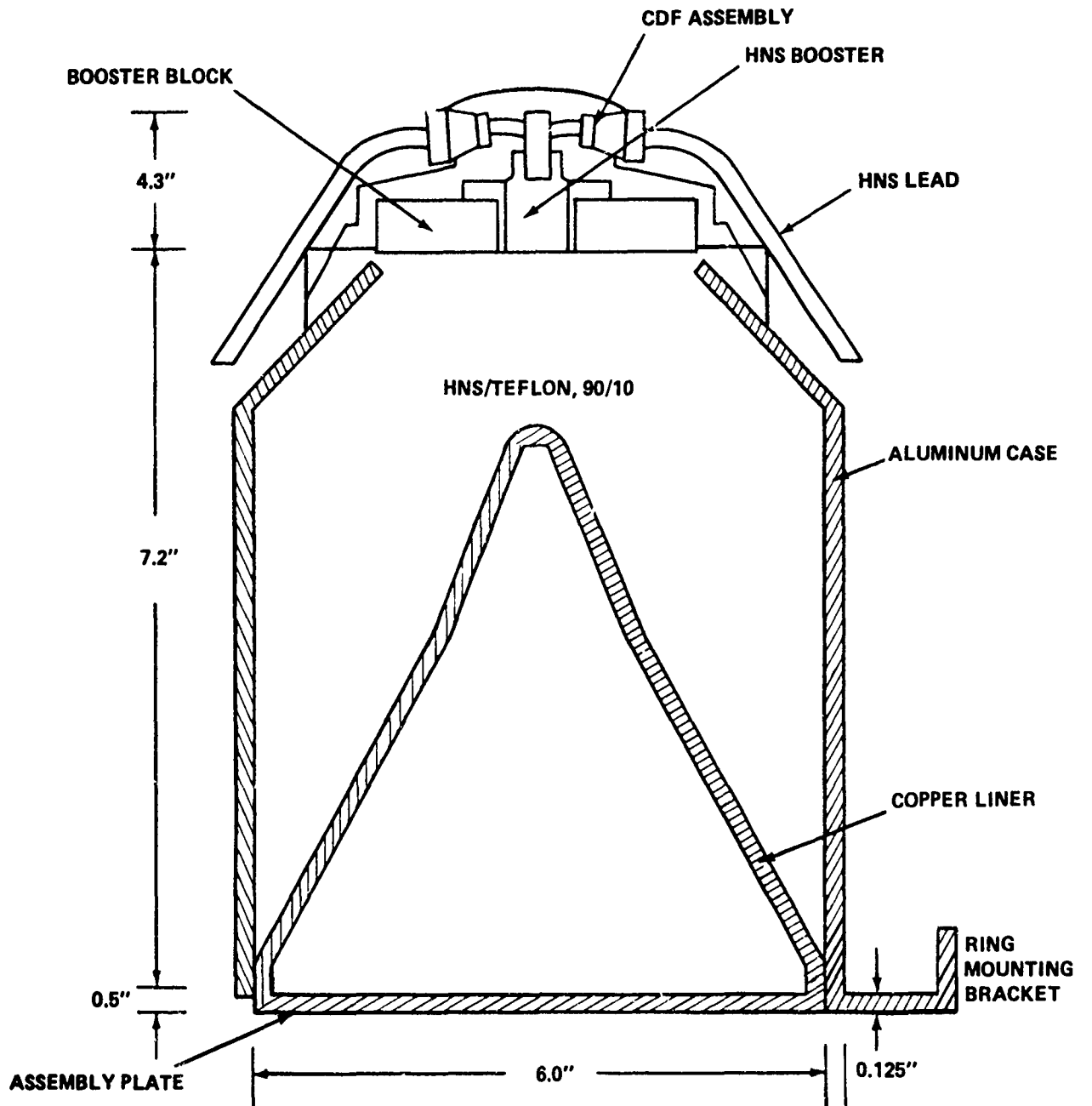


FIGURE 4-1 CONICAL TANDEM-SHAPED CHARGE ARRANGEMENT

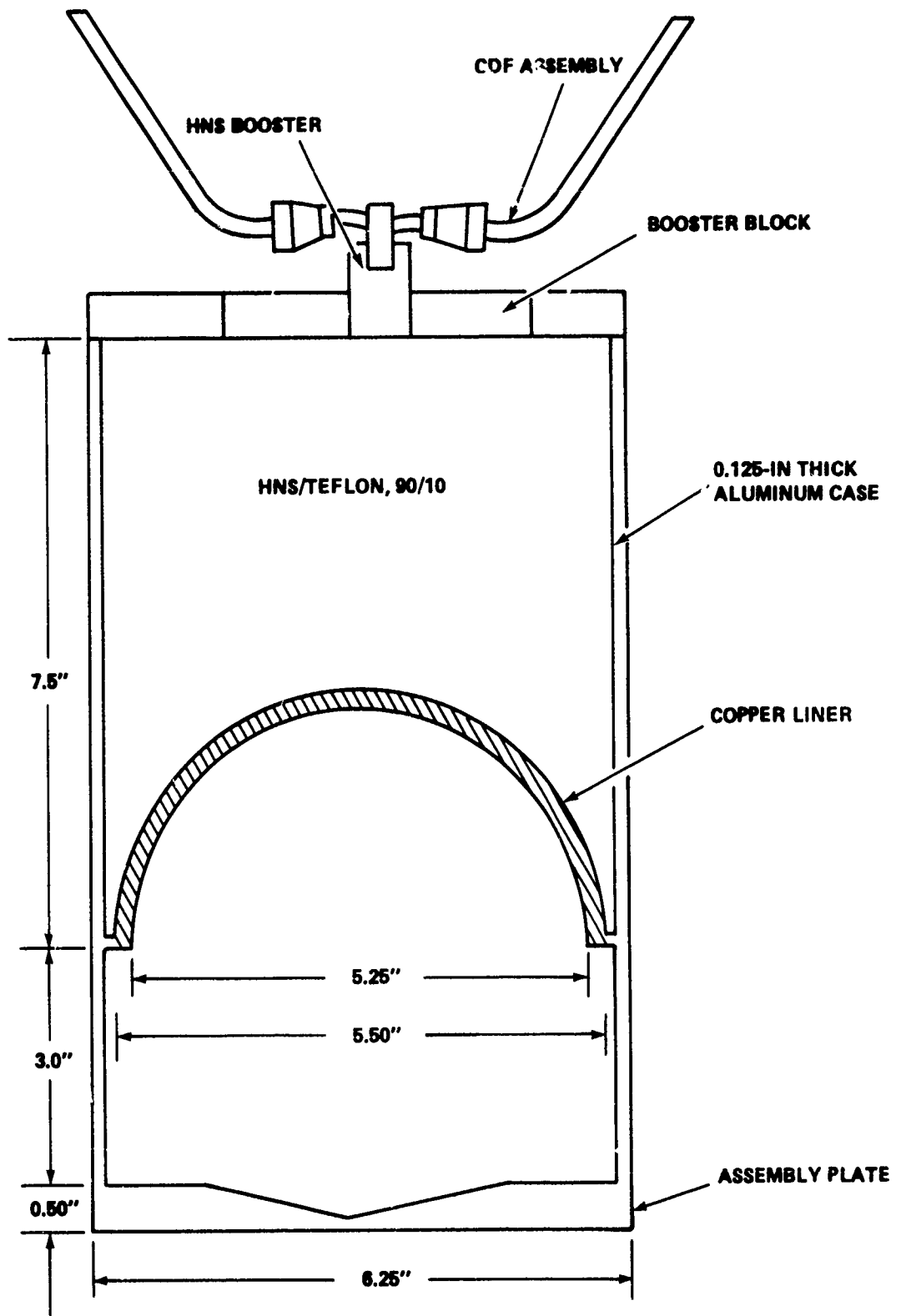


FIGURE 4-2 HEMISPHERICALLY LINED SHAPED CHARGE

It should not be difficult to destroy the LOX tank from a position in the intertank by using a shaped charge (SC). Figure 4-3 shows the location of destructively shaped charges in the intertank. The charge would be aimed so that the stream of jet particles would enter the tank in an area where the LOX is in contact with the bottom tank dome. This situation would provide a fixed air (or gas) standoff from the tank dome. (A standoff is necessary for optimum jet formation.) The impact of the jet at the entry point would load the tank locally with an extremely high-pressure shock. This loading would open up a hole in the tank wall many times larger than the hole produced by the LOX not being in contact with the wall. Further, the blast from the charge should add considerably to the destructive capability of the system. It should be noted, that at a very high altitude, there may be little, if any, air shock, yet fast-moving explosion-gas products probably would be capable of inflicting considerable damage. On entering the LOX tank, it would be desirable for the jet to pass as closely to the wall as possible in order to exert enough force on the wall to produce rupture. This would extend along a line for a distance of several feet.

If a similar shaped charge jet were used to attack the liquid H₂ tank from a position within the IT, the jet would enter the tank in an area not backed with liquid (Fig. 4-4). This would be advantageous for the blast, but not for the jet action. The blast would probably do considerable damage, venting the liquid H₂ tank at its top and blowing a large hole into the outer wall of the ET in the area of the IT.

As to the jet, the distance between the shaped charge position and the surface of the liquid H₂ will vary from a few feet in a full tank, to about 90 feet after 450 seconds of flight. If the jet is required to travel long distances, serious problems arise. Aiming the jet would be critical, since the jet should pass as closely to the wall as practical. It should also travel nearly parallel to the axis of the ET to avoid striking the wall or moving too far inward to be effective. These conditions would place stringent requirements on both manufacture and alignment of the shaped charge system. In addition, the jet elements tend to tumble with long standoffs and become misaligned, thus greatly reducing penetration in the liquid H₂.

There are little, if any, experimental data on the effects of jets impacting liquid hydrogen or oxygen. However, one can deduce reasonably well what will happen in these liquids by relating to the already known effects of jets penetrating water.

Typically, conically shaped charge jets penetrating water will generate lateral shocks which initially have very high pressures. If the tip of the jet is sharp, the duration of the high-level shock will be very short. Rarefactions from around the periphery of the contact area quickly relieve the high initial pressure. A blunt contact surface, with adequate length along the jet axis, will give a somewhat longer lasting pulse. But, in any case, lateral relief of the shock is rapid. It should be noted here that the pressure does not fall to zero at the tip immediately after impact, since a subsonic flow field exists between the shock front and the tip of the jet. The stream-lines coincident with the axis of the jet are brought to rest at the jet surface, creating an area of stagnation. Assuming that both target and jet are fluid, incompressible, and without strength, the stagnation pressure, P_s, is

$$P_s = 1/2 \rho_t U_p^2 \quad (4-1)$$

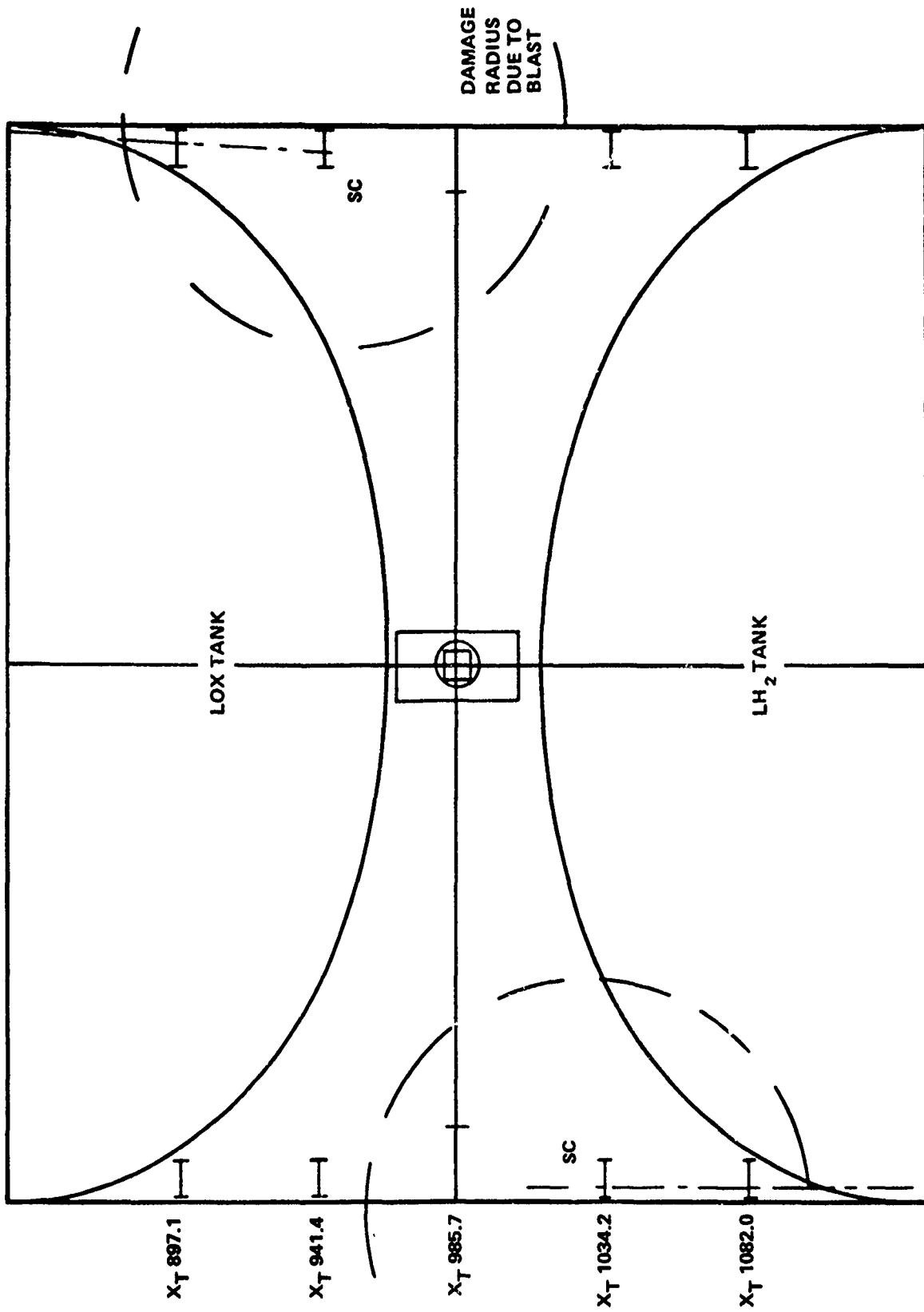


FIGURE 4-3 LOCATION OF DESTRUCT SHAPED CHARGES AND DAMAGE RADII

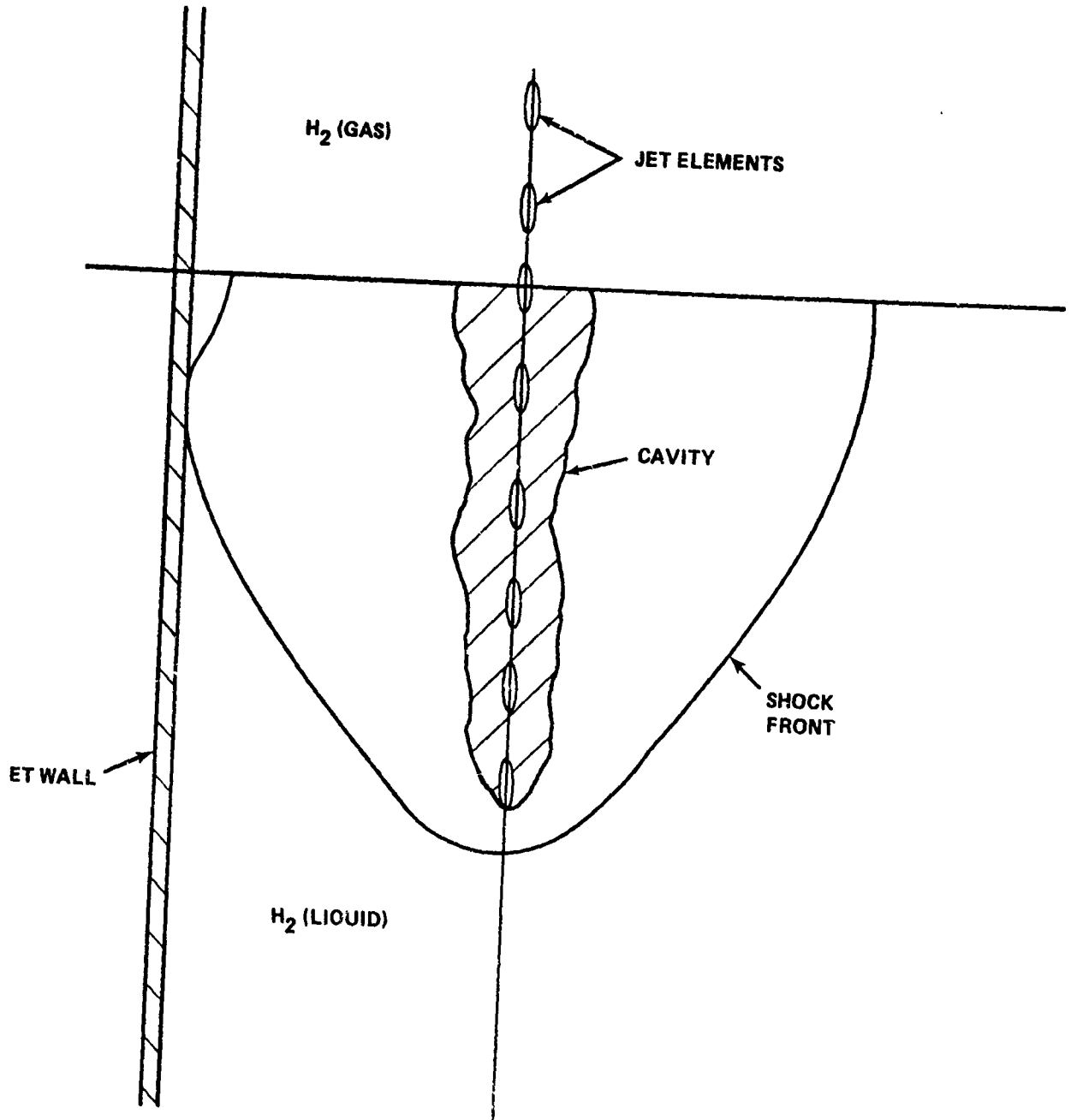


FIGURE 4-4 JET PENETRATION INTO LH₂ TANK

where ρ_t is the density of the target material and U_p is the penetration velocity. The penetration velocity is defined as the rate at which the eroding tip of the jet moves through the target. Penetration will continue until the entire jet is consumed. The relationship between U_p and the velocity of the jet in air, U_a , can be found by applying the Bernoulli equation. The continuity of pressure along the axis at the jet-target interface requires that

$$\rho_j (U_a - U_p)^2 = \rho_t U_p^2 \quad (4-2)$$

where ρ_j is the projectile (or jet) density. Thus,

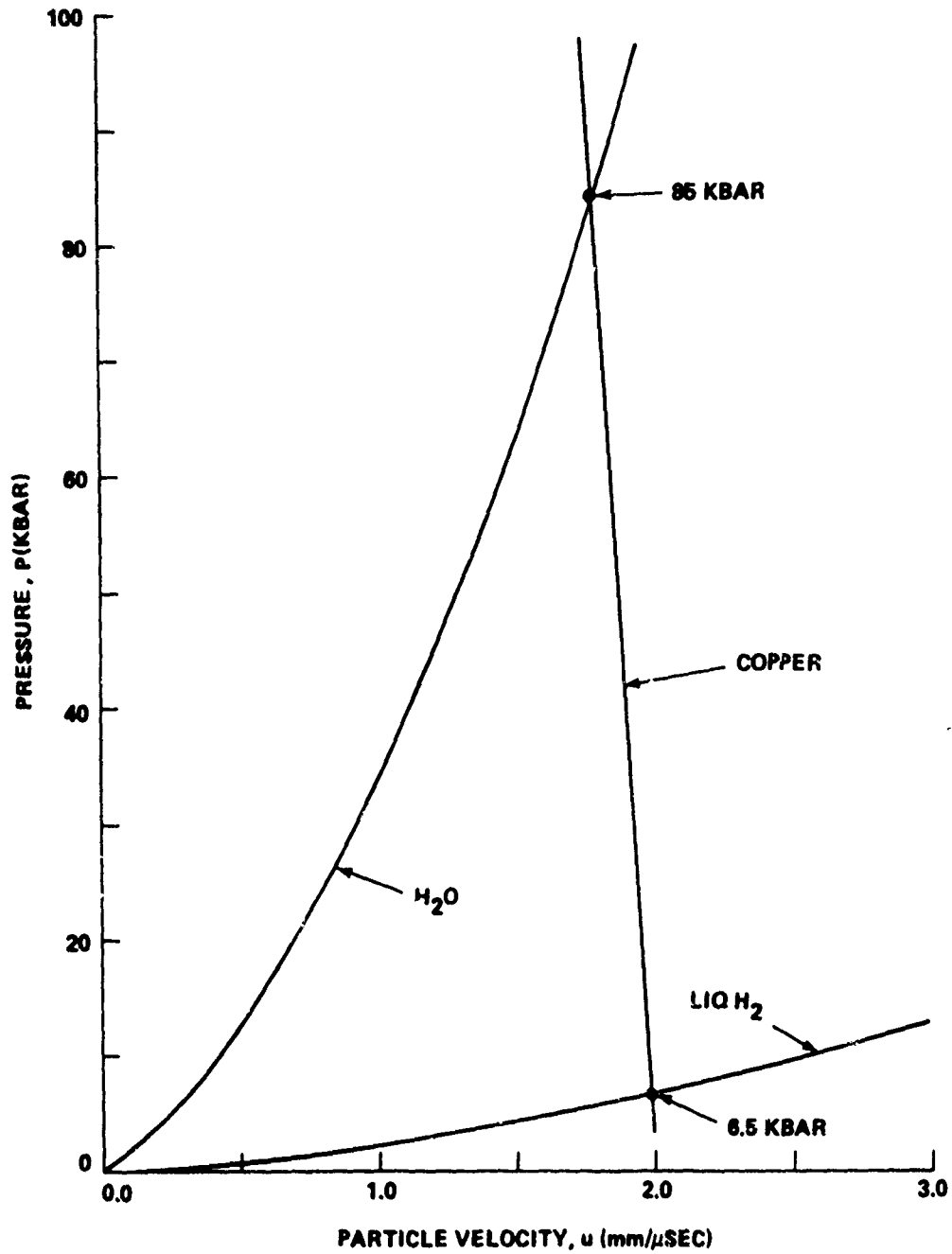
$$U_p = \frac{U_j}{1 + (\rho_t/\rho_j)^{1/2}} \quad (4-3)$$

The shock properties of water (the target) are well known. By measuring the shock wave velocity produced by the jet, the pressure at the shock front can be determined.

The pressure produced in liquid H_2 can be obtained by appropriate use of the shock Hugoniot relations between the jet material, water, and liquid H_2 . Fortunately, some data are available for liquid H_2 .¹ The pressure P versus particle velocity u curves for water and liquid hydrogen are shown in Figure 4-5. To illustrate the use of such curves, a "reflected" curve for copper is included. The curve corresponds to an arbitrarily chosen velocity of 2.0 mm/ μ sec. From the intersection points it is seen that the pressure produced in water is 85 kbar. But it is only 6.5 kbar in liquid H_2 , density = 0.071 g/cm³. For a jet moving at 5 mm/ μ sec, the initial pressure in liquid H_2 would be 30 kbar. (Actually, it would make little difference in the pressure generated if the jet were composed of aluminum rather than copper, since their densities are two orders of magnitude higher than the density of liquid H_2 .) Using Equation 4-3, it is seen that a copper jet moving at 2.0 mm/ μ sec in air will penetrate at a velocity of 1.50 mm/ μ sec in water and 1.82 mm/ μ sec in liquid H_2 . By using Equation 4-1, the stagnation pressure is found to be 7.5 kbar in water and 0.07 kbar in liquid H_2 .

Our observations of jets penetrating water have shown that the lateral shock-wave velocity falls very rapidly to a nearly constant velocity in a distance of 2 to 3 charge radii. Typically, the velocities correspond to pressures of 1 to 2 kbar for copper or aluminum jets. A comparison of the pressure versus particle velocity curves for water and liquid H_2 , Figure 4-5 shows that the peak pressures generated in the two media by the impact of a 2 mm/ μ sec copper jet would be in a ratio of ~13:1. Thus, the pressures generated in liquid H_2 would be only 0.05 to 0.10 kbar at a distance of 2 to 3 charge radii from the path of a jet. The pressures generated in LOX would be about the same as those generated in water. The density of LOX is 1.1 g/cm³.

¹van Thiel, M., Ross, M., Hoed, B.L., Mitchell, A.C., Gust, W.H., D'Addario, M.J., and Keeler, R.N., Physical Review Letters, Vol. 31, 1973, p. 979.



NOTE: FOR A JET MOVING AT 5000 M/SEC IN LIQUID HYDROGEN THE PEAK INITIAL PRESSURE WOULD BE 30 KBAR.

FIGURE 4-5 METHOD OF OBTAINING INITIAL PEAK PRESSURE GENERATED IN WATER AND LIQUID HYDROGEN BY A COPPER JET FRAGMENT MOVING AT 2000 M/SEC

The distance the jet will penetrate, X_t , in liquid H_2 or LOX can be calculated from the expression

$$X_t = \ell (\rho_j / \rho_t)^{1/2}$$

where ℓ is the length of the jet. From the expression, it can be shown that the jet will penetrate 3.8 times farther in liquid H_2 than it will in water. It will penetrate 0.94 times as far in LOX as it will in water.

Experiments have shown that the maximum penetration in water by the jet, formed from a 42-degree copper cone, is about 18 to 20 charge diameters. Thus, for a 6-inch diameter charge one can expect a jet penetration of 33 to 38 feet in liquid H_2 , and 8 to 10 feet in LOX. An aluminum hemispherical liner will give 50 to 60 percent of this penetration. If, however, the jet travels sufficiently far in air (or a low-density medium) before striking the target, the jet will break up into a number of axially aligned segments. For a copper jet from a 42- to 45-degree cone, the number of segments may be 40 to 50. (For aluminum, the number may be about half this figure.) The tip velocity of the jet can be 8 to 9 mm/ μ sec and the tail velocity 2 to 3 mm/ μ sec. The velocity gradient along the jet causes it to stretch until it breaks up into a number of segments. For very long travel distances in air, e.g., 50 charge diameters or more, the elements will become unstable in flight, begin to tumble, and lose their alignment. At 150 charge diameters it has been observed that the dispersion causes a shotgun effect on a steel target.² Needless to say, the result is a greatly reduced penetration.

The impact of each jet element at the bottom of a cavity in a liquid will produce a shockwave which rapidly decays in strength. The shocklets are distinctly seen in framing camera photographs of jets penetrating water.

An appreciable dispersion of jet elements should not occur with the jet system facing the LOX tank, since the liquid oxygen would be in contact with the inner wall of the tank at the point of entry.

EXPLOSIVE COMPOSITIONS. The plastic-bonded composition HNS/Teflon, 90/10, has high thermal stability and is easily fabricated into charges of excellent quality for use in shaped charge destruct configurations. Explosive charges of HNS/Teflon were used by NASA in its Apollo program to generate a source of seismic energy by detonation in lunar exploration.³

Table 4-1 lists physical detonation and sensitivity properties of HNS/Teflon, 90/10. Table 4-2 gives thermal cycling and shock vibrational qualification test results for a 6-pound, HNS/Teflon, 90/10, lunar charge assembly.

²Drimmer, B.E., "Penetration of Steel Targets at Long Standoffs by Steel-Cone-Lined Shaped Charges," NOLR 1145, Aug 1950.

³Kilmer, E.E., "Plastic Bonded, Thermally Stable Explosive for an Apollo Experiment," Journal of Spacecraft and Rockets, Vol. 10, No. 7, 1973, p. 463.

TABLE 4-1 DESTRUCT CHARGE SPECIFICATIONS

Explosive	HNS/Teflon, 90/10
Density (g/cm ³)	1.68
Specific heat (cal/cm/°C)	0.25
Thermal Conductivity (cal/cm/sec - °C)	5.802×10^{-4}
Melting Point (°C)	318
Detonation Velocity (m/sec)	6900
50% Initiation Pressure (kbar)	21.9
Steel Dent Output (MIIS)	43

TABLE 4-2 HNS/TEFLON, 90/10, QUALIFICATION TEST RESULTS (6-LB CHARGE)

Test*	Results
Sinusoidal Vibration (Low and high frequency)	Visual and Radiographic Inspection: No change.
Random Vibration and Boost Simulation	No performance degradation.
Thermal Cycling: -100°F, 0-3 h 250°F, 6.5-11.5 h 75°F (or ambient) 18-24 h	} Radial cracks completely across charge. } Detonation velocity unchanged.
Shock (Sawtooth shape, peak 15g, 11 ms duration)	

*NWL Technical Note TN-7/7-71, Environmental Test Procedures for Prototype Explosive Charge Assemblies for Lunar Seismic Experiments. NWL Technical Note TN-7/8-72, Design Limit Vibration and Design Limit Shock Test Procedures for Qualification Explosive Charge Assembly for Lunar Seismic Experiments. NWL Technical Note TN-7/12-72, Thermal Cycling Test Procedures for Qualification Explosive Charge Assembly.

The detonation velocity of HNS/Teflon, 90/10, is 6,900 m/sec at a loading density of 1.68 g/cm³. Its detonation pressure is 200 kbars which would make HNS/Teflon, 90/10, a more effective shaped charge explosive than TNT (~190 kbar). HNS/Teflon, 90/10, is also more sensitive. Its 50-percent initiation pressure is 21.9 kbars as compared to 40 kbars for cast TNT. The thermal stability of HNS/Teflon, 90/10, (melting point = 318°C) in a space shuttle environment offers justification for its use as the destruct charge composition despite its high cost (~\$50/pound).

LINEAR-SHAPED CHARGE DESTRUCT CONFIGURATIONS

Linear-shaped charges (LSC's) consist of an inverted V-shaped explosive load on top of a wedge-type metal liner of a fixed length (Figure 4-6 shows end and side views of an LSC). The fragment spray produced by an LSC is in the form of a thin sheet. When detonated from one end, an LSC produces a cutting effect in a metal target which, due to the nature of the fragment spray, extends beyond the charge length or width.

The principal parameters affecting the cutting ability of an LSC are:

1. Liner: material, thickness, included angle, dimensions, and shape.
2. Explosive: kind, amount, shape, and density.
3. Standoff from the target.
4. Target thickness and toughness.
5. Type of initiation.

The liner materials considered are aluminum and copper. Because of its lower density, aluminum forms a lighter LSC. For best performance, the thickness of copper and aluminum liners should be ~2 and ~6 percent, respectively, of the wedge (diameter) base. The included angle of an LSC is typically 90 degrees. Liners of greater included apex angle, e.g., 120 degrees, are used in special cases.

While a variety of explosives are used in an LSC, the high temperature environment of the Space Shuttle excludes the use of low-melting TNT-matrix explosives. RDX or HNS is the recommended explosive fill. RDX, because of its higher detonation pressure, >290 kbars compared to ~200 kbars for HNS at a loading density of 1.6 g/cm³, produces a deeper cut than HNS. HNS has much greater thermal stability.

An air standoff separating the LSC from the target is required for good cutting (Fig. 4-6). Optimum cutting for a given LSC explosive core load is obtained at a standoff distance nearly a mirror image of the height of the liner. Also, the optimum standoff varies with liner material. Because of its lower ductility, aluminum requires a longer standoff than copper to obtain equal penetration.

Materials other than metal are easily cut by an LSC. Foam materials or insulation placed within the air space standoff have only a small effect on the jet penetration. The target material, thickness, hardness, and density are parameters which must be considered in selecting or designing an LSC for particular applications. A comparison can be made of the effect of an LSC on different materials. Penetration or the LSC cutting ability is an inverse function of the square root of the materials' densities.

An LSC is generally initiated by a single detonator through a length of confined detonating fuse (CDF) connected at one end of the LSC. For certain applications such as annular destruct actions, curvilinear or flexible shaped charges (FLSC) may be used. In these cases, if dual end initiation is used, the detonation waves interact with a high-pressure (Mach) shockwave occurring at the point of interaction. Penetration of cutting will be increased at this point.

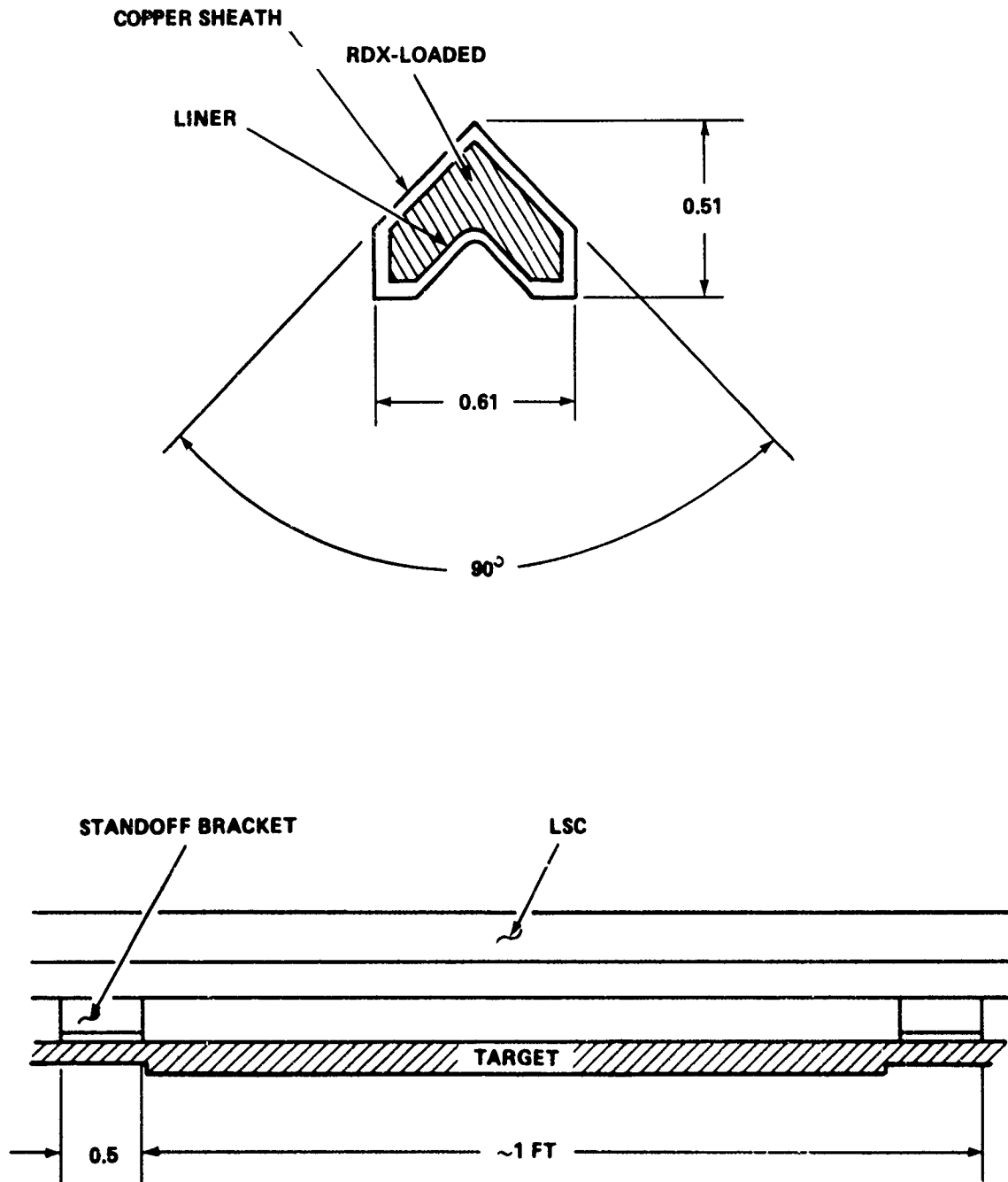


FIGURE 4-6 500 GR/FT-RDX-LOADED, CU-SHEATHED, LINEAR-SHAPED CHARGE

One particular advantage obtained by using linear-shaped charges as the IT destruct device is that LH₂ and LO₂ mixing may be minimized. A destruct system using LSC may include the following arrangements:

1. A 100-grain core load, single LSC of 90-degree apex arranged as a "Figure 8" may be located in the gore segments.

2. A curvilinear LSC of 120-degree apex, 200-grain/foot core load could be arranged within the crotch of the lower dome of the LOX tank and the IT frame. The LSC would be mounted so that the cutting action of the jet would be directed over a ~180-degree arc around the IT wall.

A similar LSC could also be mounted into the LH₂ tank/IT wall crotch. In this case, the cut would be made against the IT wall in a sector opposite the cut at the LOX tank/IT wall interface.

3. Two FLSC's would be arranged to cut a ~180-degree arc in the domes of the LH₂ and LOX tanks. The cutting action would be directed inward. These charges would be positioned back-to-back with the configurations which attack the IT walls.

4. An FLSC configuration using a 100-grain/foot RDX core load is wrapped around the SRB beam to sever it, and thereby increases SRB destruct effects on the IT.

Table 4-3 lists a description of these configurations, their target areas, locations, and explosive weights.

The above LSC's will cut large openings into the LH₂ and LOX tank domes and the IT wall. The dome and wall material will hinge under the weight of the LOX, the ullage pressure in the tanks and the force of the escaping fuels. LOX and LH₂ mixing will be minimized since the LSC will cut opposite sides of the tanks. By cutting the IT walls, any confined mixing of LH₂ and LOX will be minimized. Confinement would otherwise increase the blast potential from the explosive mixture.

The jet action from a conically or hemispherically lined shaped charge fired through the LH₂ tank dome and aimed parallel to the barrel of the LH₂ tank would assist in rupturing the LH₂ tank. This charge could be used in conjunction with the LSC configurations described above. The extent of wall rupture would depend on the level of LH₂ in the tank.

EXPLOSIVE PENETRATOR

INTRODUCTION. As originally stated, the Space Shuttle destruct mechanism was constrained to be entirely within the IT region. To reduce the explosive hazard of the mixing of hydrogen and oxygen, both tanks should not be ruptured near each other, especially if the holes feed into the confined space of the IT region. This consideration together with the fact that the LH₂ tank would empty faster through a hole in the lower end of the tank (where liquid would be forced out, while gas would be primarily vented at the top) encouraged the search for a way to vent the bottom of the tank by a mechanism housed at the top of the tank in the IT. A possible solution to the problem is the explosive penetrator.

TABLE 4-3 LSC DESTRUCT CONFIGURATIONS FOR INTERTANK OPTIONS

Option	LSC Configuration	Target Area	Location	Explosive Weight (lb)
1	Figure 8 90° Apex 100 gr/ft	LO ₂ Tank Valve LH ₂ Tank Vent	Gore Segment 941.4, - Y + Z (-Z + X) 941.4, - Y + Z (-Z + X) 1034.2, - Y - Z (-Z + Y)	0.64
2	Curvilinear 120° Apex In 200 gr/ft	LO ₂ IT Frame LH ₂ IT Frame LO ₂ /LH ₂ /IT Interfaces	LO ₂ : 852.8 LH ₂ : 1129.9 All Quadrants	10.0
3	Curvilinear 120° Apex Out 200 gr/ft	LO ₂ /LH ₂ Domes	Same as No. 2	2.46
4	SRB Umbilical Plate 100 gr/ft	SRB/ET	Beam: 985.7 - Y + Y	0.34

The explosive penetrator consists of an explosive projectile that is launched by a disposable gun. The projectile penetrates the tank in the IT region where the wall is thin (leaving only a small hole) and then proceeds in the tank to the aft end. A timing fuse would be set so that the explosive charge would explode within the tank near the end. The charge would be large enough to rupture the tank, even if the volume within which the charge exploded were occupied by gas and not liquid.

To demonstrate feasibility, a preliminary design was carried out. The following factors were considered:

1. Size of explosive charge needed in worst case.
2. Loss of velocity incurred in penetrating tank wall.
3. Velocity slowdown due to fluid drag during flight in LH₂.
4. Additional weight of projectile and launcher tube beyond that of explosive.
5. Stability against tumbling, when entering the tank, when passing through a gas-liquid interface and when flying through a liquid.

Since the explosive charge needed to rupture the tank can only be estimated, designs were carried out with two sizes of explosive charge. It was felt that 10 and 100 pounds of TNT should bracket the actual quantity needed.

The concept is simple, and the preliminary design shows it to be practical. In subsequent sections the important design factors are considered in detail.

CHARGE SIZE REQUIRED. The tank would be ruptured by the shock loading caused by the explosive charge. In the worst case, the charge would be on the tank axis away from the end. If the charge were closer to the wall, the shock loading would be greater and the required charge less. Likewise, if the charge were exploded in an empty tank, the shock loading would be reduced by the poor coupling between the charge and the gas. An increased charge weight would be needed to compensate for it. Since the tank is generally not empty, the worst case is not realistic. How unrealistic it is, is not easy to determine. The shock load needed to rupture the tank is also difficult to define accurately, because it has stiffeners and ribs that complicate calculations. As a result of estimates, it was felt that a worst-case charge would be between 10 and 100 pounds of TNT. If the tank were full, 10 pounds of TNT would be sufficient to rupture it.

VELOCITY LOSS CAUSED BY PUNCHING TANK. The work required to punch through the tank wall can be estimated. The shear strength of the wall material acts on the circumference of the projectile nose for a distance of travel equal to the thickness of the tank wall. Using typical values for wall thickness (0.09 inch), shear strength (20 Kpsi), and projectile diameter (4 inches), one finds that if the velocity is 400 ft/sec, even the slightest projectile would be slowed down by less than 10 ft/sec, which is certainly negligible.

DRAG SLOWDOWN. Over a broad range of conditions, the drag of a body can be characterized by a drag coefficient. In particular,

$$D = \frac{1}{2} C_D \rho_L V^2 A$$

where D is the drag force, ρ_L is the ambient density, V is the instantaneous velocity, A is the frontal area, and C_D is the drag coefficient. By using Newton's law, the velocity, position, and elapsed time during the flight can be determined. The deceleration and drag are related as follows:

$$\rho_p AL \, dV/dt = -D$$

where ρ_p is the projectile density, L is an effective length (so that $\rho_p AL =$ projectile mass) and t is the time. By combining the above equations and noting that

$$dV/dt = (dV/dx)(dx/dt) = \frac{1}{2} (dV^2/dx)$$

it is possible to deduce that

$$dV^2/dx = -(C_D \rho_L / L \rho_p)$$

Since the right-hand side of this equation is a constant, it can be easily solved to obtain

$$\ln (V_0/V_f) = C_D (\rho_L / \rho_p) (\Delta x / L)$$

where V_0 is the initial velocity, V_f is the final velocity, and Δx is the length of the flight path. From this equation it can be seen that for a fixed geometry

$(\Delta x/L)$ it is the velocity ratio (V_0/V_f) and not the magnitude of the velocity that matters. The identity $dx/dt = V$ can be used in conjunction with the relation between V and x , that was just found, to solve for the flight time, Δt . The result is

$$(C_D \rho_L V_0/2 \rho_P L) \Delta t = (V_0/V_f) - 1$$

The time-of-flight equation is used to ensure that the projectile cannot reach the end of the tank, even if it should encounter no resistance during the flight.

STABILITY. The projectile can be guided by the launch tube during the penetration of the tank wall so that it will not be set off-course at this point. If this is not practical, then simply firing the launcher perpendicularly to the tank skin, in an area where there are no stiffeners, should ensure that the projectile travels into the intended direction.

If a sharp pointed projectile enters a liquid at a shallow angle, there is a tendency to "skip" and be deflected off-course. This problem has been studied in connection with air-launched torpedoes. By blunting the nose, this tendency can be largely eliminated. Although the drag is larger, it is still acceptable.

To ensure stability during the flight, it is necessary to have the weight distributed as far forward as possible. Since the nose must be hardened to punch the tank wall, this condition will be easily met. Small stabilizing fins would also be used.

TYPICAL DESIGN. As mentioned in "Charge Size Required," p. 4-16, the weight of TNT necessary to rupture the tank would be in the 10- to 100-pound range. The exact figure depends upon the degree to which the explosive is surrounded by liquid at the time of detonation.

The nose of the projectile would be weighted for stability, and to harden it in order to punch the tank. The casing would be a larger percentage of the total package weight for the smaller projectile, but would not amount to more than 20 percent of the total.

As stated earlier, the percentage slowdown in velocity is independent of the initial velocity. Even for modest velocities, the slowdown caused by punching the tank is negligible. In view of these facts, a modest launch velocity is sufficient. This means that the "gun" can actually be a thin-walled tube. A launch velocity of 400 ft/sec was arbitrarily picked. A preliminary design of the launcher was based upon a simplified picture of the launch process. It was assumed that a constant pressure acts on the base of the projectile for a distance equal to the length of the projectile. The pressure necessary to achieve 400 ft/sec was calculated to be about 2000 psi. With this pressure, the wall thickness of the launch tube and the necessary powder charge can be estimated. The result of this calculation shows that the launcher weight would be on the order of 30 percent of the projectile charge weight.

Based upon a launch velocity of 400 ft/sec and a tank length, the flight time would be somewhat less than 1/4 seconds to prevent the projectile from exiting the tank. A drag coefficient C_D , based upon frontal area, would not exceed one, even for the blunt shapes used in this design. Calculations show that with this drag and

the 1/4-second flight time, the velocity at the end of the flight will still be on the order of 250 ft/sec. The projectile will have traversed about 75 percent of the tank length, even if its flight is entirely in the LH₂.

CONCLUSIONS. If it is necessary to confine all destruct equipment to the IT region, then this scheme appears to be a practical method for effectively producing a large hole in the aft end of the LH₂ tank as demanded by the minimum mixing requirement. A preliminary design shows that the additional weight of casing and launcher probably would not exceed the weight of the charge itself. Charges on the order of 10 to 100 pounds of TNT would probably be necessary. It may require some experimentation to fix the minimum charge that could be trusted to rupture a nearly empty tank.

OTHER SYSTEMS

Only brief note is made of three other destruct systems confined to the IT that were explored. One utilized the Misznay-Schardin flying plate technique to produce damage. A second used flat, pancake-like charges. The third called for a delay time between the rupture of the LOX and LH₂ tanks so as to minimize the extent of mixing.

In the Misznay-Schardin technique, a solid metal disc is driven at high velocity by an explosive charge. The disc will easily penetrate the LOX and LH₂ domes and, in conjunction with the high hydrodynamic pressures it generates in the liquid O₂ and H₂, further structural damage would occur to the tanks. This system was discarded from further consideration because of the advanced development required for its design. A closely controlled propagation of the detonation wave through the explosive is required to drive the plate without breaking it up into small, ineffective fragments. Additionally, the long distances the plate has to travel at late times into flight before it encounters liquid H₂, makes it unlikely that the plate will maintain its flat impact on the liquid H₂. Consequently, it will lose its effectiveness.

The use of flat, flexible sheets of explosive glued to the LOX and LH₂ domes and the IT wall was considered briefly, but no particular advantage was offered by these pancake-like charges. LSC's could do the job as effectively and with less explosive weight.

In the third system, the delay system, the time between the rupture of the LOX and LH₂ tanks would be spaced some seconds apart. In this concept, upon receiving the destruct signal, the IT wall would be severed by an LSC, aerodynamic forces would separate the LOX and LH₂ tanks and put them into different trajectories, and then, at some selected delay time built into the explosive fusing system of the destruct ordnance attached to each tank, the LOX and LH₂ tank domes would be ruptured by LSC's. The apparent complexities of this system negated its further consideration.

DISCUSSION AND COMPARISONS OF IT-SITED DESTRUCT SYSTEMS

The basic explosive ordnance items considered for the destruct of the LH₂ and LOX tanks and the IT walls are described in the preceding sections of this chapter. The explosive principles involved in their functioning are also described there and in the appendices. These preceding sections indicate the location of the ordnance in the IT and also give the extent of the damage to be attained.

As could be expected, sites and arrangements other than those described could be selected for effective destruct actions. For instance, hemispherically or conically shaped charges could be directed at the LOX and LH₂ domes so that the jets penetrate and follow a near tangent path within the domes. The penetrations and the large hydrodynamic jet-induced shock wave forces in the LOX would produce a large tear in the LOX dome. Penetrations and a much smaller rip would be produced in the nonliquid-backed LH₂ dome.

As another example of explosive charge options available, the LSC's could be made to sever the domes and IT wall in almost any length cut desired, from a short length to completely around the structures. A 360-degree cut hardly seems necessary; a 180-degree cut is discussed in "Linear-Shaped Charge Destruct Configurations," p. 4-12, but a 90- or even 45-degree cut may be adequate depending on the combinations of ordnance types and sites chosen.

Figure 2-2 (three sheets, p. 2-8 thru 2-10) illustrates and summarizes types and locations considered as options for IT-located destruct ordnance. The damage areas are also qualitatively shown.

As discussed in Chapter 1, the merits of any particular ordnance destruct system can be compared on the basis of the effectiveness of the system in producing structural failure of the ET, providing rapid dispersal of the LOX and LH₂, and minimizing mixing between the dumped LOX and LH₂ (thus minimizing potential blast yield). The system can further be compared in its effectiveness in keeping the weight of the ordnance package low, providing commonality of ordnance types, holding anticipated development time to a minimum, and selecting locations for the ordnance which are compatible with the IT structural design and environment. Cost of the ordnance package per flight and for development, verification, and demonstration are important factors to be considered in the selection of any particular system; however, they were not in the purview of this task. Nevertheless, costs were treated qualitatively in some cases.

The following paragraphs present the major advantages and disadvantages of the options covered in the earlier sections of this chapter. Where deemed necessary, additional explanatory comments are provided.

Single Large Bare Charge. Advantages: (1) One large charge, centrally initiated and centrally located in the IT, produces omni-directional explosion forces which effectively perforate the IT walls and the LOX and LH₂ tank domes and sever the SRB beam (severing the beam enhances the ET destruct resulting from SRB destruct actions). (2) Little development time and cost are required; the explosive and damage principles involved in this option are well in hand.

Disadvantages: (1) A large charge weight (approximately 390 pounds), is required to produce the necessary damage at all altitudes of concern. (2) The cost of the charge is high because of the large quantity of explosive required. If TATB explosive is used, the cost per flight is about \$6,000. If the explosive is HNS, an explosive with better thermal properties, the cost is about \$24,000. (These costs include estimated amortized development costs.) (3) There is a high probability of mixing of the LOX and LH₂ in the LH₂ tank and the IT producing a potentially large blast yield.

Small Bare Charges. Advantages: (1) Two small charges weighing about 20 pounds each placed in the crotch between the IT walls and LOX and LH₂ domes would produce 4- to 5-foot diameter holes in the IT walls and LH₂ dome with a somewhat smaller hole in the LOX dome. (2) The cost and development time should be relatively small.

Disadvantages: (1) There is limited working space in the crotch locations to position the charges. (2) A large degree of LOX and LH₂ mixing can be expected in the IT and LH₂ tank.

Focused Blast Charge. Advantage: (1) One centrally located charge can defeat the LH₂ and LOX domes and the IT walls.

Disadvantages: (1) The charge weight required is about 200 pounds. While this is about half the weight required for the centrally located bare charge with omnidirectional blast, it is still large. Hence, (2) costs are high, about \$6,000 per charge per flight if TATB is the explosive of choice and about \$15,000 if HNS is the explosive. (3) Mixing of the LH₂ and LOX remains a problem.

Cased Charges. Advantages: (1) Case fragments would penetrate and weaken the dome and IT structures enhancing blast produced damage. (2) Only one centrally located charge is required.

Disadvantages: (1) A 300- to 400-pound device is required with about 200 pounds of explosive contained in the steel case. (2) The cost of the device per flight is estimated to be about \$6,000 and \$15,000, depending upon the explosive material (TATB or HNS) used. (3) The case fragments would be a hazard to the orbiter. (4) Mixing of LOX and LH₂ would take place to a large degree.

Continuous Rod Charge. Advantages: (1) One centrally located device would rupture the LOX and LH₂ domes and the IT walls. (2) A relatively small weight of explosive, about 20 pounds, is required in the 70-pound device. (3) Only modest development time would be required since military technology provides the major design principles.

Disadvantages: (1) Mixing of LOX and LH₂ would take place to a large degree. (2) Continuous rod fragments could be a hazard to the orbiter.

Conically Lined Shaped Charges. Advantages: (1) The device weight is 16 pounds with only 10 pounds of explosive. (2) This leads to a low cost per device, about \$5,000 per unit with HNS. (3) The jet produced by this charge in a 6-inch diameter unit can penetrate 22 inches of steel. It would be sufficiently effective for the intended destruct purposes, even after traveling through about 50 feet of air or gas, 35 feet of liquid H₂, or 10 feet of liquid O₂.

Disadvantages: (1) The specifications for manufacturing the charge may be difficult to attain for achieving the required accuracy for the jet trajectory. (2) The jet is most effective for LOX and LH₂ tank destruct when the jet travels through the liquid propellant close to the tank walls. This poses little problem for the LOX tank where in normal flight the LOX is in contact with the lower dome. But, the LH₂ is not in contact with the upper dome, and as the time into flight increases, the LH₂ is farther and farther away from the point of jet penetration, thus reducing the damage possibilities on the LH₂ tank wall.

Hemispherically Shaped Charges. Advantages: (1) The device weight is only 16 pounds with only 10 pounds of HNS. (2) It is easier to fabricate than the conically shaped charge, hence, its cost is less and estimated to be \$4,000. (3) Although it has less penetration capability than the tandem conically shaped charge, it is adequate. (4) More importantly, the jet can be directed more accurately than the conically shaped charge jet.

Disadvantages: (1) As with the conically shaped charge jet, the hemispherically shaped charge jet is less effective in rupturing the LH₂ tank wall as the LH₂ level moves farther and farther from the jet source.

Linear-Shaped Charge. Advantages: (1) Linear-shaped charges are low in weight, about 0.3 to 0.4 pounds per foot with only 100 to 200 grains of explosive per foot. Obviously, the total weight of the LSC's required is determined by the length used in any particular configuration. Since in most of the options discussed, 25 to 50 feet of LSC could be used, the total weight of the ordnance would range between 10 and 20 pounds with at most only about 1-1/2 pounds of explosive being used. (2) LSC's have been qualified by NASA for space mission utilization, thus qualification for use on the Space Shuttle should be relatively easy.

Disadvantages: (1) Considerable difficulty would be encountered in placing the LSC's in the crotch locations called for in some of the options. (2) The severe cold environment in the crotch position forms ice that would negate the air standoff required for effective LSC operations, i.e., the purge N₂ will solidify.

Explosive Penetrator. Advantages: (1) It is the only system which tackles the mixing problem by directing the explosion forces against the lower portions of the LH₂ tank.

Disadvantages: (1) The total system weight is high, requiring about 100 pounds of explosive in the 20-pound case. Additional weight is added by the launcher in the IT and by the propellant required to drive the projectile. (2) The cost of development would be very high since delayed fusing is required for effective operation of the projectile.

Comparing the advantages and disadvantages of the various explosive types and options leads to the selection of two possible ordnance destruct systems for ET destruct. These systems combine the best features of the options studied (but as indicated below, the systems leave much to be desired).

One system utilizes five explosive elements (see Figure 2-3, p. 2-11). The system consists of the following:

1. An LSC in the crotch of the LOX tank to cut up to a 180-degree arc in the LOX dome.
2. A similar LSC in the crotch of the LH₂ tank to cut the LH₂ dome in a sector opposite the LOX tank cut.
3. LSC's located in the crotch areas and back to back with the LSC's cutting the domes. These LSC's are directed at the IT walls.
4. A conically shaped charge to rupture the LH₂ tank wall in the presence of liquid H₂.

5. An LSC wrapped around the SRB beam to break the beam and thus enhance the ET destruct through SRB destruct actions.

This system will assure destruct of the ET. However, it suffers the disadvantages of the individual elements detailed earlier: difficulty of placing LSC's in the crotch areas and assuring conically shaped charge jet alignment with the LH₂ tank wall. The major disadvantage, however, is that LOX and LH₂ mixing will undoubtedly occur to a large degree. An additional disadvantage of this five-element system is that five elements complicate initiation and fusing problems.

The second total system tends to avoid some of these disadvantages. It uses only three elements for ET destruct (see Fig. 2-4, p. 2-12).

1. A conically shaped charge directed at the LOX tank dome and wall.
2. A hemispherically shaped charge directed at the LH₂ tank dome and wall on the side opposite the LOX tank destruct element.
3. A hemispherically shaped charge positioned so that the jet travels parallel and close to the LH₂ tank wall so that upon entering and traveling in the liquid H₂, large shock forces in the LH₂ rupture the nearby wall.

As with the five-element system, the three-element system has obvious shortcomings: mixing of the LOX and LH₂ can still take place to a large degree and there is no commonality of the ordnance items. (The conically shaped charge was selected for LOX tank destruct because of its greater penetration capabilities, the hemispherically shaped charge for the LH₂ tank because of the greater accuracy in jet alignment).

In summary of the destruct systems located in the ET, it is evident that no system adequately meets the considerations deemed important. Destruct is predicted for all devices and systems, but weight, development costs and mixing of LOX and LH₂ are not minimized. These problems, to a large extent are circumvented by the use of ordnance external to the ET as described in the next chapter.

CHAPTER 5

EXPLOSIVE SYSTEM OPTIONS: DEVICES OUTSIDE INTERTANK

INTRODUCTION

A previous report* discusses shaped charge configurations and specifies the trajectories of high-velocity jet fragments which could rip apart the LO₂ tank when explosively propelled from locations within the solid rocket boosters (SRB's).¹ No consideration was given to the more difficult design problem, i.e., shaped charge jet action which could defeat the LH₂ tank. This section describes two options which can defeat both the LOX tank and the LH₂ tank by ordnance located outside these tanks.

HYBRID (HEMISPHERICALLY LINED SHAPED CHARGES) SYSTEM. This system consists of two hemispherically lined shaped charges each loaded with ~10 pounds of heat-resistant explosives, either HNS/Teflon, 90/10, or TATB. One charge is located within the intertank (IT) area and aimed to defeat the LOX tank. A second charge is positioned inside the cross-beam orbiter attachment. This charge is aimed to destruct the lower section of the LH₂ tank.

LINEAR-SHAPED CHARGES. Two copper-sheathed linear-shaped charges with 500- or 750-grain/foot loads of RDX are recommended for positioning within the electrical cable trays outside the LOX and LH₂ tanks. These charges, each weighing ~10 pounds, will accomplish destruct action by severing ~20-foot-long sections of the tank barrels. The ability of linear-shaped charges (LSC's) to sever the LH₂ and LOX tank walls was demonstrated in mock-ups of the ET arrangement.

The design of the above systems, specifications, advantages and disadvantages, tests and analyses, which established LSC's as the preferred ordnance option, are described in the following.

HYBRID SYSTEM

In the preceding chapter it was concluded that jet fragments from a linear-shaped charge and either hemispherically or conically lined shaped charges could rupture the LOX tank and produce rapid LOX dumping. By locating these charges in the intertank, the jet fragments could be directed to rip the bottom dome of the tank. However, if similar charges were directed against the top of the LH₂ tank

*Now published as Phase I of the present report.

¹"Study Report on Space Shuttle Range Safety Command Destruct System Analysis and Verification," by NSWC/WOL for NASA George Marshall Space Flight Center, AL 35812, under NASA-Defense Purchase Request H-13047B of 15 May 1975; 2 Feb 1976.

dome, the tank would be vented only, without dumping the LH₂ during normal flight trajectory. Moreover, the possibility of explosive mixing would be of real concern. A large explosive yield could result if the LOX were dumped into the opened LH₂ tank.

It is therefore necessary to cause the LH₂ tank to fail at a point as far away from the LOX tank as possible. Maximum possible destruct separation of ~100 feet would occur if the aft area of the LH₂ tank were affected. Thus the bottom dome of the LH₂ tank could be ruptured by a charge placed in the crossbeam orbiter attachment. If the LH₂ tank bottom dome were ruptured, the action of gravity, ullage pressure, and other forces would ensure rapid dumping with a minimum of mixing. Design of a "hybrid" system is therefore advantageous. This system uses one shaped charge located in the IT to defeat the LOX tank and a similar shaped charge to rupture the LH₂ tank from a location in the crossbeam orbiter attachment.

LOX TANK DESTRUCT CHARGE. In the hybrid system a hemispherically lined shaped charge of a design described in the previous section (Fig. 4-2) is located on a frame in the IT area. Alternative mounting arrangements for this charge are shown in Figure 5-1. (Table 5-1 lists the weights of components for the two mounting arrangements.) In mounting arrangement A, the charge is aimed forward and attached within ± 45 degrees of the -Z-axis by a bracket which makes an angle of 2.5 degrees to a frame at Station X_T 941.4. A built-in standoff of one charge radius (3 inches) is provided for this charge (Fig. 5-2).

This charge in the alternative arrangement B, has no built-in standoff (Fig. 5-3) and is mounted within a 6-inch-diameter hole cut into the web of the frame at Station X_T 897. The flange makes an angle of 2.5 degrees with the frame, as in arrangement A. In arrangements A and B, the charge is mounted with its center 5.5 and 3.5 inches, respectively, away from the IT wall.

In addition to the mounting alignment, three other factors affect the accuracy of aiming the shaped charge jet. These factors principally arise from fabrication imperfections and are listed below with an estimate of their probable deviation:

1. Variations in wall thickness of the metal liner (± 0.005 in).
2. Tilt of the liner axis relative to the charge axis (± 0.005 in).
3. Initiator misalignment (± 0.005 in).

Based on these considerations it is estimated that the jet may deviate in its propagation in the X-direction, ± 1.5 degrees from a line extending through the central charge axis. This deviation is indicated in Figure 5-1, showing three jet paths with angular displacements, 0° (-1.5° total), 1.5° (nominal), and 3.0° ($+1.5^\circ$ total). The primary shock damage regions listed in Figure 5-1 correspond to the above jet paths. Each penetration path in the LOX has a different length and following the shorter path (3° deviation), the jet will exit the LOX tank wall. (This path length is predicted to be ~30 inches as compared to ~40 inches for the other paths.)

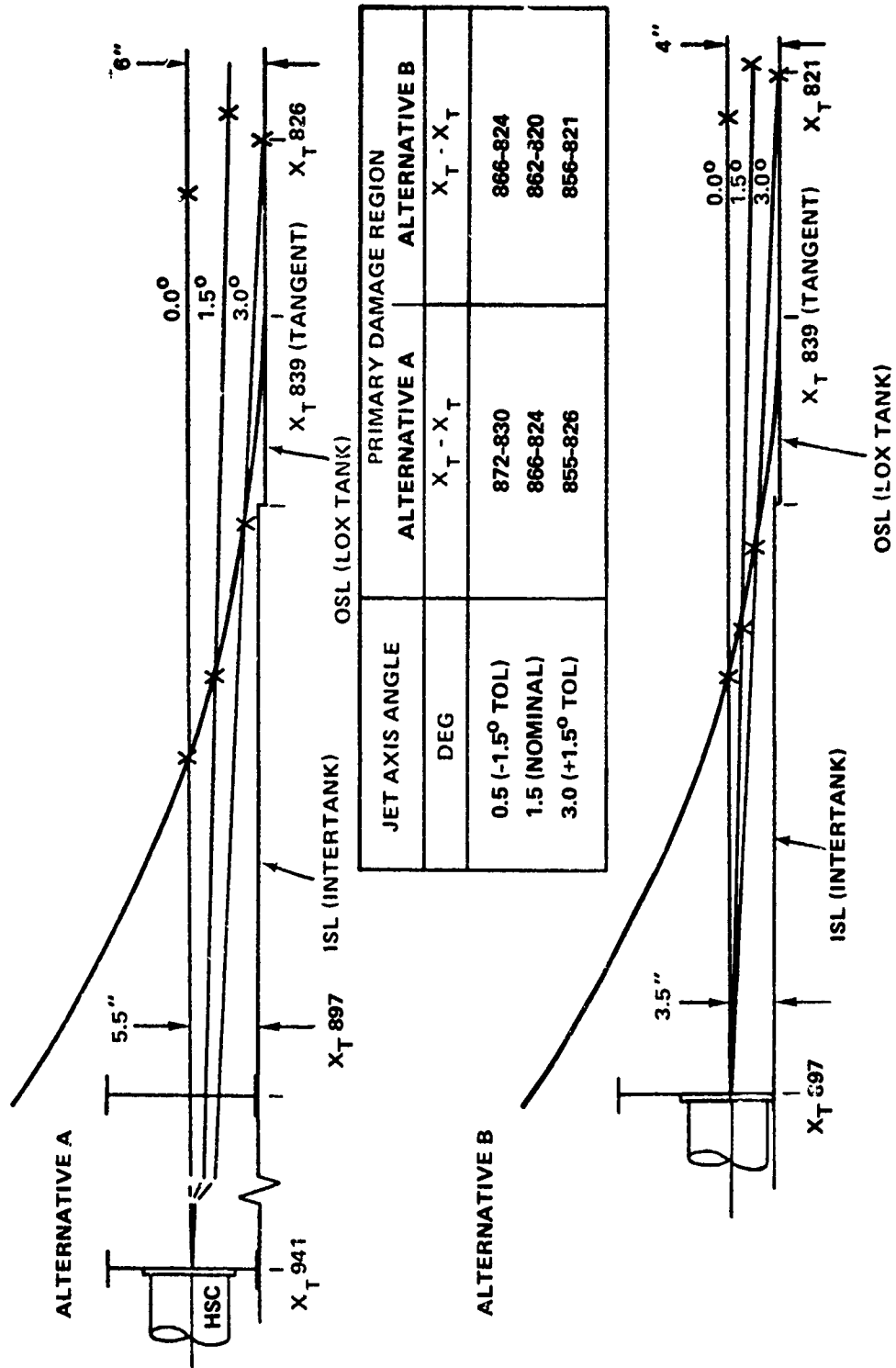


FIGURE 5-1 HEMISPHERICALLY LINED CHARGE PLACEMENT IN INTERTANK

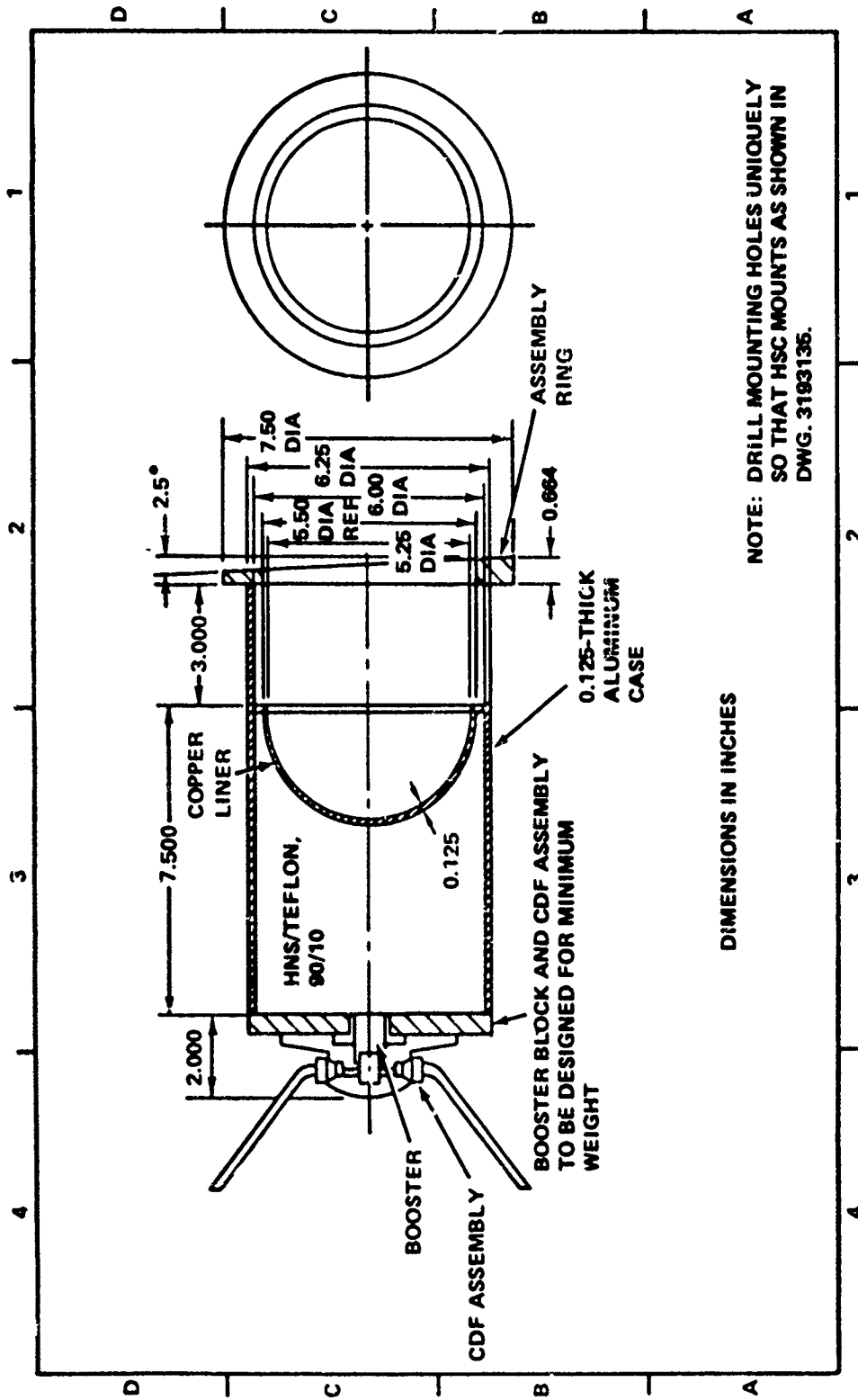


FIGURE 5-2 HEMISPHERICALLY LINED SHAPED CHARGE FOR ALTERNATIVE ARRANGEMENT A

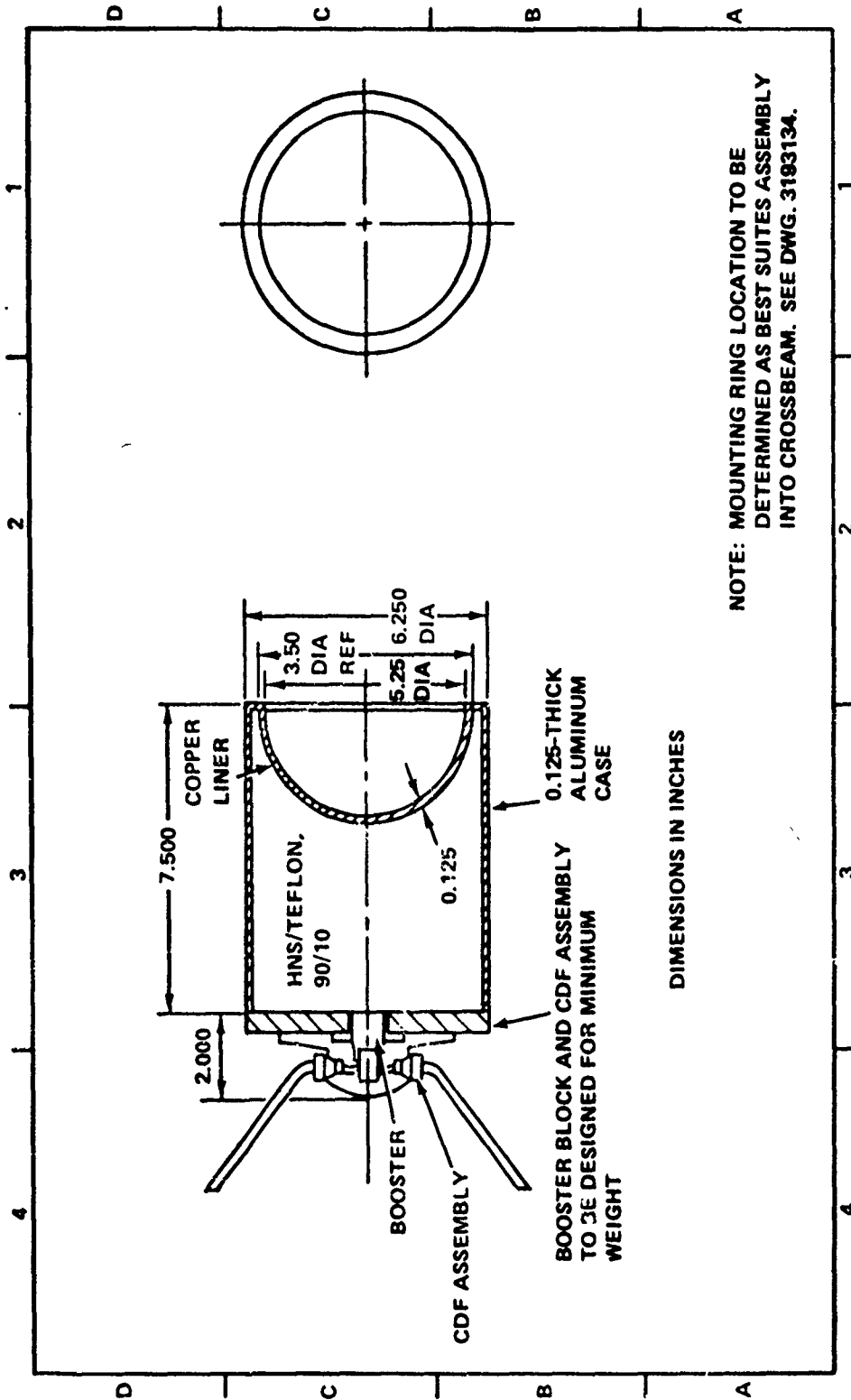


FIGURE 5-3 HEMISPHERICALLY LINED SHAPED CHARGE FOR ALTERNATIVE ARRANGEMENT B

TABLE 5-1 WEIGHTS OF COMPONENTS FOR HEMISPHERICALLY LINED SHAPED CHARGES IN HYBRID SYSTEM

Component	HSC Alternate A Basic (1b)	HSC Alternate B (1b)	HSC Cross-Beam (1b)
Booster Block (0.5 in AL)	1.53	1.53	1.53
Shell (0.125 in AL)	1.80	1.80	1.80
Bulkhead (0.125 in AL)	0.08	0.08	0.08
Liner (0.125 in Cu)	1.82	1.82	1.82
HNS/Teflon	<u>10.00</u>	<u>10.00</u>	<u>10.00</u>
Subtotal	15.23	15.23	15.23
Assembly Ring (AL)	0.80	0.80	-
Standoff Shell (0.125 in AL)	<u>0.72</u>	-	-
Total	16.75	16.03	15.23*

*Mounting bracket not included.

Shock loading produced by the jet propagation in the LOX will rupture the tank wall. The explosion products gases will also load the IT wall and the LOX tank dome. Experiments at simulated high altitude indicate gas loading from the destruct charges will encompass a 5-foot radius surrounding the charge.² This loading helps ensure destruct action. Figure 5-4 outlines the area of the LOX tank dome (heavy line) which should be catastrophically damaged by the action of a destruct charge located at alternative site A.

ET CROSS-BEAM CHARGE FOR LH₂ TANK DESTRUCT. The placement of a hemispherically lined shaped charge designed to rupture the LH₂ from a location in the cross-beam is shown in Figures 5-5 and 5-6. The charge is mounted at a position in the center of the cross-beam ($X_T = 2043$, $Y_T = -48$, $Z_T = +587$). The charge is aimed so that the jet will propagate in the -Z, +X-direction. After entering the LH₂ tank ($X_T = 208$, $Y_T = -48$, $Z_T = 550$) the jet will exit from the tank dome after ~5 feet of propagation within the LH₂. Figure 5-7 shows the region of lower dome damaged by the shock from the jet. Tank rupture and subsequent LH₂ dumping will be enhanced by the impact on the tank of high-velocity fragments and debris propelled by the explosion of the charge in the cross-beam.

²Liddiard, T. P., Naval Surface Weapons Center, unclassified data taken from limited distribution report, 30 June 1971.

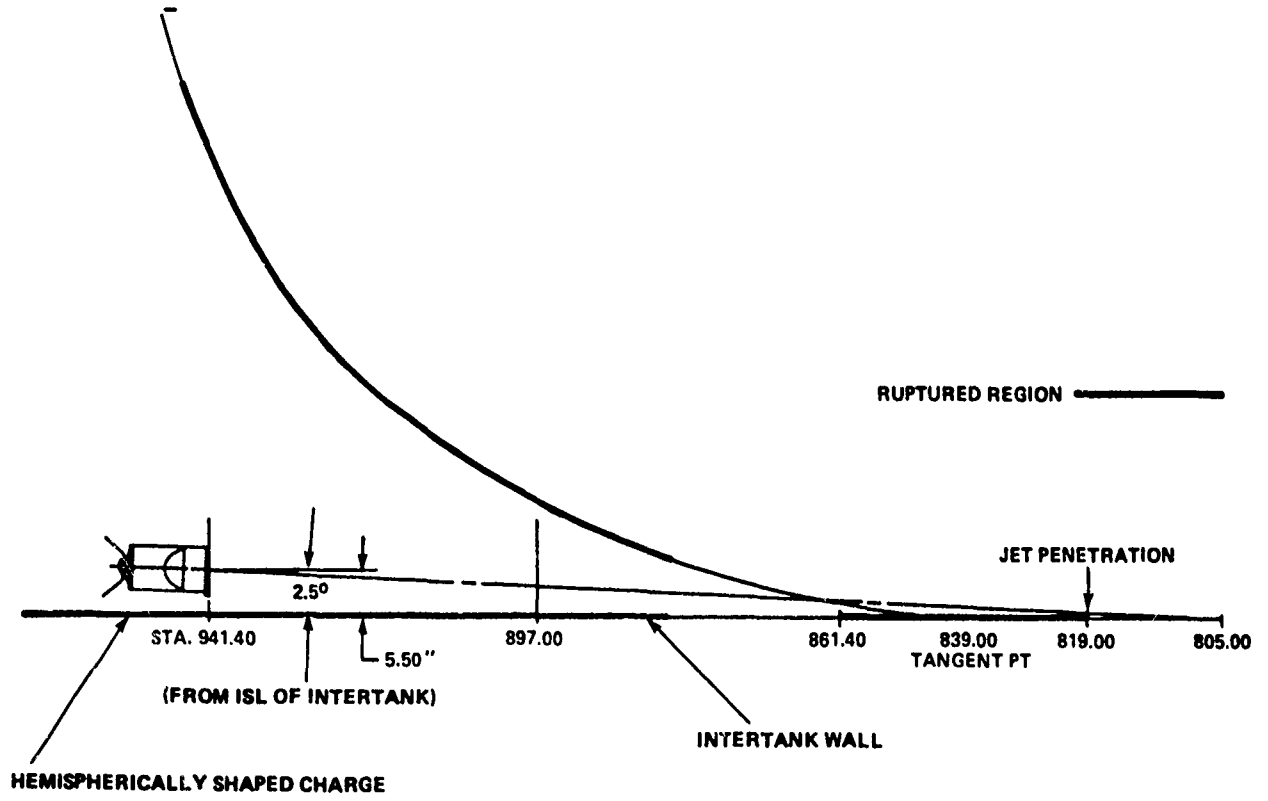


FIGURE 5-4 MOUNTING LOCATION OF CHARGE IN INTERTANK

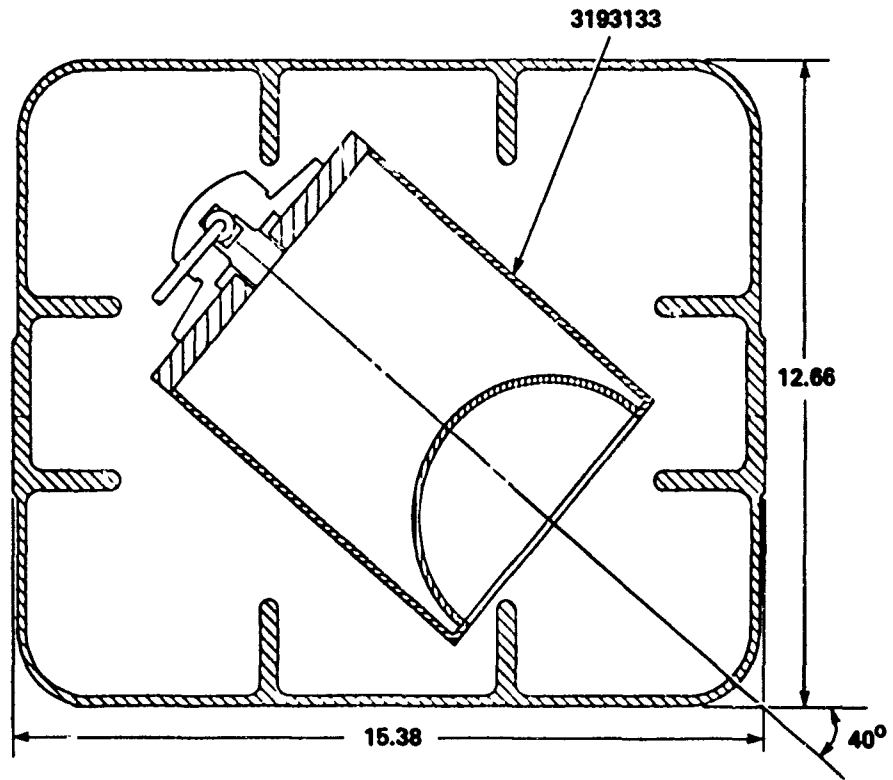


FIGURE 5-5 MOUNTING LOCATION OF CHARGE IN CROSSBEAM

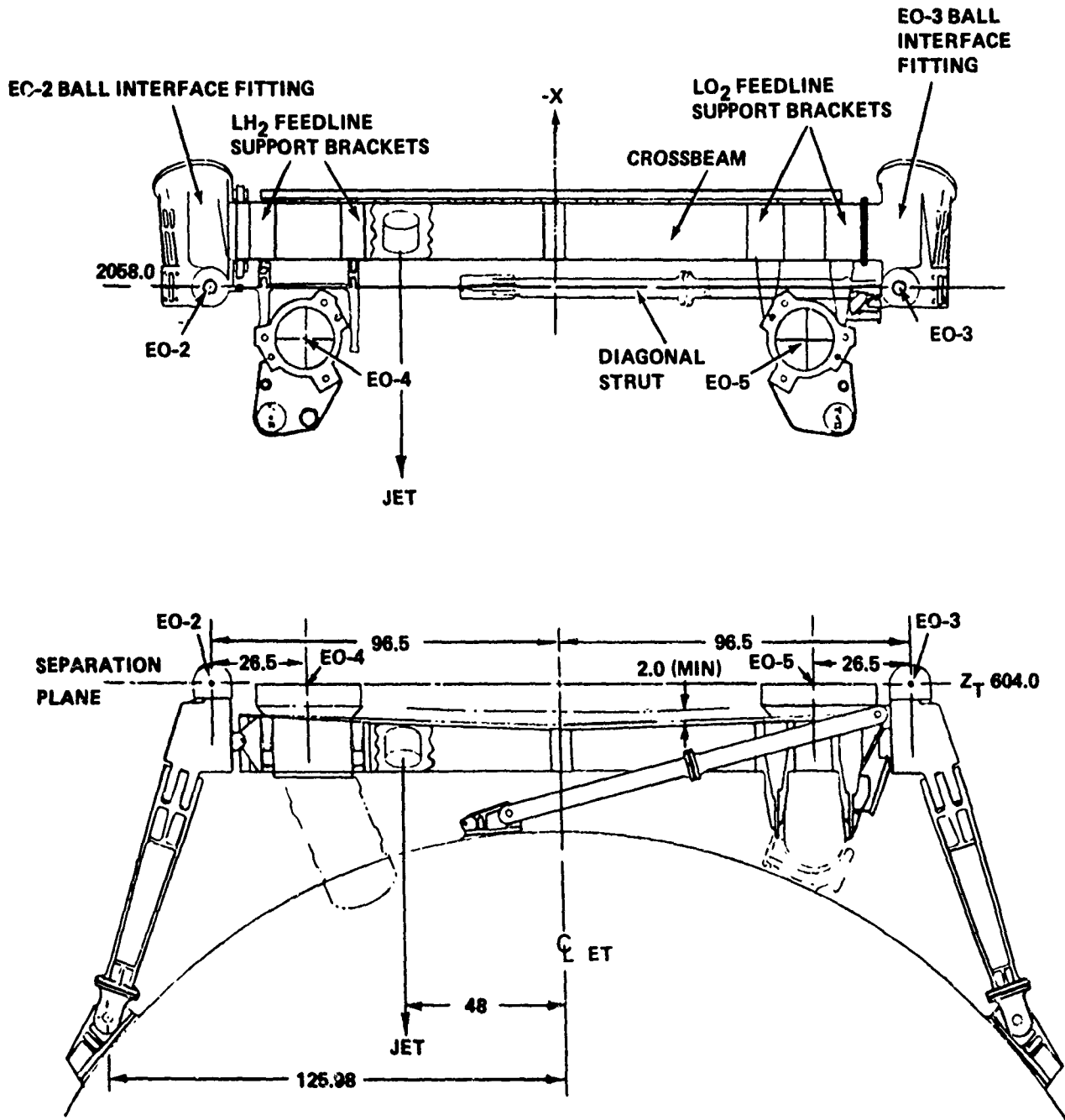


FIGURE 5-6 CHARGE PLACEMENT IN CROSSBEAM

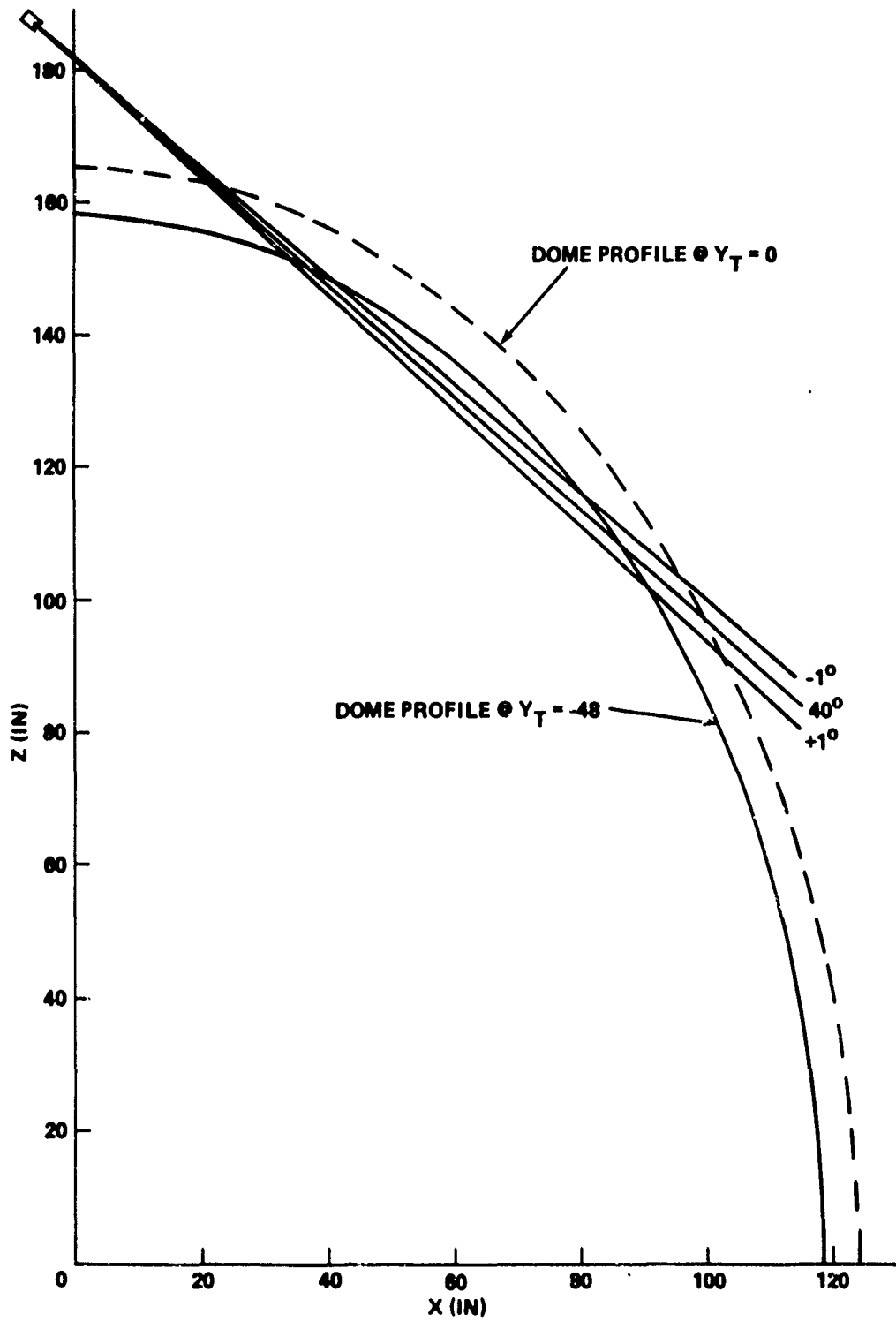


FIGURE 5-7 REGION OF LH₂ TANK DOME ATTACKED BY DESTRUCT SHAPED CHARGE IN ORBITER CROSSBEAM

LINEAR-SHAPED CHARGES ON ET

TARGET CONSIDERATIONS. Space is available in the electrical cable trays (Fig 5-8) outside the LH₂ and LOX tanks for positioning of the LSC's. Figures 5-9 and 5-10 are sketches supplied by Martin Marietta Company, Michoud, Louisiana, of the cable tray details. The bottoms of the cable trays (2024-T8511 aluminum) are ~0.126 inch thick and covered with an insulating layer (SLA) of a similar thickness. The standoff from the cable tray bottoms to the skins of the LH₂ and LOX tanks is 3.06 inches and 4.16 inches, respectively. Layers of insulation (SOFI) with a density of 2.6 pounds/foot³ cover the tank skins. The length of the gaps from the tray bottom to the tank wall makes the 2219T-87 aluminum skin covering the tanks an unusually distant target for LSC cutting action.

The thickness of the LH₂ tank skin is ~0.18 inch. The skin of the LOX tank is thicker, ranging up to 0.196 inch. Each cable tray is supported by brackets at several places along the barrel section of the tank. Each LOX tank bracket consists of a cast beam (Fig. 5-8) attached to two vertical supports that are fastened to pads. The beam is located directly in the path of an LSC jet as shown in the cross-section view (Fig. 5-11). This increases the total thickness of aluminum which must be cut to about 2.6 inches (Fig. 5-12). A similar situation exists on the LH₂ tank.

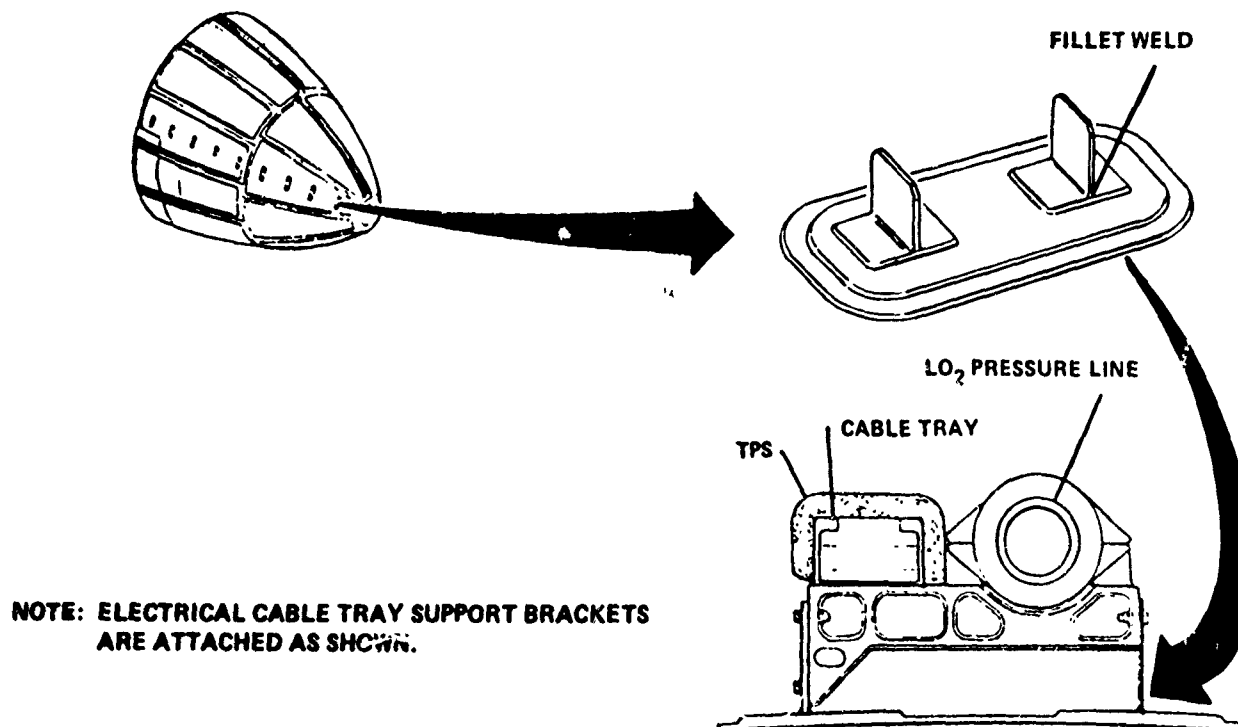


FIGURE 5-8 SKIN PAD AND WELDS ON TANK FORWARD AND AFT GORE SECTIONS

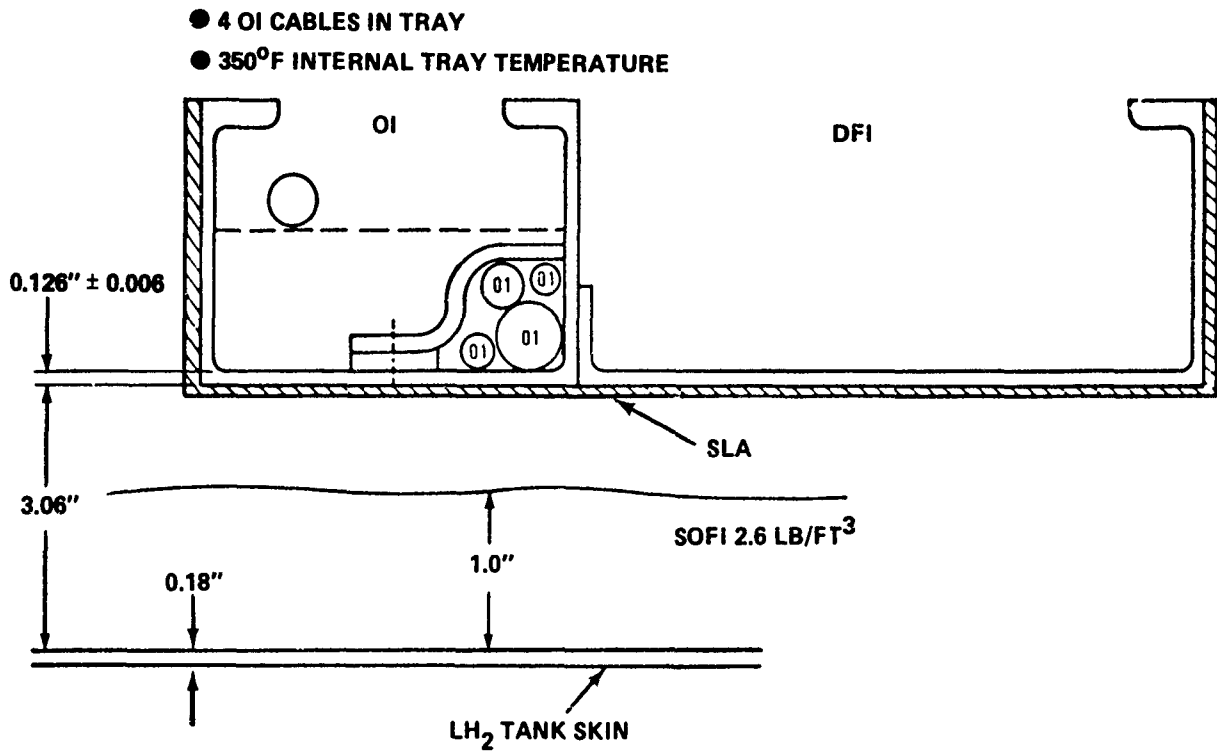


FIGURE 5-9 LH₂ CABLE TRAY GEOMETRY

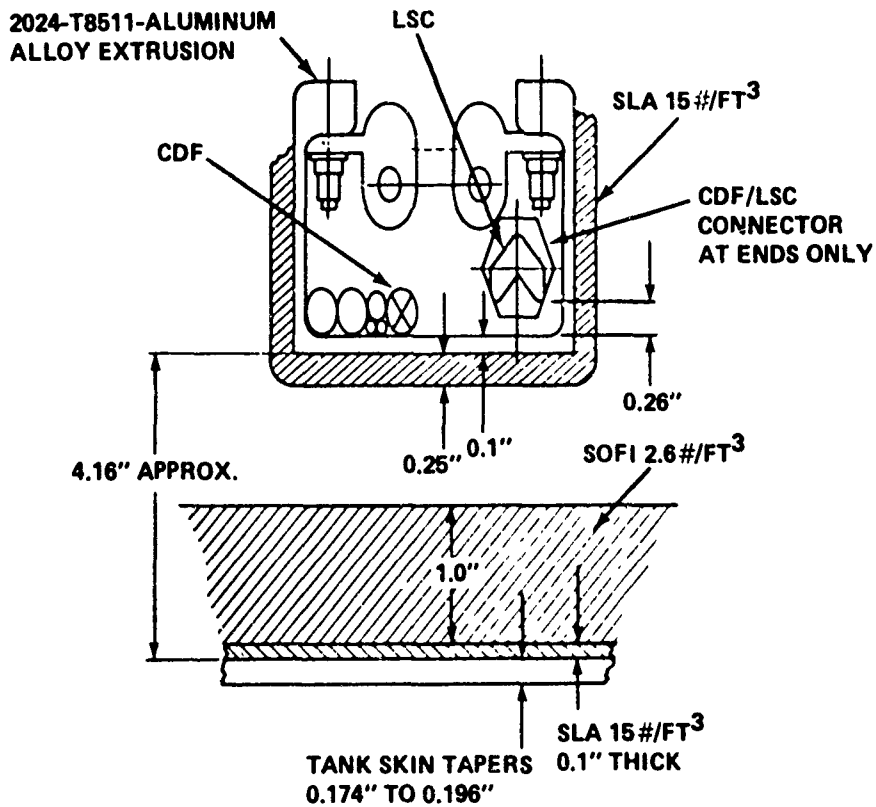


FIGURE 5-10 LOX CABLE TRAY GEOMETRY

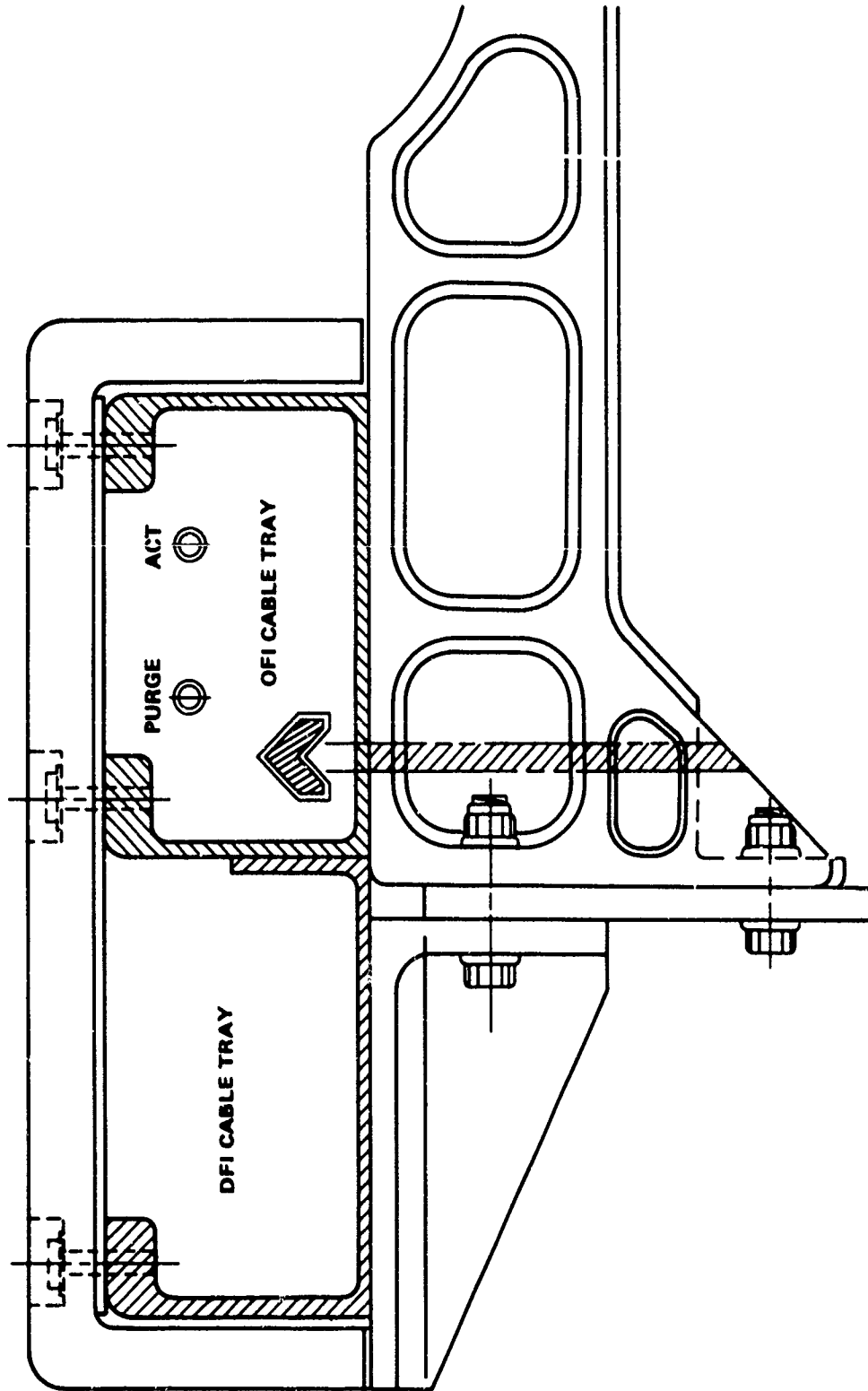


FIGURE 5-11 CABLE TRAY BRACKETS ON LOX TANK

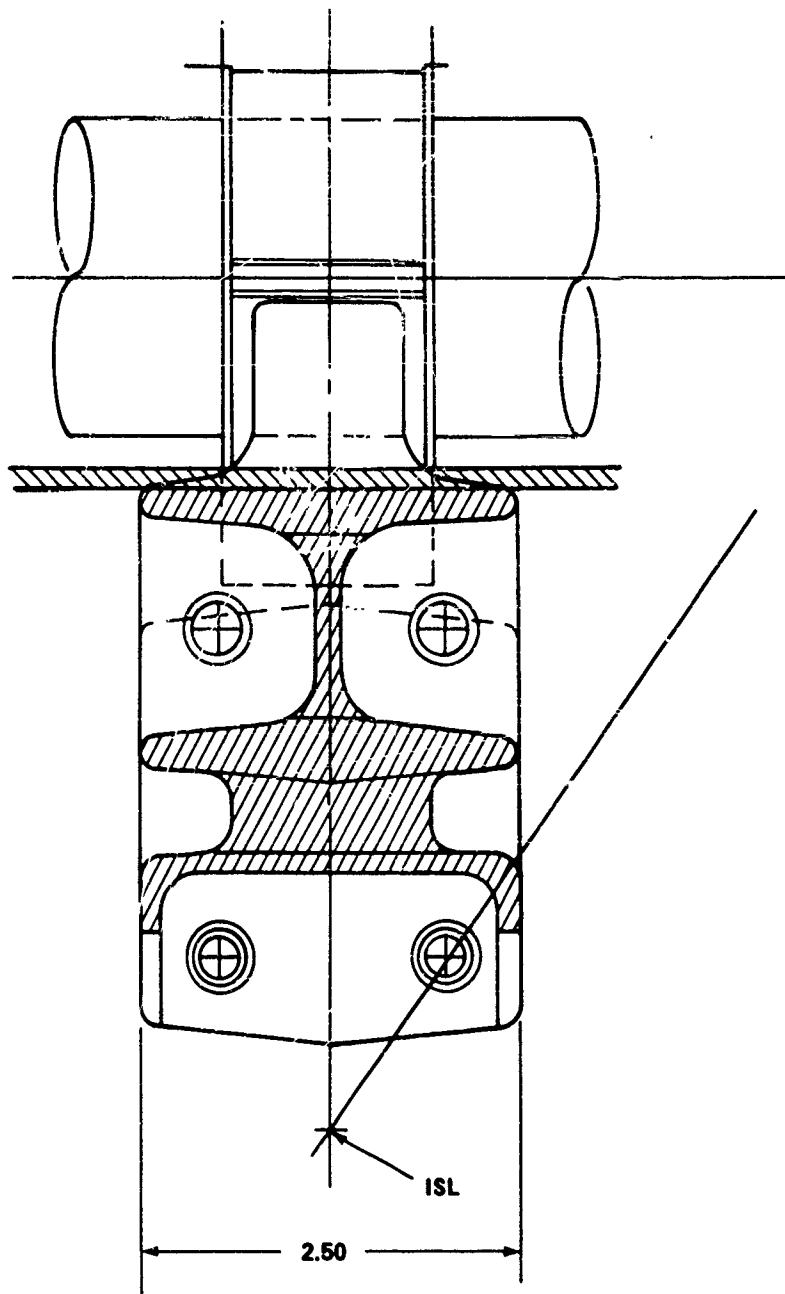


FIGURE 5-12 BEAM CROSS SECTION

TEST CONSIDERATIONS. The following factors make it necessary to establish the feasibility of using LSC for destruct action from a position within the electrical cable trays:

1. The uncommonly long standoff required for the LSC jet to reach the target skin.
2. The thickness of metal to be cut.
3. The requirement to use an LSC of minimum size, and explosive weight (core load) capable of performing destruct action on the target skin.
4. The interior dimensional constraints of the cable trays.

Therefore, the objectives of the test program were the following:

1. Prepare a test arrangement simulating the cable tray bottom, tank wall geometry, and materials. Also, simulate insulation on the trays and tanks.
2. Demonstrate that an LSC located in the cable tray would cut through the tank wall.
3. Study the effect of standoff.
4. Specify the type, minimum gross weight, and size of the LSC required to accomplish the cut.

TEST ARRANGEMENTS. The LSC test arrangements used to simulate the ET configurations on the LH₂ and the LOX tanks are shown in Figures 5-13 and 5-14, respectively. In these tests, the brackets supporting the cable tray were not simulated or modeled.

The cable tray bottom was simulated by 0.125-inch-thick 2024T-3 aluminum, covered by 0.125-inch-thick styrofoam (Figure 5-13) or 0.25-inch-thick cork (Figure 5-14). Standoff to the tray bottom for the LSC was provided by styrofoam spacers of the desired height.

The target plates simulating the tank skins were 0.1875-inch-thick 2024T-3 aluminum. (This thickness was a convenient mean since the thickness of the LO₂ tank skin (Fig. 5-10), except for bracket and bracket mounting pads, varies from 0.174 to 0.196 inch.) Each plate was 12 inches long by 12 inches wide. One side of the plate facing the simulated tray bottom was covered by 1-inch-thick styrofoam as in Figure 5-13, or with 1-inch-thick styrofoam and 0.125-inch-thick cork as shown in Figure 5-14. The styrofoam and cork were used to simulate the SOFI and SLA insulations on the tank and the tray. In several tests the 0.1875-inch-thick plate was placed on top of a 1-inch-thick aluminum plate. Through this plate residual penetration as a measure of LSC effectiveness was obtained.

The free surfaces of the tank plates (and residual plates) were at liquid nitrogen temperature (-320°F) during the tests. The LSC's were at ambient temperatures within the simulated cable tray. The LSC's were detonated when the LH₂ in the container had just evaporated below the tank plate surface facing the cable tray bottom.

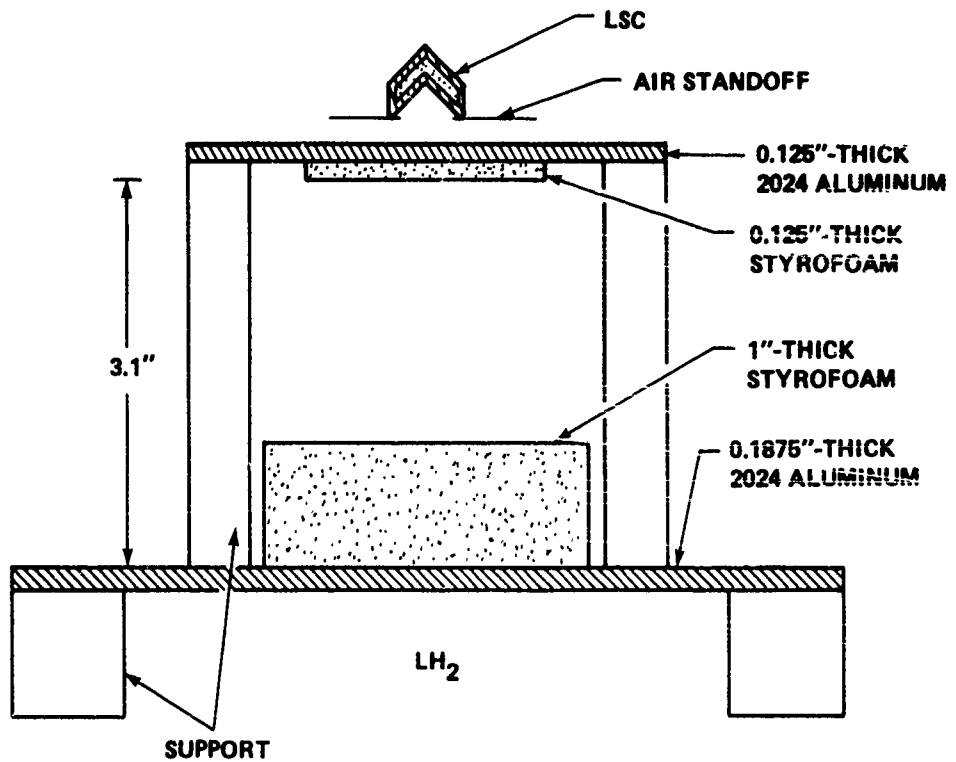


FIGURE 5-13 TEST ARRANGEMENT (LH₂ TANK)

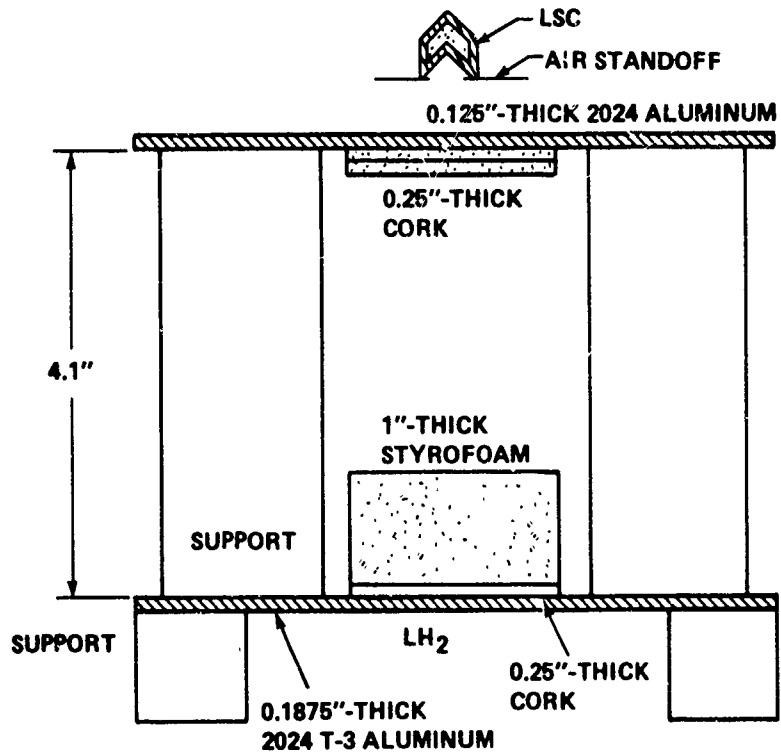


FIGURE 5-14 TEST ARRANGEMENT (LO₂ TANK)

Initiation of the LSC was by a No. 6 detonator fastened to one end of the LSC. Aluminum- and copper-lined linear-shaped charges loaded with RDX were used in the tests. Standoff distances were varied from 0 to about 1.5 inches.

RESULTS. The test results obtained with the simulated ET arrangement for the LH₂ tank are given in Table 5-2. In all tests using aluminum LSC's with 400 grain loads of RDX, no cuts were obtained through the 0.1875-inch-thick, simulated LH₂ tank skin. At 1.0-inch and 1.5-inch air standoffs (Shots 7 and 8) from the first plate (simulated cable tray bottom) partial cuts were obtained.

No jet penetration or cutting was obtained in the ET arrangement (Fig. 5-13) at zero standoff from the first plate using Cu LSC's with 500 grains and 750 grains RDX core loads. However, at 0.26-inch standoff, and a core load of 500 grains, Cu LSC's (Shots 2 and 6) produced clean cuts through the 0.1875-inch-thick, simulated LH₂ tank skin. An examination of the two severed halves of these plates indicated that the shaped charge jet in making the penetration and cut removed a ~0.25-inch wide section from the plates. The cutting actions of Cu LSC (Shot 2) on the simulated cable tray bottom and simulated LH₂ tank skin plate are shown in Figure 5-15.

TABLE 5-2 TEST RESULTS OF RDX-LOADED LINEAR-SHAPED CHARGES (LH₂ TANK)

Shot No.	LSC Specifications						Standoff (in)	LH ₂ Tank Skin Result
	Core Load (gr/ft)	Liner Metal	Apex Angle (deg)	Height (in)	Width (in)	Gross Weight (lb/ft)		
1	400	Al	120	0.463	0.540	0.135	0.260	No cut
2	500	Cu	90	0.513	0.605	0.410	0.260	Cut
3	500	Cu	90	0.513	0.605	0.410	0.0	No cut
4	750	Cu	90	0.620	0.740	0.500	0.0	No cut
5	750	Cu	90	0.620	0.740	0.500	0.0	No cut
6	500	Cu	90	0.513	0.605	0.410	0.260	Cut
7	400	Al	120	0.463	0.540	0.135	1.0	Fracture, cut 1/3 through
8	400	Al	120	0.463	0.540	0.135	1.5	Slightly less cut than Shot 7

SIMULATED
CABLE TRAY
BOTTOM



SIMULATED
LH₂ TANK
SKIN



FIGURE 5-15 RESULTS OF LINEAR-SHAPED CHARGE (COPPER-LINER, 500-GR/FT, RDX-LOADED) ACTION ON SIMULATED CABLE TRAY/LH₂ TANK

Table 5-3 lists the results obtained with the simulated ET arrangement for the LOX tank. Copper LSC's with an RDX core load of 500 grains were used except in one test (Shot 5) in which the core load was 400 grains. Tests were made at standoff distances of 0.26 inch and 0.50 inch from the 0.125-inch-thick, simulated cable tray bottom. The simulated tank skin was severed cleanly in each test despite the large gap (4.1 inches) separating the skin and the cable tray bottom.

An average residual penetration is listed in Table 5-3 for Shots 4, 5, and 6. These data are also shown schematically in Figure 5-16. The residual penetration is the depth of cut measured at 1-inch intervals along the length of the 1-inch-thick 2024 aluminum plate which backed the 0.1875-inch target plate simulating the LOX tank skin.

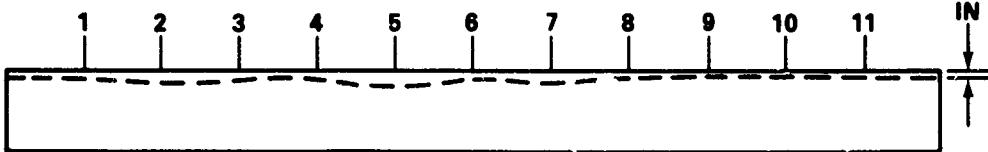
DISCUSSION. Short time requirements and unavailability of actual ET materials prevented an exact duplication of the ET arrangements (Fig. 5-8). No attempt was made, for example, to duplicate the bracket arrangement and mounting pad on the ET. These materials affect the LSC cutting actions. An evaluation based on the test results is given in a following section. Any differences in mechanical properties or heat treatment between 2024T-3 aluminum or 2024T-8511, are considered of little consequence in affecting LSC performance. Similarly, the differences in actual ET insulation and insulation used in the test arrangements could not detrimentally affect LSC penetration or cutting action. (Penetration or cutting is an inverse function of the square root of material densities. Test material densities and actual ET materials do not differ significantly.)

An aluminum LSC was tested because a considerable weight saving (see Table 5-2) could be obtained if it were successful in ET destruct action. The results, however, indicate that successful use of aluminum LSC's would require a core load of 500 grains or greater and LSC's with the usual apex angle of 90 degrees rather than 120 degrees, as used in these tests. The most effective standoff for aluminum LSC's would be ~1 inch. This standoff requires some modification of the cable tray interior to accommodate the LSC.

TABLE 5-3 TEST RESULTS OF RDX-LOADED LINEAR-SHAPED CHARGES (LOX TANK)

Shot No.	LSC Specifications					Gross Weight (lb/ft)	Standoff (in)	Average Residual Penetration (in)	Result
	Core Load (gr/ft)	Liner Metal	Apex Angle (deg)	Height (in)	Width (in)				
1	500	Cu	90	0.51	0.61	0.41	0.50		Cut
2	500	Cu	90	0.51	0.61	0.41	0.26		Cut
3	500	Cu	90	0.51	0.61	0.41	0.26		Cut
4	500	Cu	90	0.51	0.61	0.41	0.26	0.081	Cut
5	400	Cu	90	0.46	0.54	0.31	0.50	0.004	Cut
6	500	Cu	90	0.51	0.61	0.41	0.50	0.057	Cut

SHOT NO.	AVERAGE RESIDUAL PENETRATION											
	1	2	3	4	5	6	7	8	9	10	11	IN
4	0.094	0.111	0.101	0.079	0.130	0.101	0.124	0.068	0.034	0.021	0.029	0.081
5	0.000	0.001	0.006	0.046*	0.010	0.002	0.006	0.002	0.003	0.005	0.004	0.004
6	0.028	0.127	0.067	0.098	0.016	0.004	0.004	0.086	0.135	0.041	0.022	0.057



*REJECTED IN CALCULATING AVERAGE RESIDUAL PENETRATION ACCORDING TO PROBABILITY LAWS.

FIGURE 5-16 RESIDUAL PENETRATION AT 1-INCH INTERVALS

As expected, copper is a more effective liner material than aluminum under the constraints of the small standoff from the tray bottom plate. This 0.125-inch-thick plate provides a considerable impediment to the penetration and cutting action of the LSC jet on the tank wall. It is estimated that the presence of this plate defocuses the fragment spray to such an extent that the penetration is reduced by ~50 percent. This effect is much more detrimental on the fragments from a linear-shaped charge than on the jet from a conically-lined shaped charge. Initiation of the explosive at one end of an LSC forms a high-speed blade from the collapsed liner. The collapse is markedly affected by the explosive core load. The concentration of fragment energy from an LSC differs considerably from the energy of the jet from a conically lined shaped charge. As a consequence, an LSC is much less effective when the standoff between a double-plate target is increased.

Copper LSC's with 500-grain core load initiated at 0.26-inch standoff performed satisfactorily in all tests. Increasing the standoff to 0.50 inch did not affect the performance. A standoff of 0.50 inch is considered optimum for a copper LSC at 500 grain core load. However, the presence of the cable tray bottom reduces the explosive blast effect. This result tends to offset the advantage of a longer standoff. The data in Table 5-3 show the average residual penetration in the 1-inch-thick backup plate to be 0.081 inch for 0.26-inch standoff and 0.057 inch for 0.50-inch standoff. Copper LSC's with an RDX core load of 400 grains also cut through the simulated LOX tank skin. The residual penetration, however, was just 0.004 inch.

A more effective LSC in the LOX tank geometry would have a 750-grain RDX core load. The 750-grain LSC would produce a ~60 percent deeper cut than the 500-grain LSC. This conclusion is reached in the following way. The penetration and cut of a given material by a linear-shaped charge are proportional to the core load of the charge raised to a power, k , i.e.,

$$\frac{C_1}{C_2} = \left(\frac{W_1}{W_2} \right)^k \quad (5-1)$$

where C is the penetration for a core load, W. The total penetration in two plates of 2024-T3 aluminum, forming the LO₂ tank wall and the residual plate, (Table 5-3) was 0.1915 inch and 0.2445 inch for 400-grain and 500-grain core loads, respectively. These data in Equation 5-1 give $k = 1.09$. Thus, for a 750-grain core load, a 0.381-inch-deep cut is predicted.

BRACKET FAILURE ANALYSIS. The tests were not designed to include the cable tray brackets which exist at three places along the LOX tank barrel section and four places along the LSC installation on the LH₂ tank. However, the following discussion shows that the brackets will not prevent complete severing of the tank walls over the entire lengths of the LSC's. Differences in bracket design, spacing and skin thickness in the LOX and LH₂ tank installations preclude a common analysis and, in fact, introduce different failure modes.

LOX Tank Bracket. Figure 5-11 shows the brackets that are in the LSC jet path. The bottom of the bracket is 2.6 inches from the lower interior surface of the cable tray. The total thickness of aluminum to be cut at these three places is about 2.6 inches. This thickness is ~8 times the thickness of aluminum cut in the tests, although the distance the jet must travel before encountering the material is less.

Assume that the jet from an LSC has an effective range which depends upon the standoff distance and the amount of material encountered in that range. A 500-grain/foot Cu LSC at optimum standoff (0.5 inch) will cut 1.44 inches of aluminum within a range of 1.94 inches. In the simulated cable tray/LOX tank geometry, this charge cut a total aluminum thickness of 0.369 inch at a range of 4.73 inches. Linear interpolation of these data (Fig. 5-17) yields a material cut thickness of ~1.0 inch within a range of 3 inches. The maximum accumulated thickness of the cable tray and bracket material is approximately 2.6 inches. The analysis indicates, therefore, that the 500-grain/foot LSC cannot cut the entire bracket at the position given.

Two improvements can be made. First, the LSC can be located on the opposite side of the cable tray. This would reduce the bracket thickness to be cut to about 2 inches. In addition, increasing the RDX core load to 750 grain/foot will increase the likelihood of a complete cut.

However, severing of the bracket is not required, as an analysis based on fracture mechanics shows. Assuming that the bracket shields the skin, none of the support pads below the bracket is removed. A ligament remains in the skin with the cross section illustrated in Figure 5-18.

The total load, F, to be carried by one ligament and bracket at a ΔP across the skin of 15 psi (minimum ΔP expected in barrel section during ascent - vapor pressure of LOX inside of tank, negligible atmospheric pressure external to tank) is

$$F = \Delta P R \ell = 15 (165.5)(39) = 96,800 \text{ lb} \quad (5-2)$$

where R is the radius of the barrel section and ℓ is the bracket to bracket spacing. If the bracket is not completely severed, some portion of the hoop load will be carried by the bracket. That load will be limited by the ultimate tensile capability of the remaining bracket material or the fully plastic bending moment capability of the vertical bracket supports.

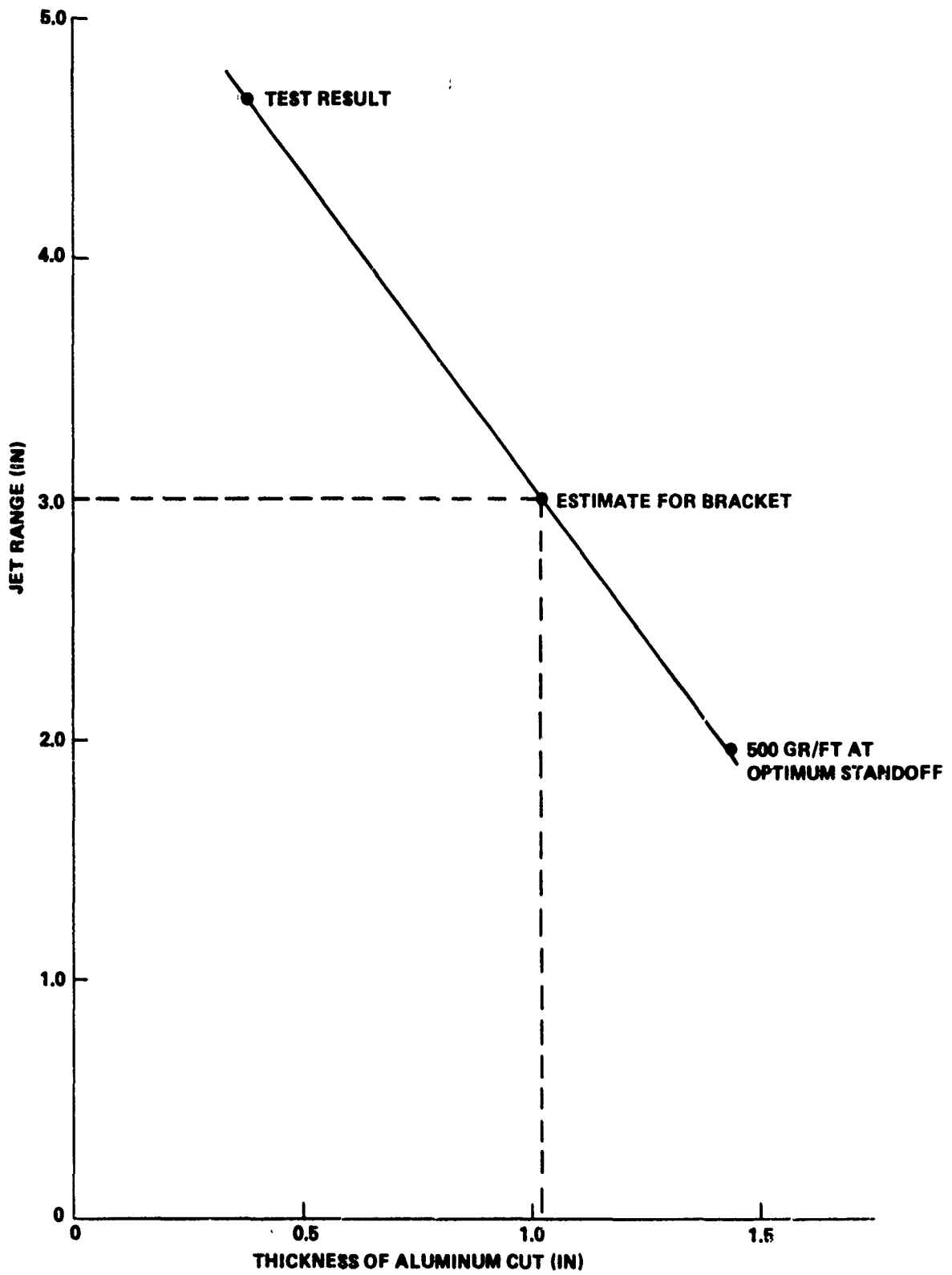
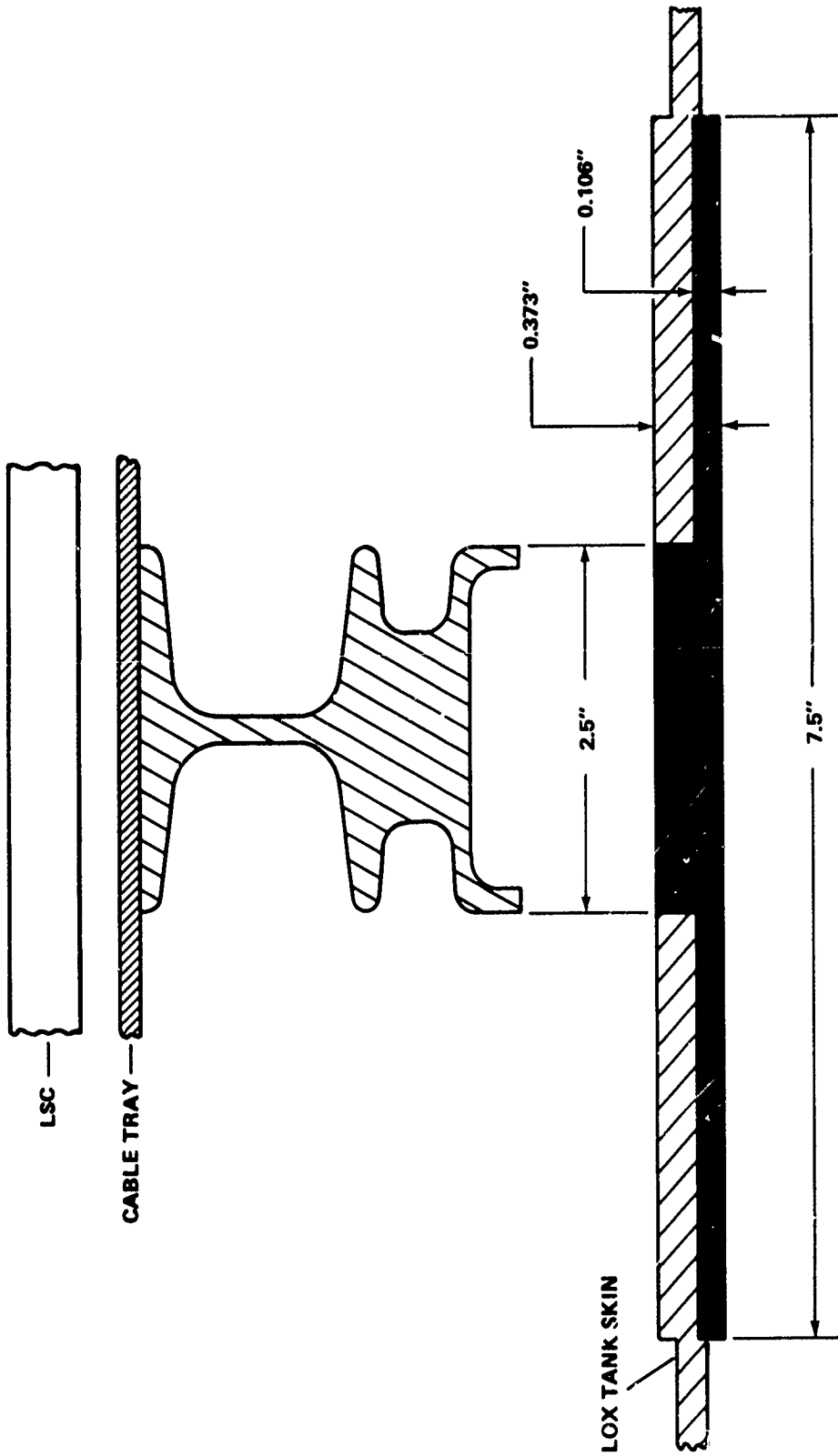


FIGURE 5-17 500-GR/FT TEST RESULT FOR CABLE TRAY APPLICATION



■ SECTION OF SKIN PAD NOT CUT BY LSC - A = 1.45 IN²

FIGURE 5-18 LIGAMENT REMAINING IN LOX TANK SKIN AFTER LSC CUT

The fully plastic bending moment capability of the right-hand vertical support (looking forward) is only.

$$M_P = \sigma_o \frac{bh^2}{4} = 75,000 \frac{(3.5)(0.080)^2}{4} = 420 \text{ in-lb} \quad (5-3)$$

where b = width and h = thickness of the bracket support. At a bracket load of about 200 pounds, a plastic hinge will form at the base of the support and the support will rotate with no further increase in load transmission. Therefore, the tank wall will still carry at least 99.8 percent of the load, giving an average tensile stress of

$$\sigma = \frac{F}{A} = \frac{96,800 - 420}{1.46} = 66,000 \text{ psi} \quad (5-4)$$

where A is the cross sectional area of the ligament. The resultant tensile stress is some 9,000 psi less than the ultimate strength of the 2219-T87 aluminum at -296°F.

However, consideration of fracture mechanics suggests that the flaws cut into the skin will propagate through the ligaments. Consider the flaw pattern of Figure 5-19. For thin-walled cylindrical pressure vessels ($R/t = 50$) with long cracks, the critical hoop stress for crack extension is:³

$$\sigma_H^* = \frac{K_c}{(\pi c \phi_3)^{1/2}} \left[1 + 1.61 \frac{c^2}{R^2} \left(50 \tanh \frac{R}{50t} \right) \right]^{-1/2} \quad (5-5)$$

where

$$\phi_3 = 1. \text{ for } \sigma^* \ll \sigma_o$$

2c = crack length

R = vessel radius

t = wall thickness

For a K_c of 110 ksi $\sqrt{\text{in}}$ (stress intensity factor for 2219-T87 aluminum) the above equation gives the critical hoop stress to cause fracture at 12,000 psi. For a ΔP of 15 psi, the gross stress carried by the tank wall is 13,300 psi. Therefore, the ligament will fail by crack extension. Once the ligament fails, the bracket or bracket support will rupture by gross deformation.

³Hahn, G.T., Sarrate, M., and Rosenfield, A.R., "Criteria for Crack Extension in Cylindrical Pressure Vessels." Journal of Fracture Mechanics, Vol. 5, No. 3, 1969, p. 187.

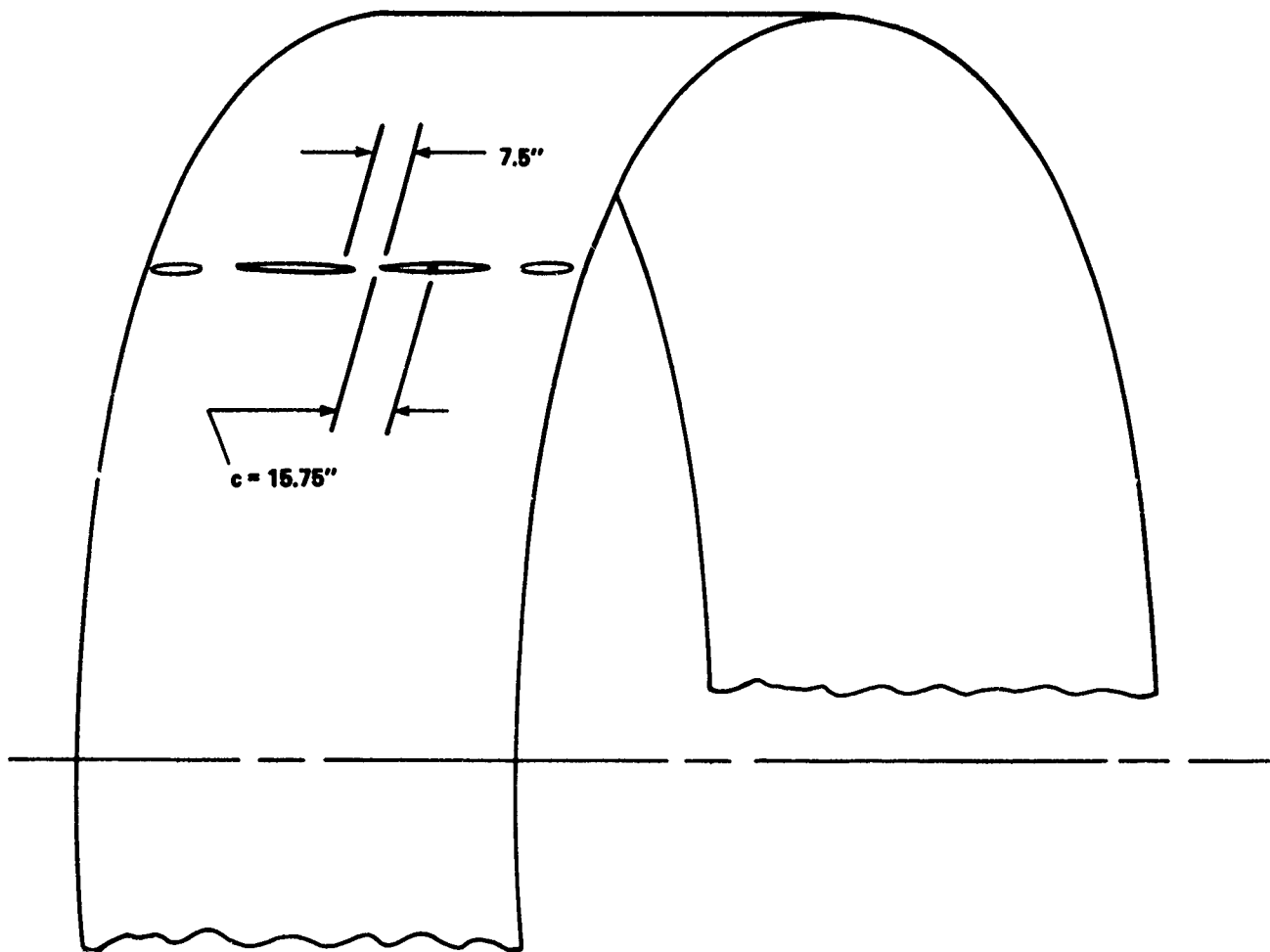


FIGURE 5-19 FLAW PATTERN - LOX TANK BARREL SECTION

LH₂ Tank Bracket. The LH₂ tank cable tray brackets are placed at approximately 65-inch intervals. In contrast to those of the LOX tank, the vertical supports are relatively stiff and allow the bracket to carry considerable hoop load (Fig. 5-20). However, all but a small portion of the web will be cut by a 500-grain/foot, copper-lined LSC. The remaining cross sectional area (<0.1 inch²) can carry an ultimate load of less than 4,000 pounds ($\sigma_0 = 38,000$ psi for A356-T6 aluminum). A 750-grain/foot LSC, on the other hand, will completely sever the bracket.

Assume in either case that the skin is shielded by the brackets. The minimum load to be carried by each ligament and bracket is

$$F = \Delta P R \ell = 15(165.5)(65) = 161,000 \text{ lb} \quad (5-6)$$

Again, ΔP is 15 psi (the minimum ΔP expected across the tank skin -- vapor pressure of LH₂ inside of tank, negligible atmospheric pressure outside of tank).

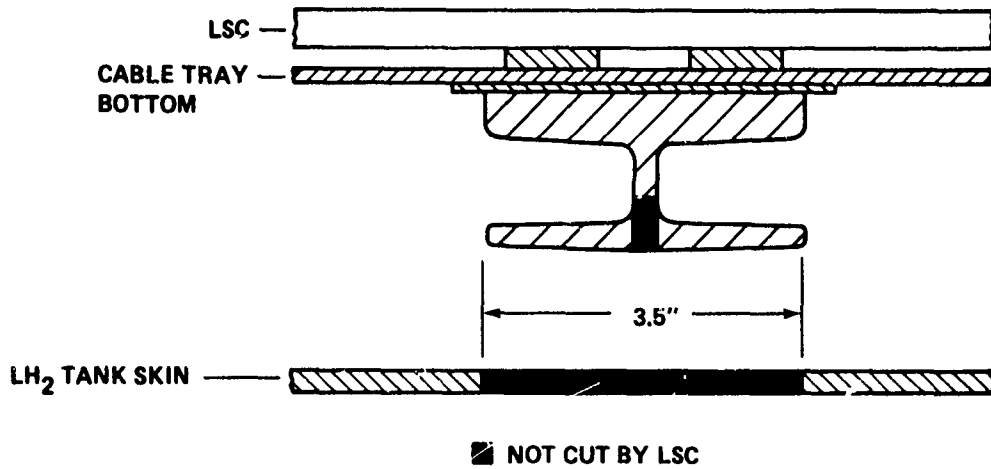
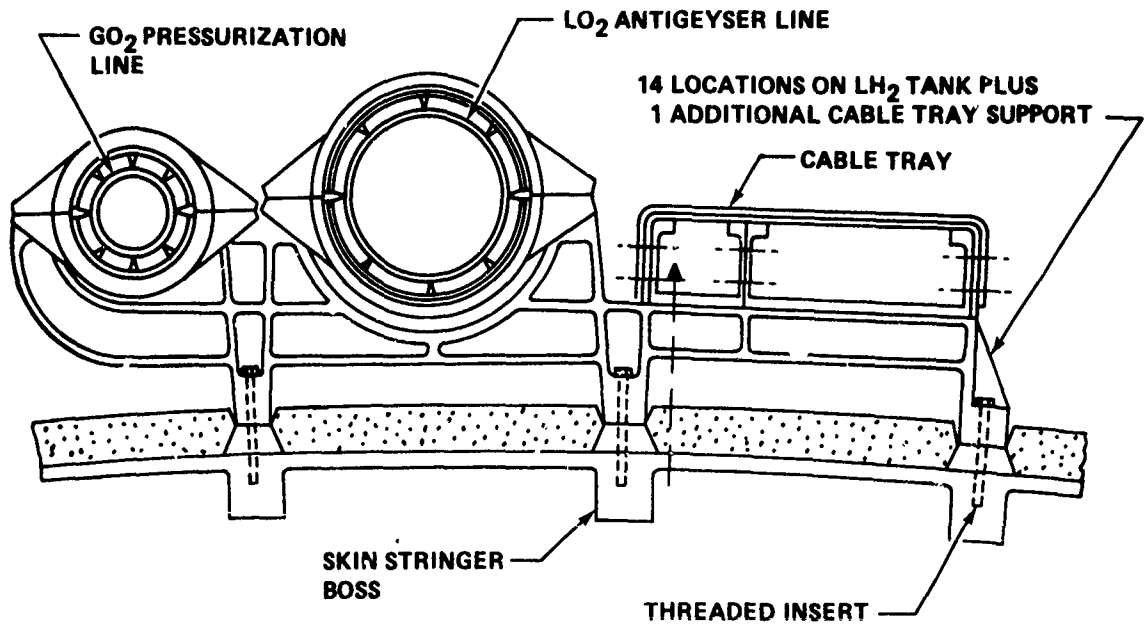


FIGURE 5-20 LH₂ TANK CABLE TRAY BRACKET

The resultant ligaments remaining in the skin have cross sectional areas of 0.09 inch² or less (Fig. 5-20). Subtracting the 4,000-pound load carried by a partially severed bracket gives a stress in the ligament of

$$\sigma = \frac{F}{A} = \frac{161,000 - 4,000}{0.9} = 174,000 \text{ psi} \quad (5-7)$$

This grossly exceeds the ultimate strength of the 2219-T87 aluminum, and the ligaments will fail by gross yielding.

SUMMARY AND CONCLUSIONS. It has been demonstrated that two copper-lined, RDX-loaded linear-shaped charges, weighing ~10 pounds each can catastrophically destruct the LH₂ and LOX tanks from locations in the electrical cable trays. Tests were made using simulated ET/cable tray geometry to establish linear-shaped charges as effective destruct ordnance. The test results give confidence in successful LSC destruct against actual ET configurations. The tests and analysis indicate that LSC with an RDX core load of 500 or 750 grain/foot will produce a depth of cut which will exceed destruct action requirements. The analysis was made using fracture mechanics to examine LSC destruct action at places on the tank barrel section where brackets support the cable tray. The analysis shows that while LSC jet action alone will not produce skin severance at these places, stress crack extensions will result and cause skin failure. The specifications for the 500-grain/foot charges are summarized in Table 5-4.

TABLE 5-4 SUMMARY OF RECOMMENDED LINEAR-SHAPED CHARGE SPECIFICATIONS

Component/Characteristic	Specification
Liner Type	Copper
Apex Included Angle	90 deg
Sheathing	
Height	0.620 in
Width	0.740 in
Explosive	RDX
Load	750 gr/ft
Gross Weight	0.500 lb/ft
Recommended Standoff	0.5 in
Temperature Exposure Limitations	High: 325°F/0.5 h (not over 400°F, 10 sec) Low: -320°F

COMPARISON OF SYSTEMS WITH DEVICES OUTSIDE INTERTANK

As with the destruct options using ordnance contained in the IT, it is useful to compare the merits and demerits of the two systems investigated which employ ordnance outside the IT. The hybrid system, as its name is intended to imply, uses explosives both inside and outside the IT. The other system uses LSC's outside the IT.

The features of interest for both options are summarized in the following:

HYBRID SYSTEM. Advantages: (1) Only two ordnance devices are employed; both are hemispherically shaped charges. The commonality goal is attained. (2) The weight of each device is about 16 pounds with 10 pounds being explosive. (3) The accuracy of jet alignment can be adequately attained. (4) Mixing of LH₂ and LOX is minimized because of the long distance between the rupture areas, i.e., the bottoms of the LOX and LH₂ tanks. (The hybrid system provides the largest distance between rupture areas of all the options studied in this task). (5) The cost of each charge is relatively low (about \$4,000) since the thermally stable HNS explosive is used.

Disadvantages: (1) The cross beam design requires substantial modification to accept and correctly position the charge directed at the LH₂ tank lower dome. (2) The cross beam location may impose severe temperature and vibration environments on the destruct charge. This would require shock mounts and temperature controls to abate the situation, which, in turn, would add weight to the system.

LSC'S IN OPERATIONAL INSTRUMENTATION CABLE TRAYS. These LSC's are shown in Figure 5-21.

Advantages: (1) Only two ordnance devices are required, both LSC's. (2) LSC's have been qualified by NASA for space vehicle applications; hence, qualification for Space Shuttle applications should be relatively easy. (3) To obtain 20-foot long cuts in the LH₂ and LOX tanks, 40 feet of LSC are required. The total weight of the LSC's would be about 20 pounds with only 4 pounds of this being explosive for 750-grain/foot LSC's. (4) The feasibility of LSC's located in the operational instrumentation (OI) cable trays has been demonstrated in mock-up tests.

Disadvantages: (1) Some rerouting of OI cables is necessary to accommodate the LSC's. (According to early indications this can be accomplished.)

CONCLUSIONS

Comparison of the characteristics of the hybrid and LSC systems described in this chapter indicates that the better system to obtain assured ET destruct with minimal mixing of the LH₂ and LO₂ is the option using LSC's mounted into the OI trays. Remembering the characteristics of the options described in Chapter 4 dealing with destruct systems located in the IT leads to the conclusion that the LSC system in the OI trays is, indeed, the best of all options analyzed. It best meets the technical and operational objectives, guidelines, and concerns given in the work statement as initially stated and as they evolved.

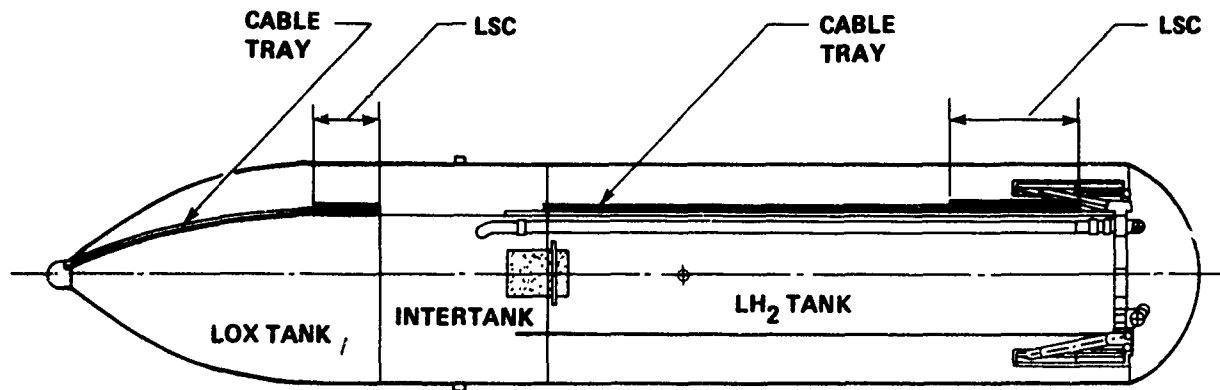


FIGURE 5-21 TWO-ELEMENT DESTRUCT SYSTEM, LSC/CABLE TRAY
INSTALLATION - ET TOP VIEW

The LSC system effectively destructs the LH₂ and LOX tanks. Large initial ruptures, about 20 feet long, assure rapid dumping of the liquid propellants. Because the rupture areas are separated by a long distance - at the lower ends of both tanks - minimal mixing of the LOX and LH₂ will take place. Hence, minimal potential blast yield of the mixture can be expected. There is commonality of the ordnance items; similar LSC's are used for LH₂ and LOX tank destructs. The LSC's are relatively light weight, approximately 20 pounds being required for the total package. Only about 4 pounds of this weight is explosive. The cost of the LSC itself should be low, less than \$1,500 per flight. Another attribute of the LSC option is that LSC's have been qualified for space vehicle operations by NASA; qualification for the Space Shuttle should be relatively easy. An equally important advantage in LSC use is that NASA personnel have experience and competence in handling this item. The other explosive items considered, while not novel, may not be as familiar.

In the study, more work was done on this LSC system than on the other systems. This system's feasibility was demonstrated by test. Mock-ups were made of the OI tray/ET geometries. Copper sheathed 500-grain/foot LSC's effectively cut the simulated ET skins. Although the brackets supporting the OI trays were not modeled, analysis indicates that the LSC would cut enough of the bracket to violate its structural integrity and thus not inhibit ET destruct. If larger LSC's can be accommodated in the OI trays, (and indications are they can), it is recommended that a 750-grain/foot, copper-sheathed LSC be used. This would cut the brackets more effectively.

BIBLIOGRAPHY

- Ahrens, T.J., Allen, C.F., and Kovach, R.L. "Explosive Gas Blast: The Expansion of Detonation Products in Vacuum," Journal of Applied Physics, Vol. 42, 1971, p. 815.
- Ammann and Whitney, "Shock Wave Parameters for Spherical TNT Explosion in Free Air at Sea Level," unpublished chart, undated.
- Baker, W.E., et al, "Assembly and Analysis of Fragmentation Data for Liquid Propellant Vessels," NASA CR-134538, Contract No. NAS 3-16009, Southwest Research Institute, San Antonio, Texas, Jan 1974.
- Brennan, J.A., Edmonds, D.K., and Smith, R.V., "Two-Phase (Liquid-Vapor), Mass-Limiting Flow With Hydrogen and Nitrogen," Advances in Cryogenic Engineering, Vol. 14, 1969, pp. 294-298.
- Drimmer, B.E., "Penetration of Steel Targets at Long Standoffs by Steel-Cone-Lined Shaped Charges," NOLR 1145, Aug 1950.
- Farber, E.A., Klement, F.W., and Bonzon, C.F., "Prediction of Explosive Yield and Other Characteristics of Liquid Rocket Propellant Explosions," Final Report, NASA-CR-137372, N74-20589, Contract No. NAS 10-1255, University of Florida, Gainesville, 30 Jun 1973.
- Fertis, D.G., Dynamics and Vibration of Structures, (New York: John Wiley & Sons, Inc., 1973).
- Granstrom, S.A., "Loading Characteristics of Air Blasts from Detonating Charges," Acta Polytechnica, 1956, 196. Also, Trans. of the Royal Institute of Technology, Stockholm, Sweden, No. 100.
- Hahn, G.T., Sarrate, M., and Rosenfield, A.R., "Criteria for Crack Extension in Cylindrical Pressure Vessels," Journal of Fracture Mechanics, Vol. 5, No. 3, 1969, p. 187.
- Holt, M., ed., Basic Developments in Fluid Dynamics (New York: Academic Press, 1965).
- Humphreys, J.S., "Plastic Deformation of Impulsively Loaded Straight Clamped Beams," Journal of Applied Mechanics, Mar 1965, pp. 7-10.
- Jack, W.H., Jr., and Armendt, B.F., Jr., "Measurements of Normally Reflected Shock Parameters from Explosive Charges Under Simulated High Altitude Conditions," BRL R 1280, AD 469014, Aberdeen Proving Ground, Maryland, Apr 1965.

Jack, W. H., Jr., "Measurements of Normally Reflected Shock Waves from Explosive Charges," BRL Memo Report No. 1499, Aberdeen Proving Ground, Maryland, 1963.

Kilmer, E. E., "Plastic Bonded, Thermally Stable Explosive for an Apollo Experiment," Journal of Spacecraft and Rockets, Vol. 10, No. 7, 1973, p. 463.

Liddiard, T. P., Naval Surface Weapons Center, unclassified data taken from limited distribution report, 30 June 1971.

"Study Report on Space Shuttle Range Safety Command Destruct System Analysis and Verification," by NSWC/WOL for NASA George C. Marshall Space Flight Center, AL 35812, under NASA-Defense Purchase Request H-13047B of 15 May 1975; 2 Feb 1976.

Sutherland, L. C., "A Simplified Method for Estimating the Approximate TNT Equivalent from Liquid Propellant Explosions," Paper before 15th Annual Explosives Safety Seminar, San Francisco, 20 Sep 1973.

van Thiel, M., Ross, M., Hoed, B. L., Mitchell, A. C., Gust, W. H., D'Addario, M. J., and Keeler, R. N., Physical Review Letters, Vol. 31, 1973, p. 979.

Willoughby, A. B., Wilton, C., and Mansfield, J., "Liquid Propellant Explosive Hazards. Final Report-Dec. 1968. Vol. I - Technical Documentary Report, Vol. II - Test Data, Vol. III - Prediction Methods," AFRPL-TR-68-92, URS-652-35, URS Research Co., Burlingame, California.

APPENDIX A

BASIC BARE-CHARGE BLAST DATA

D. Lehto

CHARGE AT SEA LEVEL

The peak shock pressure from bare spherical TNT charges in sea-level air is quite well defined. Figure A-1 shows the results of a WUNDY calculation. These data may be scaled reasonably well to high altitudes, i.e., low nitrogen pressures in the intertank (IT). In a vacuum, however, the air shock no longer exists, and the damage is done by the expanding explosion product gases.

The reflected impulse at sea-level conditions is shown in Figure A-2. Experimental data are shown from two sources. The Ammann Whitney curve^{A-1} is fitted to experimental data of Granstrom^{A-2} for free-air TNT charges. The Jack data are for pentolite and are scaled to TNT for Figure A-2.^{A-3}

According to the usual Sachs scaling procedure, impulse and distance should scale from Condition 1 to Condition 2 as

$$I_2/I_1 = (a_{01}/a_{02}) (p_{02}/p_{01})^{2/3} (w_2/w_1)^{1/3} \quad (A-1)$$

$$r_2/r_1 = (p_{01}/p_{02})^{1/3} (w_2/w_1)^{1/3} \quad (A-2)$$

A-1 Ammann and Whitney, "Shock Wave Parameters for Spherical TNT Explosion in Free Air at Seal Level," unpublished chart, undated.

A-2 Granstrom, S.A., "Loading Characteristics of Air Blasts from Detonating Charges," Acta Polytechnica, 1956, 196. Also, Trans. of the Royal Institute of Technology, Stockholm, Sweden, No. 100.

A-3 Jack, W.H., Jr., "Measurements of Normally Reflected Shock Waves from Explosive Charges," BRL Memo Report No. 1499, Aberdeen Proving Ground, Maryland, 1963.

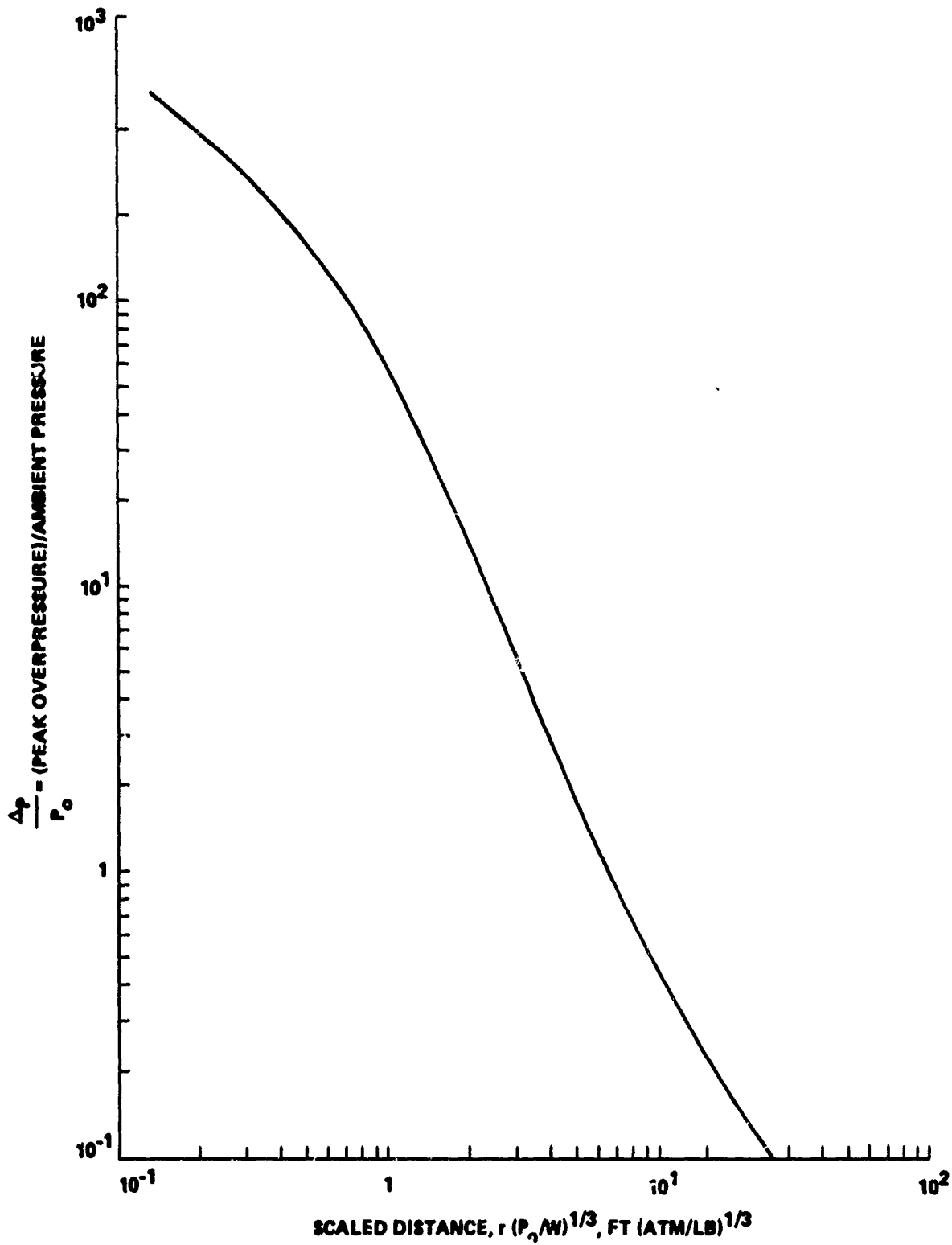


FIGURE A-1 PRESSURE VS. DISTANCE FOR TNT CHARGE

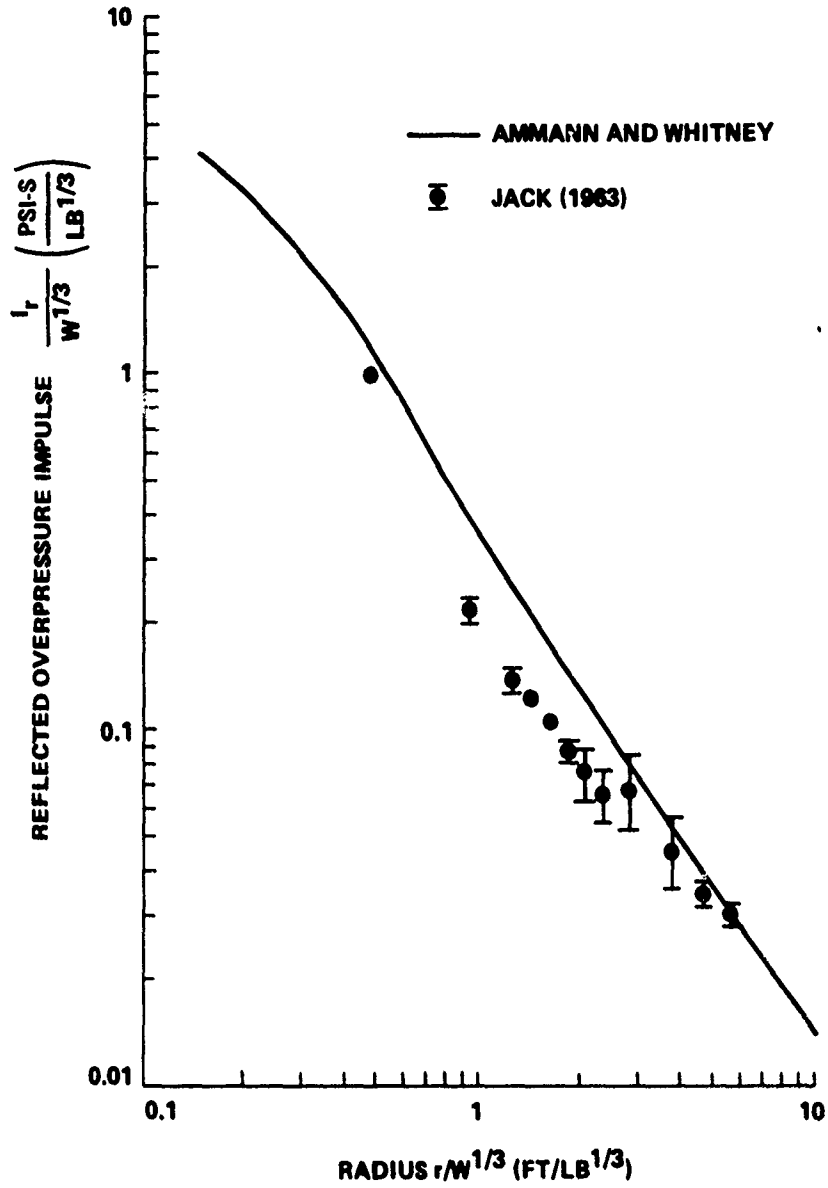


FIGURE A-2 REFLECTED IMPULSE FROM TNT SPHERE IN SEA-LEVEL AIR

where

I = reflected impulse

a_0 = ambient sound speed

p_0 = ambient pressure

W = charge mass (or, more correctly, the energy of explosion)

r = distance

Figure A-2 may be yield-scaled accurately, but p_0 scaling is questionable close to the charge because the charge radius is fixed and does not obey Equation A-2. Figure A-2 will only be used to correlate plate damage data taken at sea level conditions. Figures A-1 and A-2 may be used to get the approximate overpressures and reflected impulses from propellant explosions when the TNT equivalent weight is known.

CHARGE IN VACUUM

Charges that will work at any ambient pressure from 1 atm to essentially zero are needed. Since it is known that the impulse at a given distance from a charge decreases monotonically with pressure to its vacuum value, impulse versus distance data in a vacuum must be used to arrive at conservative charge masses.

Jack and Armentdt measured the reflected impulse from 1/8-pound pentolite charges for ambient pressures from 0.3 to 0.0007 atm.^{A-4} The latter pressure is accepted here as being close enough to vacuum. Figure A-3 shows the data for 0.0007 atm scaled from pentolite to TNT. Also shown are a point from a rough TUULI (formally called TUTTI) hydrocode calculation and a point obtained by integrating a pressure-time record of Ahrens, et al for a 2.6-gram HNS charge at 10^{-7} atm.^{A-5} The line drawn through the data is fitted by

$$I_r/W^{1/3} = 0.135 (r/W^{1/3})^{-1.853} \quad (\text{TNT in vacuum}) \quad (\text{A-3})$$

from which the charge weight needed to give a desired I_r at r is

$$W = 8.21 I_r^{0.951} r^{1.95} \quad (\text{TNT in vacuum}) \quad (\text{A-4})$$

^{A-4} Jack, W.H., Jr., and Armentdt, B.F., Jr., "Measurements of Normally Reflected Shock Parameters from Explosive Charges Under Simulated High Altitude Conditions," BRL R 1280, AD 469014, Aberdeen Proving Ground, Maryland, Apr 1965.

^{A-5} Ahrens, T.J., Allen, C.F., and Kovach, R.L., "Explosive Gas Blast: The Expansion of Detonation Products in Vacuum," Journal of Applied Physics, Vol. 42, 1971, p. 815.

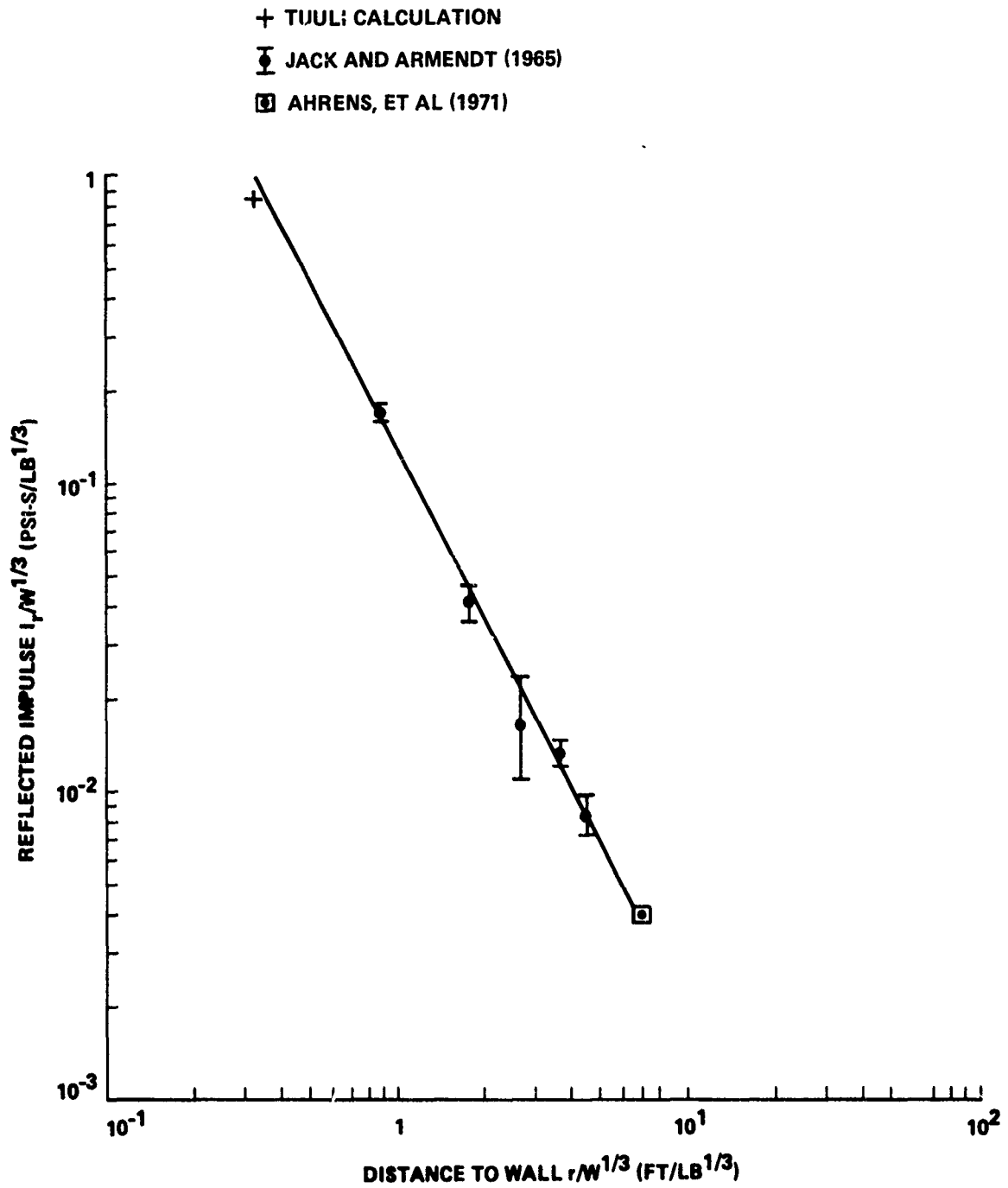


FIGURE A-3 REFLECTED IMPULSE FROM TNT CHARGE IN VACUUM

where

W = weight of TNT charge in pounds

I_r = reflected impulse (psi-s)

r = distance from charge center (ft)

Table A-1 gives the charge weights needed to put holes into the dome of the LH₂ tank at sea level conditions. To find the charge weights needed in vacuum, the impulse from the Ammann and Whitney curve (Fig. A-2) is read, which yields the charge weight to give this same impulse in vacuum from Equation A-4.

The result is that a 20-pound TNT charge detonated at a 2-foot standoff distance will blow an at least 4-foot diameter hole into the IT LH₂ tank dome for all IT conditions from 1 atm pressure to vacuum.

TABLE A-1 EFFECTS OF TNT CHARGE AT STANDOFF DISTANCE OF 2 FEET FROM LH₂ TANK DOME

Desired hole diameter (ft) for metal thickness of 0.11 in	0.9	2.4	3.7	4.7	6.1	7.2	8.5	9.8
Desired hole diameter (ft) for metal thickness of 0.15 in	0.0	1.2	2.9	3.9	5.2	6.3	7.4	8.6
TNT charge weight (lb) to perforate steel* at sea level	1.0	2.0	5.0	10.0	25.0	50.0	100.0	200.0
Reflected impulse I_r (psi-s) to perforate steel at sea level (from Amman and Whitney curve)	0.125	0.214	0.455	0.829	1.93	3.46	6.27	10.6
Reflected impulse (psi-s) to perforate aluminum (0.45 times I_r for steel)	0.056	0.096	0.205	0.373	0.869	1.56	2.82	4.79
TNT charge weight (lb) needed for enough reflected impulse to perforate aluminum at sea level	0.36	0.73	1.95	3.9	10.3	20.0	39.0	72.0
TNT charge weight (lb) needed for enough reflected impulse to perforate aluminum in vacuum	2.0	3.4	7.0	12.4	28.0	48.0	85.0	141.0

*Rolled homogeneous steel armor plate.

APPENDIX B

EFFECTS OF HIGH-EXPLOSIVE CHARGE IN LIQUID HYDROGEN

D. Lehto

INTRODUCTION

One of the possible ways to destruct the LH₂ tank is to fire an explosive charge into the LH₂. An explosion in the liquid would give much greater wall loading than an explosion in the vapor. We want to know how large a charge is needed at the axis of the tank to give a wall-reflected impulse of 0.4 psi-sec.

Most of the available calculations and experiments on explosions in liquids are for water. These results are not directly usable here because LH₂ and water have widely differing properties; the densities, for example, differ by a factor of 14. Instead of scaling from water to LH₂, an approximate equation of state for LH₂ is set up, and the flow with a one-dimensional hydrocode is calculated.

EQUATION OF STATE OF LH₂

The Hugoniot of LH₂ has been measured by van Thiel and Alder (1966).^{B-1} The shock velocity versus particle velocity relation is curved. Here the lower-pressure section is emphasized and the approximate fit made as follows:

$$u_s = c_o + s u_p \quad (B-1)$$

where

u_s = shock velocity

c_o = ambient sound speed = 1.122×10^5 cm/s

s = 1.831

u_p = particle velocity behind the shock front

^{B-1} van Thiel, M., and Alder, B.J., "Shock Compression of Liquid Hydrogen," Molecular Physics, Vol. 10, 1966, pp. 427-435.

The Hugoniot based on Equation B-1 is

$$P_H = K_O \mu(1 + \mu)/[1 - \mu(s - 1)]^2 \quad (B-2)$$

where

P_H = Hugoniot pressure

$K_O = \rho_O c_O^2$ = bulk modulus

ρ_O = ambient density = 0.0703 g/cm³ for boiling LH₂ at 1 atm

c_O = ambient sound speed = 1.122 × 10⁵ cm/s

$\mu = (\rho/\rho_O) - 1$ = compression

ρ = density

$s = 1.831$

Using the Hugoniot as a reference curve, an equation of state may be written:

$$P = P_H (1 - 0.5 \Gamma \mu) + \Gamma \rho E \quad (B-3)$$

where

$P = P(\rho, E)$ = pressure

Γ = Gruneisen parameter

E = internal energy

Examination of the tables of Vargaftik gives $\Gamma = 2.0$, which was used in these calculations.^{B-2} An alternative would have been to use the Dugdale-MacDonald relation

$$\Gamma = 2s - 1 = 2.662 \quad (B-4)$$

Isentropes from Equation B-3 do not agree well with those of Vargaftik, but this equation of state is good enough for estimating blast effects.

^{B-2} Vargaftik, N.B., Tables on the Thermophysical Properties of Liquids and Gases (New York: John Wiley & Sons, Inc., 1975).

RESULTS OF EXPLOSION CALCULATIONS

The explosion of a spherical 1-pound pentolite charge in LH₂ was calculated with the WUNDY hydrocode.^{B-3} The LSZK equation of state with burn was used for the pentolite and Equation B-3 was used for the LH₂. The initial value of E was chosen to make P equal one atmosphere in the LH₂. One pound of pentolite is equivalent to about 1.24 pounds of TNT.

Figure B-1 shows the calculated peak pressure versus distance for LH₂ and, for comparison, for the same charge in water and air. The bottom figure shows the results for impulse. Keeping in mind that both impulse and radius scale with the cube root of the charge weight and that the reflected impulse is approximately twice the incident impulse (for a nearly incompressible fluid), the desired impulse of 0.4 psi-sec at a distance of 13 feet requires a charge weight of 4 pounds. If the explosion were to occur in the vapor instead of in the liquid, a charge weight of roughly 100 pounds would be needed.

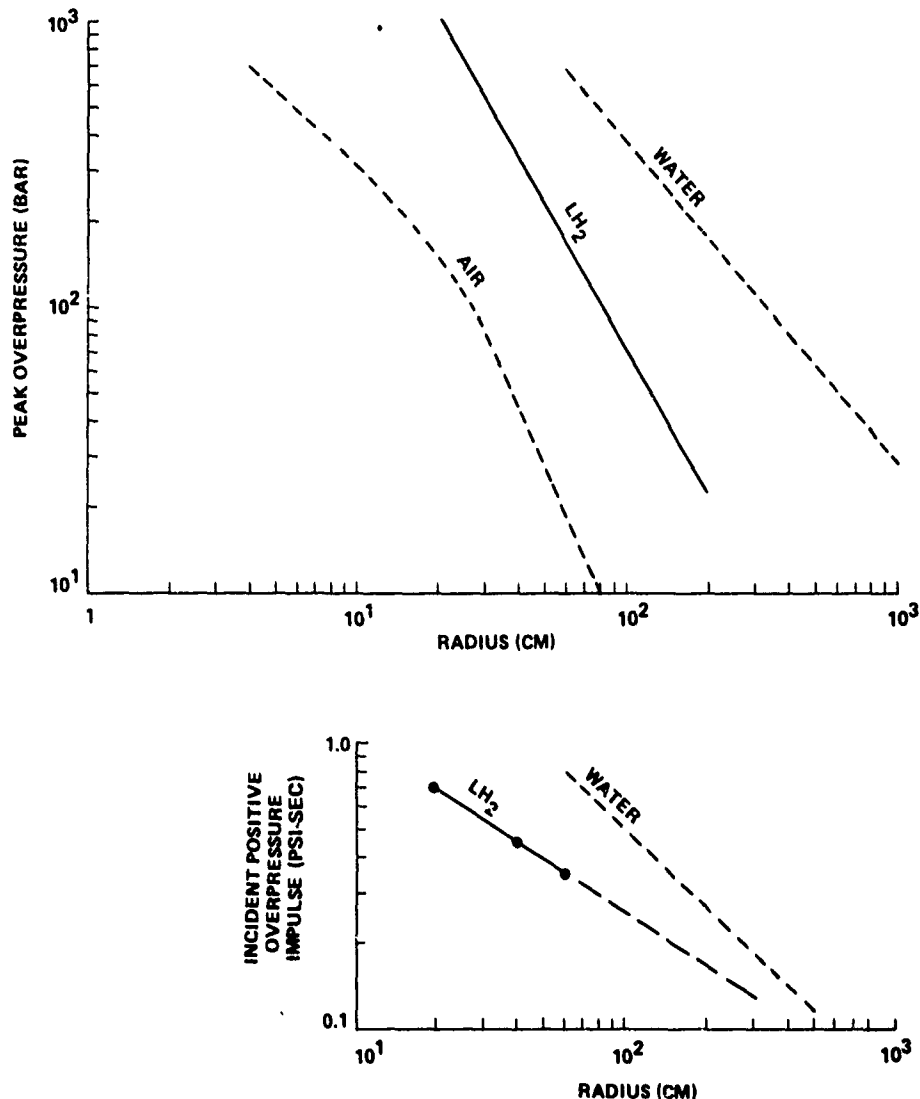


FIGURE B-1 BLAST FROM 1-LB SPHERICAL PENTOLITE CHARGE IN LIQUID PARA-HYDROGEN

B-3Lehto, D. and Lutzky, M., "One-Dimensional Hydrodynamic Code for Nuclear-Explosion Calculations," Naval Ordnance Laboratory NOLTR-62-168, Mar 1965.

APPENDIX C

FLOW FROM RUPTURED TANKS

D. Lehto

INTRODUCTION

This appendix considers the speed of cryogen venting in case of a simple hole in each tank opened up by the destruct charges as the only damage.

VEHICLE STANDING ON LAUNCH PAD

It is assumed that the only venting is due to holes opened up near the bottoms of the LH₂ and LO₂ tanks and that the external tank (ET) remains standing upright on the pad. The velocity of the outflow can be approximated by

$$u = fC_d (2gz)^{1/2} \quad (C-1)$$

where

u = flow velocity

f = correction factor for gurgling flow

C_d = discharge coefficient = 0.62

g = acceleration of gravity

z = fluid head

This is simple open-top tank flow ($f = 1$) with a correction factor, f , to account for reduction of the effective velocity by the alternating outflow of liquid and inflow of air. If the liquid flow and air flow take equal amounts of time, then $f \cong 0.25$. (A rough confirmatory test with a perforated water-filled can gave $f = 0.20$.)

Integrating Equation C-1 to give the time t needed to drop the liquid level from height z_0 to z when the vent area is A gives

$$tA = \left(z_0^{1/2} - z^{1/2} \right) C_1 / f \quad (C-2)$$

where

t = time after venting begins

A = vent area

z_0 = liquid level at time $t = 0$

z = liquid level at time t

$f = 0.25$

$C_1 = \sqrt{2} A_t / (C_d \sqrt{g}) = 114,000 \text{ ft}^{3/2} - \text{sec for LH}_2; 42,189 \text{ for LO}_2$

$A_t = \text{cross sectional area of tank} = 5.56 \times 10^5 \text{ cm}^2$

$g = \text{acceleration of gravity} = 981 \text{ cm/sec}^2$

This calculation can be done in a much more complicated way with allowance for the initial push by the ullage pressure and with spurt-by-spurt calculation of the flow with allowance for boiling near the top of the tank when the ullage pressure is below atmospheric. The gurgling flow of the simple model would then be called two-component, two-phase countercurrent intermittent flow. Enough of this elaboration was carried out to permit confidence in the simple model.

The simple model results for venting of the tanks are shown in Figure C-1. For a hole area of 100 ft^2 , the times to spill 90 percent are 37 seconds for LO_2 and 61 seconds for LH_2 .

The two liquids would pour onto the launch pad and spontaneously detonate when a few thousand pounds had been mixed. A large hydrogen-burning flame would engulf the vehicle. The effects of the detonation and flame may cause massive dumping of the remaining liquids.

VEHICLE IN FREE FALL

Dumping from tanks in free fall will occur if the orbiter and SRB's are detached or all thrust is cut off.

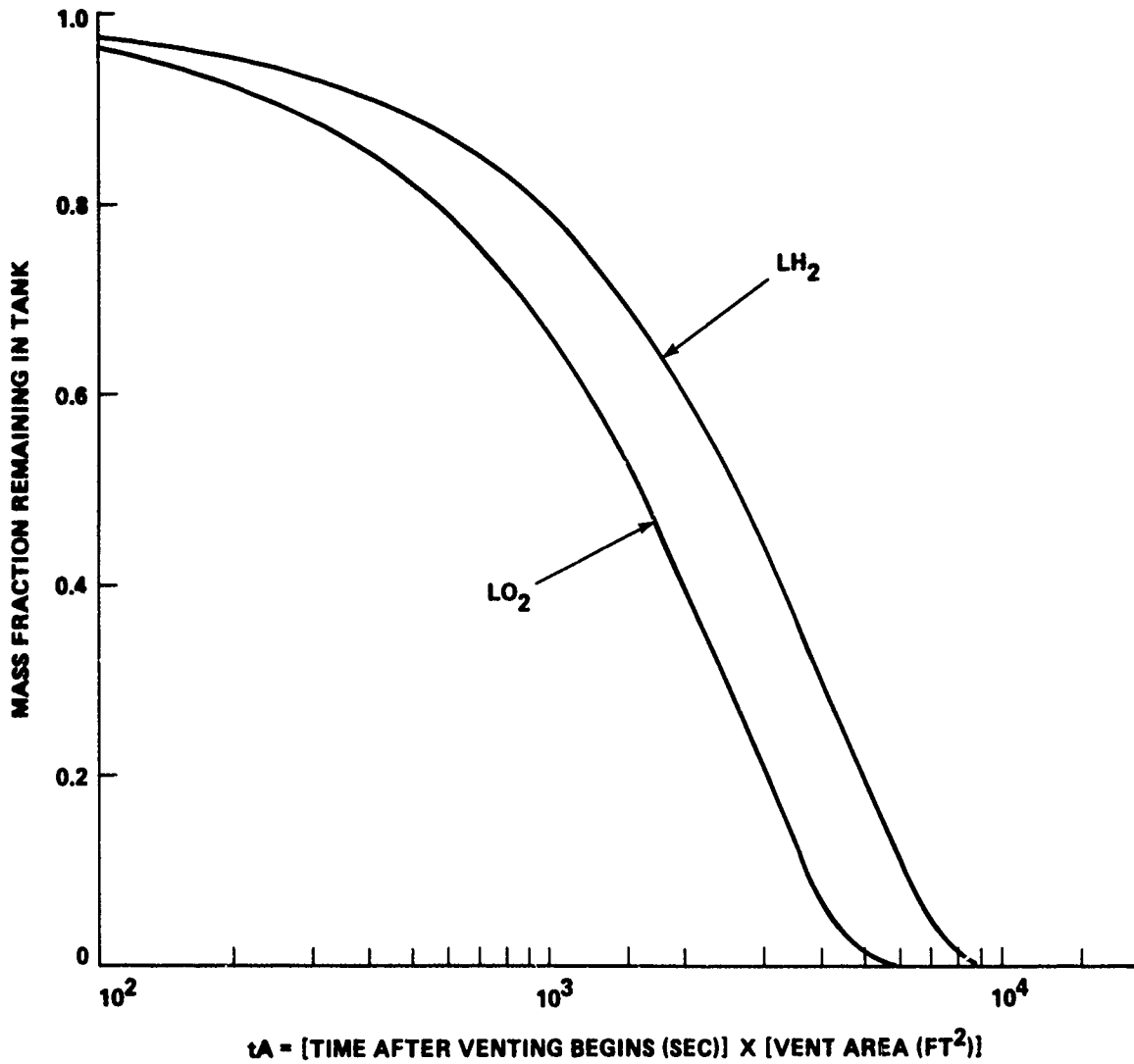


FIGURE C-1 SPILLING OF LH₂ AND LO₂ FROM ET TANKS OPENED AT BOTTOM WHILE ON LAUNCH PAD

It is assumed that the liquid in the tank has time for both heat and mass transfer and follows isentropic expansion from its boiling point at one atmosphere pressure as long as it remains in the tank. It is further assumed that when this boiling fluid exits through the opening in the tank, the pressure change is so fast that there is time for heat transfer but not for mass transfer. This metastable-flow model was worked out by Tangren, et al^{C-1} and applied to cryogenics by Smith^{C-2} and Brennan, et al.^{C-3} Their expression for choked flow is

$$G_c^2 = \Gamma p / (x v_g) \quad (C-3)$$

where Γ is an effective adiabatic exponent defined as

$$\Gamma = (x C_{pg} + (1 - x) C_f) / (x C_{vg} + (1 - x) C_f) \quad (C-4)$$

where

G_c = mass flow (g/cm²·sec)

p = pressure at exit plane (dyne/cm²)

x = quality = mass fraction of vapor phase

v_g = specific volume of vapor phase (cm³/g)

C_{pg} = constant-pressure specific heat of vapor phase

C_{vg} = constant-volume specific heat of vapor phase

C_f = specific heat of liquid phase.

Brennan, et al compare results from Equation C-3 with experimental data for liquid nitrogen and for liquid hydrogen. In both cases, for low x , the experimental G_c is about a factor of 1.4 greater than that from Equation C-3. (There is apparently a calculation error in the curves shown for hydrogen in footnote C-3; using Equation C-3 gives lower G_c values than shown. These lower values lie below the experimental points in the same way as for nitrogen.)

Equation C-4 assumes that the gas and liquid phases have time to reach equal temperatures. If there is no time for heat transfer, $C_f = 0$ can be placed into

C-1 Tangren, R.F., Dodge, C.H., and Seifert, H.S., "Compressibility Effects in Two-Phase Flow," Journal of Applied Physics, Vol. 20, 1949, pp. 637-645.

C-2 Smith, R.V., "Some Idealized Solutions for Chocking, Two-Phase Flow of Hydrogen, Nitrogen, and Oxygen," Advances in Cryogenic Engineering, Vol. 8, 1963, pp. 563-573.

C-3 Brennan, J.A., Edmonds, D.K., and Smith, R.V., "Two-Phase (Liquid-Vapor), Mass-Limiting Flow with Hydrogen and Nitrogen," Advances in Cryogenic Engineering, Vol. 14, 1969, pp. 294-298.

Equation C-4 yielding $\Gamma = C_{pg}/C_{vg}$, which is the adiabatic exponent of the gas phase. Figures C-2 and C-3 show the experimental data of Brennan, et al and the flow rates from Equation C-3 for Γ values of 2.0, 1.4, and 1.0. For low quality, Γ from Equation C-4 is nearly 1.0. These figures show that $\Gamma = 1.4$ gives a better fit to the data than does Γ from Equation C-4. Therefore, $\Gamma = 1.4$ is used for both hydrogen and oxygen (because oxygen is similar to nitrogen).

Thus far only critical flow has been discussed. This occurs only when the ratio of tank pressure to outside pressure exceeds a certain critical value. When it is less than this value, the flow is subsonic and Equation C-3 does not apply.

The excluded-volume equation of state for adiabatic flow is as follows:

$$p(v - B)^\Gamma = \text{constant} \quad (\text{C-5})$$

where

p = pressure

v = specific volume of the mixed phases

$B = (1 - x)v_f$ = excluded volume

x = quality

v_f = specific volume of the liquid phase

Γ = adiabatic exponent = 1.4

Combining Equation C-5 with the adiabatic energy equation

$$h + \frac{1}{2} u^2 = \text{constant} \quad (\text{C-6})$$

where

h = enthalpy

u = particle velocity

gives the desired expression for particle velocity

$$u^2 = \frac{2}{\Gamma - 1} p(v - B) \left[(p_o/p)^{(\Gamma-1)/\Gamma} - 1 \right] + 2B (p_o - p) \quad (\text{C-7})$$

the mass flux

$$G = u/v \quad (\text{C-8})$$

● DATA FROM BRENNAN, ET AL (SEE FOOTNOTE C-3, p. C-4)

— CALCULATED FROM

$$G_c^2 = \frac{\Gamma P_T}{x V_g}$$

Γ = AS SHOWN

P_T = THROAT PRESSURE

x = QUALITY

V_g = SATURATED VAPOR-SPECIFIC VOLUME (CM³/g) AT THROAT

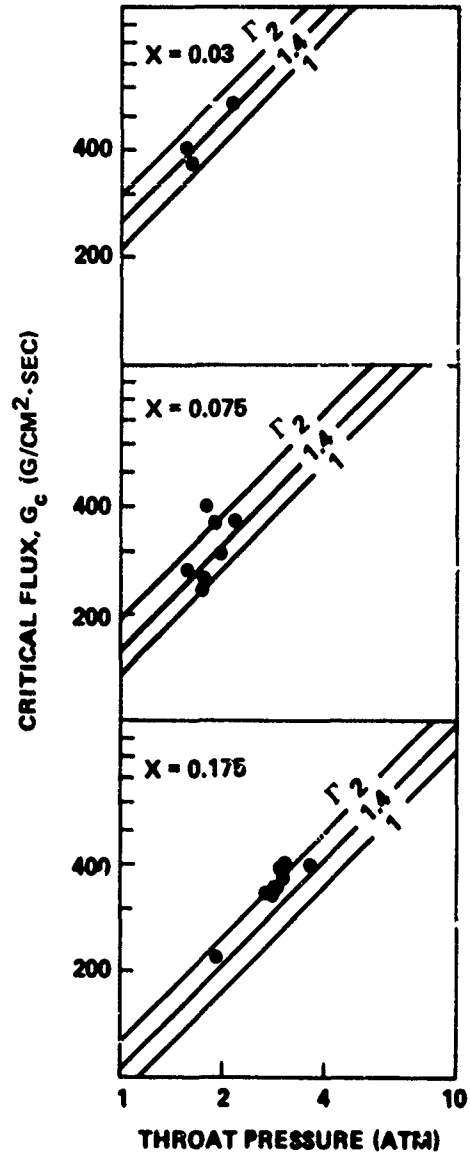


FIGURE C-2 CRITICAL FLOW MASS FLUX OF HYDROGEN LIQUID/VAPOR MIXTURE

● DATA FROM BRENNAN, ET AL (SEE FOOTNOTE C-3, p. C-4)

— CALCULATED FROM

$$G_c^2 = \frac{\Gamma P_T}{x V_g}$$

Γ = AS SHOWN

P_T = THROAT PRESSURE

x = QUALITY

V_g = SATURATED VAPOR-SPECIFIC VOLUME (CM³/g) AT THROAT

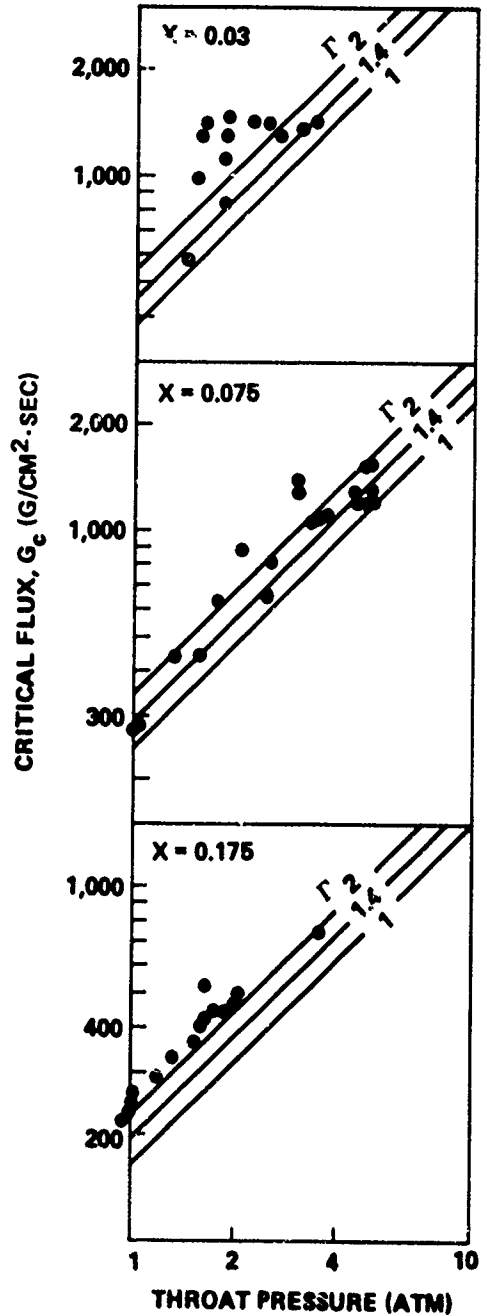


FIGURE C-3 CRITICAL FLOW MASS FLUX OF NITROGEN LIQUID/VAPOR MIXTURE

the sound speed

$$c^2 = \Gamma p v^2 / (v - B) \quad (C-9)$$

and the critical mass flux (identical to Equation C-3)

$$G_c^2 = \Gamma p / (v - B) \quad (C-10)$$

This study did not explicitly solve for the critical pressure ratio; instead, G and G_c were calculated and the smaller value was used.

Figures C-4 and C-5 show the p - v expansion paths for the LH_2 and LO_2 , respectively. The pressure drops faster with increasing volume for the metastable flow than for the fluid in the tank. There is not enough time inside the nozzle to evaporate more liquid or to transfer heat from the liquid to the gas phase that is being cooled by expansion. These processes take place after the gas has left the nozzle.

Figures C-6 and C-7 show the results from integration of Equations C-7 and C-10 for LH_2 and LO_2 dumping, respectively, in free fall. During the early stages of the flow, the pressure in the tank remains above the boiling point, and the flow is driven by the ullage pressure. When the ullage pressure drops to 1 atm, the fluid throughout the tank begins to boil, and the outflow changes from liquid to bubbly liquid. Note that for a flight time of 10 seconds, over 80 percent of the LH_2 present at lift-off is still in the tank when the flow stops. When the pressures inside and outside the tank have become equal, the only force available for forcing more fluid out of a perforated tank is the acceleration of aerodynamic drag or spinning.

Figures C-8 and C-9 show the mass fluxes at a flight time of 100 seconds. The break in the curves occurs where bubbly flow is just beginning and the zero quality gives an infinite flow rate in Equation C-3.

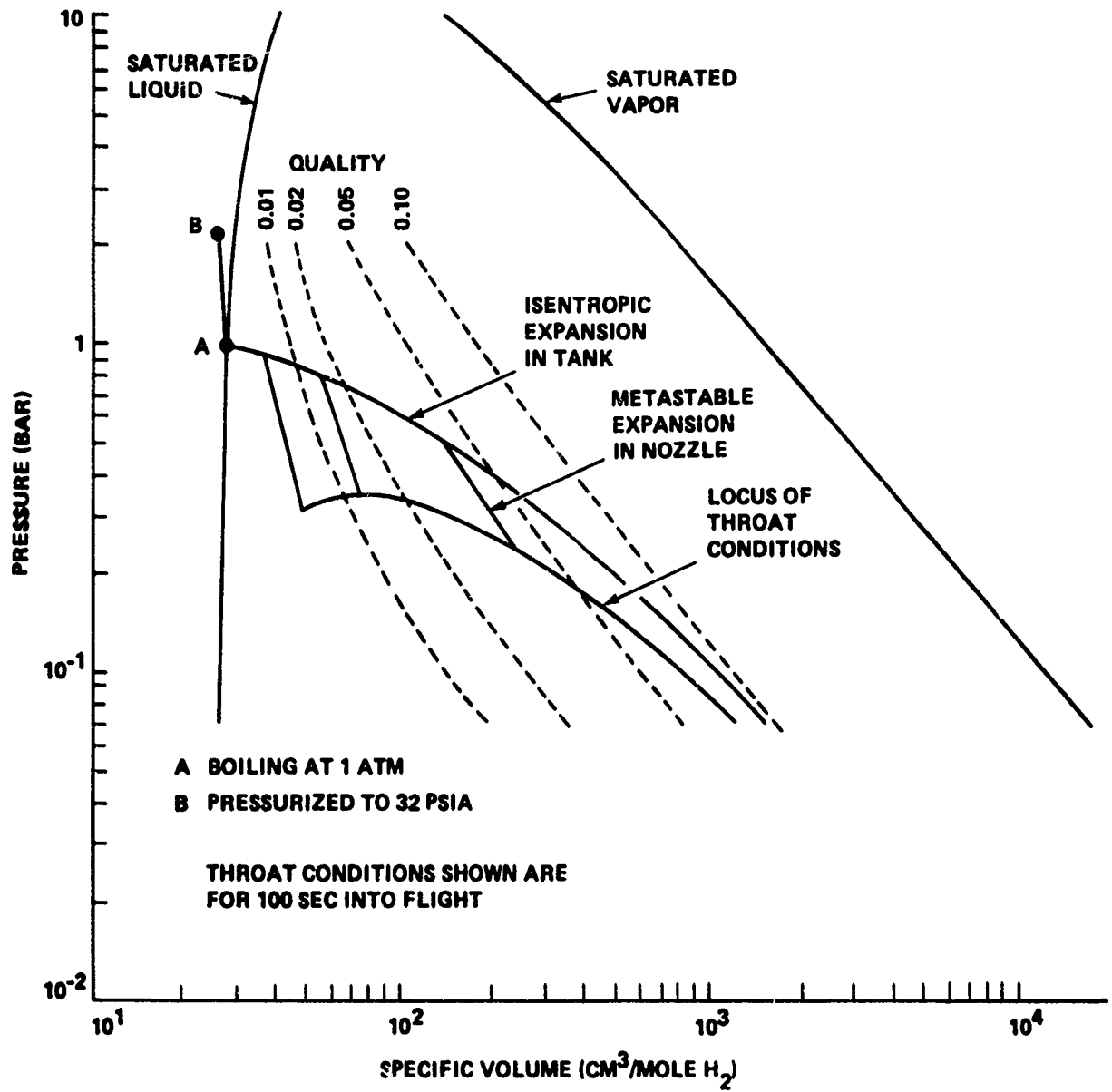


FIGURE C-4 P-V EXPANSION PATHS FOR LH₂

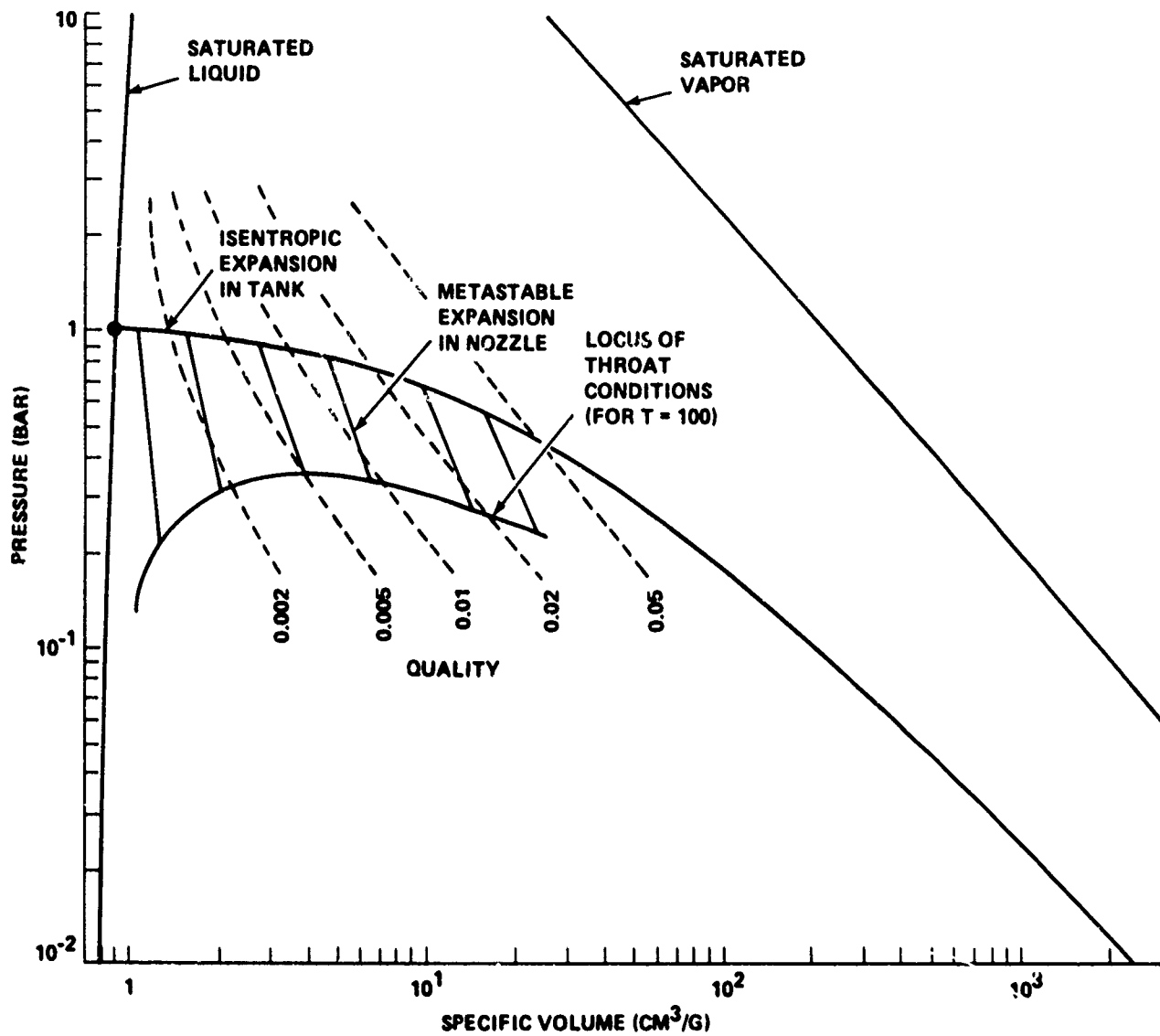


FIGURE C-5 P-V EXPANSION PATHS FOR LO₂

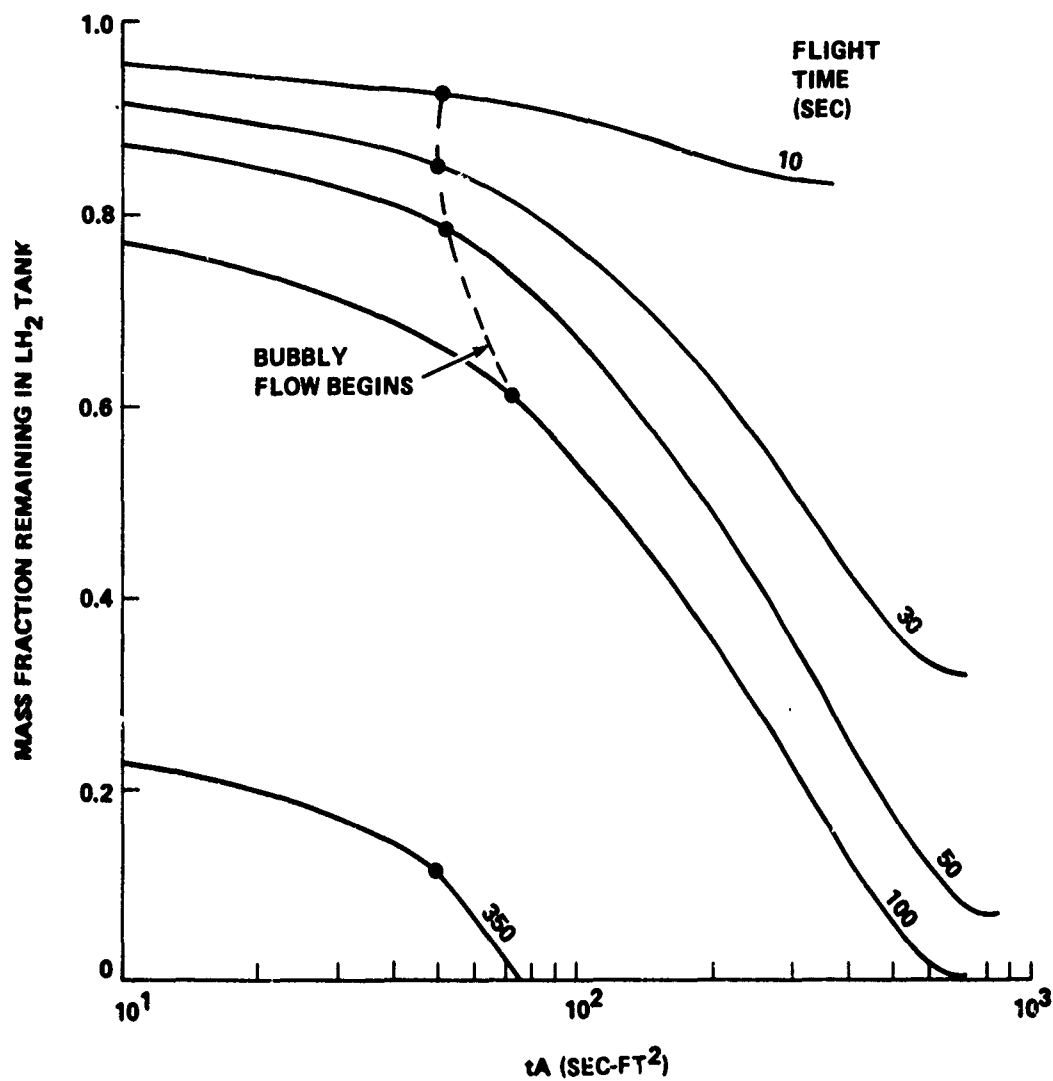


FIGURE C-6 DUMPING OF LH₂ DURING FREE FALL

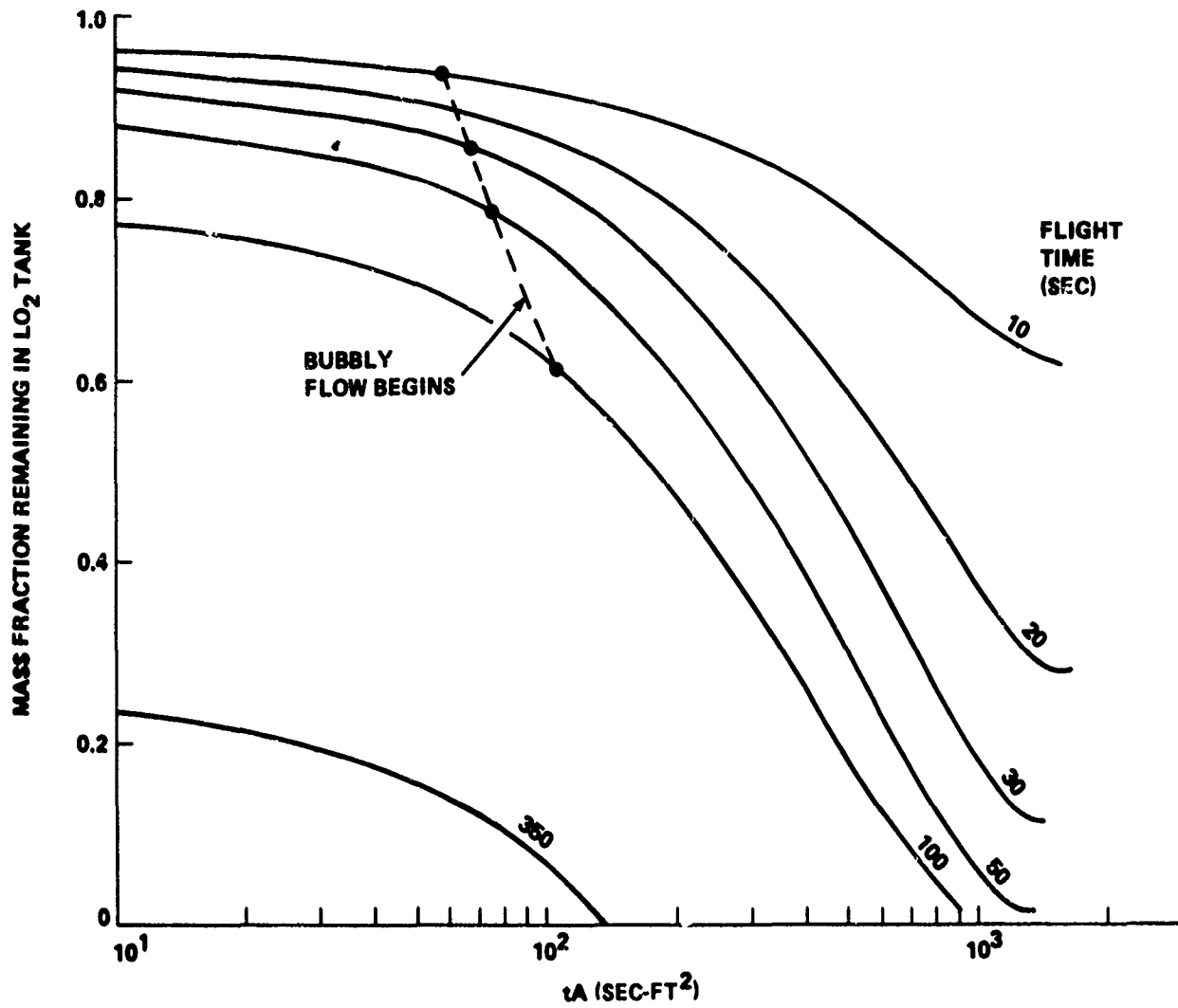


FIGURE C-7 DUMPING OF LO₂ DURING FREE FALL

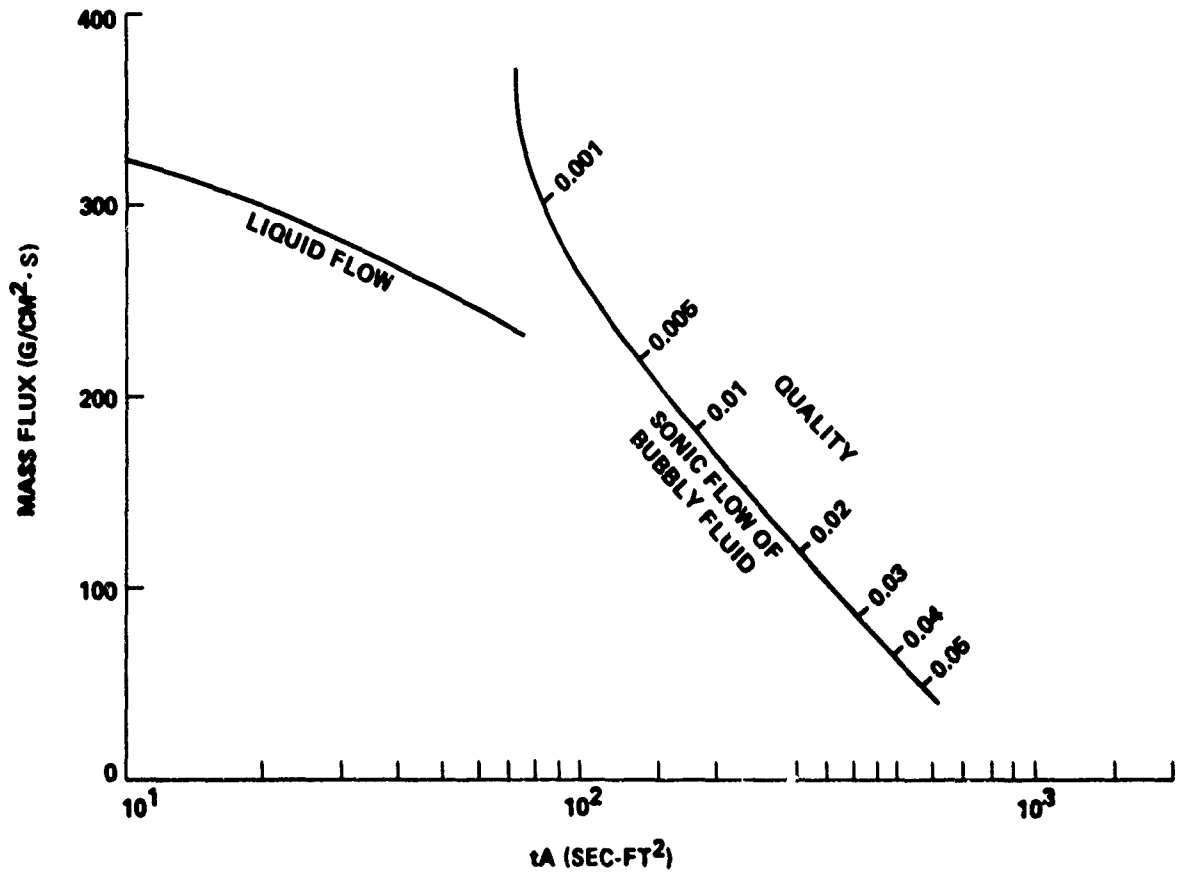


FIGURE C-8 MASS FLUX OF LH₂ DURING FREE FALL AT FLIGHT TIME OF 100 SECONDS

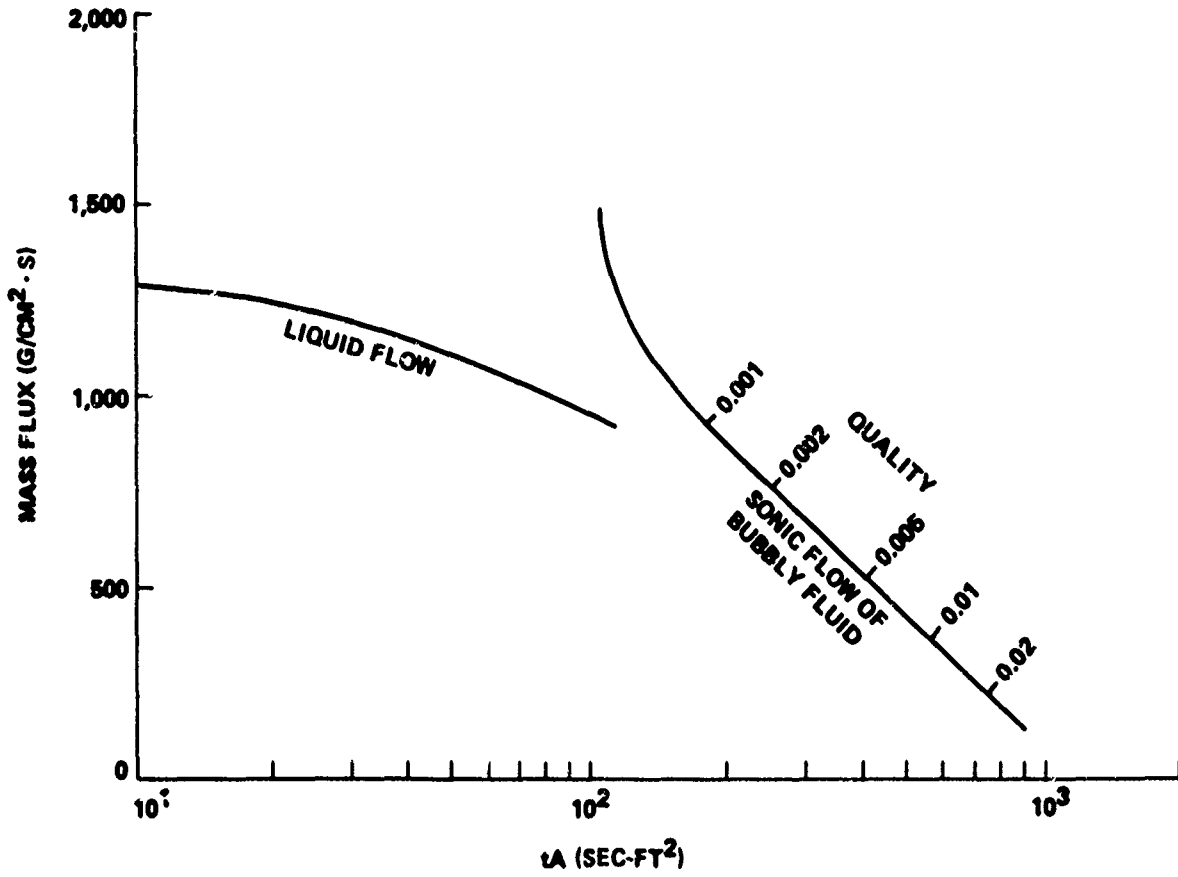


FIGURE C-9 MASS FLUX OF LO_2 DURING FREE FALL AT FLIGHT TIME OF 100 SECONDS

APPENDIX D
SHOCK STRENGTH SCALING LAWS

R. Phinney

INTRODUCTION

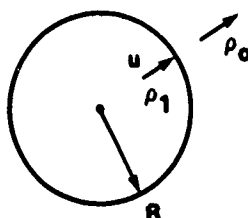
Blast wave theory treats the wave propagation caused by the instantaneous point release of energy. A similarity solution can be found for the hydrodynamic equations together with strong shock limiting forms of the shock jump equations. For a review of the progress in the field see Sakurai's chapter devoted to "Blast Wave Theory."^{D-1}

Typically, the released energy propagates with the wave and is confined to a thin layer behind it. The shock layer's thickness grows linearly with distance traveled by the shock. The energy in this layer is a combination of kinetic energy associated with the particle motion behind the shock, as well as the compressive work of increasing the density. Simple scaling laws can be derived without actually formulating and solving the corresponding hydrodynamic equations. By assuming that the released energy remains in a thin layer behind the shock, the problem is simplified to the point where all one needs to know are the shock relations that give the properties just behind the shock in terms of the upstream values. Using this technique, some scaling laws of particular interest are developed below.

SPHERICAL WAVES IN A LIQUID

Consider first the spherical wave caused by the point release of the energy E . After some time, the wave has expanded to the radius R . At this instant, the particle velocity is u , and the density behind the shock is ρ_1 . The wave velocity is $dR/dt = U$, and the density in front of the wave is ρ_0 . The basic assumption then is that the energy E is contained in a layer of thickness aR , where a is assumed small. The volume of the layer that contains the energy is $(aR)(4\pi R^2)$. The conservation of energy can be written

$$E = \frac{1}{2} \rho_1 u^2 (4\pi aR^3)$$



(D-1)

^{D-1}Holt, M., ed., Basic Developments in Fluid Dynamics (New York: Academic Press, 1965).

(noting that for liquids the energy of compression is small compared to that of the particle motion).

The shock jump can be completely characterized and all the properties behind it determined by any single parameter that defines its strength. A convenient strength parameter is the density "condensation" $\mu = \rho_1/\rho_0 - 1$. The shock Hugoniot can usually be approximated quite well by a quadratic

$$\Delta p = A\mu + B\mu^2 \quad (D-2)$$

with $A = \rho_0 C^2$ and $B = (2k - 1) \rho_0 C^2$ where Δp is the pressure jump, C is the sound speed in front of the wave, and k is a material constant that characterizes the curvature of the Hugoniot.

Conservation of mass and momentum across the shock can be used to generate the following simple equations

$$\rho_1/\rho_0 = U/(U - u) \quad (D-3)$$

and

$$\Delta P = \rho_0 Uu \quad (D-4)$$

Manipulation of the above equations will produce the result

$$\frac{E}{\rho_0 C^2} = 2\pi a R^3 (\mu + 1) \left[\frac{\mu}{1 - (2k - 1)\mu} \right]^2 \quad (D-5)$$

which relates the instantaneous density jump to the shock radius, $E/\rho_0 C^2$ being a constant for any particular case. The pressure is related to the density through the quadratic Equation D-2 which can be solved to give

$$\mu = \frac{\sqrt{1 + 4(2k - 1) \frac{\Delta P}{\rho_0 C^2}} - 1}{2(2k - 1)} \quad (D-6)$$

In the weak wave limit which corresponds to a large enough radius R , the equations simplify to

$$\frac{E}{\rho_0 C^2} = 2\pi a R^2 \left(\frac{\Delta P}{\rho_0 C^2} \right)^2 \quad (D-7)$$

Although the constant a cannot be determined by this simple theory, it is not necessary to know it if ratios are formed in which it cancels out. For example, tests in water can be used to predict the shock strength in a cryogen. Likewise, the shock strength dependence on radius is given by Equation D-7.

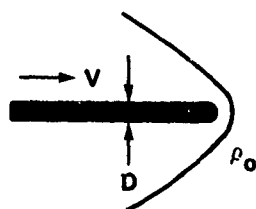
As a check on the above procedure, the same process was followed for shocks in gases. The resulting relationship was the same as the commonly used "Sachs scaling law" for explosives in air.^{D-2} Sachs' law is derived empirically from test data in which E and R were varied systematically and the pressure jump measured. The fact that Sachs scaling was correctly predicted gives confidence that the method is reasonable and can be extended to shocks in liquids.

SHOCK FROM SHAPED CHARGE JETS

The technique outlined above can also be applied to another problem of interest, namely the pressure waves produced by a shaped charge jet. For this case, we assume that the energy imparted to the wave reflects itself as a drag that acts upon the head of the jet. In fact, the jet appears to be a line source of energy that creates a quasi-cylindrical wave.

The energy transmitted to the wave is the work done in moving through the distance Δx against the drag force.

$$\Delta E = \text{drag} \cdot \Delta x$$



(D-8)

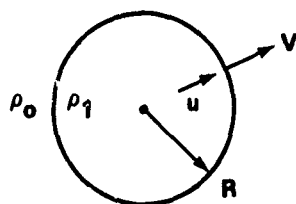
The line energy density is $\bar{E} = \Delta E / \Delta x$ which is just the drag force on the jet. The drag force in turn can be characterized by a drag coefficient C_D , which is defined by the relation

$$\text{drag} = \frac{1}{2} \rho_0 V^2 \left(\frac{\pi}{4} D^2 \right) C_D \quad (D-9)$$

where ρ_0 is the ambient density, V is the jet velocity, and D is the jet diameter.

If the jet velocity is high enough, the wave propagation can be considered cylindrical. In a plane perpendicular to the axis of the jet a situation similar to the spherical wave discussed above exists. As before, it is assumed the energy is concentrated in a thin layer behind the shock. The following equation results:

$$\bar{E} = (2\pi R aR) \rho_1 u^2$$



(D-10)

^{D-2}Ericsson, U., and Edin, U., "On Complete Blast Scaling," Physics of Fluids, Vol. 3, 1960, p. 893.

or, noting that \bar{E} = drag and using Equation D-9

$$\frac{\frac{1}{2} \rho_o V^2 \frac{\pi}{4} D^2 C_D}{\rho_o C^2} = 2\pi a R^2 (\rho_1/\rho_o) (u/c)^2 \quad (D-11)$$

which for weak shocks simplifies to

$$\frac{\frac{\pi}{8} D^2 V^2}{C^2} C_D = 2\pi a R^2 u^2 = 2\pi a R^2 \left[\frac{\Delta P}{\rho_o C^2} \right]^2 \quad (D-12)$$

This can be further simplified to

$$\frac{\Delta P}{\rho_o C^2} = \sqrt{\frac{C_D}{16a} \left(\frac{V}{C} \right) \left(\frac{D}{R} \right)} \quad (D-13)$$

This relation, like the one for spherical shocks, can be used to estimate shock pressures if values of a and C_D can be guessed or derived from tests. In any case, the relation can be used to plan and evaluate model tests or to apply results to other ambient fluids of different distances.

DISTRIBUTION

Copies

National Aeronautics and Space
Administration
Marshall Space Flight Center
ATTN: J. A. Roach (EL-42)
Alabama 35812

National Aeronautics and Space
Administration
Kennedy Space Center
ATTN: B. Rock (SF-ENG)
Florida 32899

National Aeronautics and Space
Administration
Lyndon B. Johnson Space Center
ATTN: R. Rose
Houston, TX 77058

President
Naval War College
Newport, RI 02840

Superintendent
Naval Postgraduate School
ATTN: Library
Monterey, CA 93940

Superintendent
Naval Academy
Annapolis, MD 21402

Commander
Harry Diamond Laboratories
2800 Powder Mill Road
ATTN: Technical Library
Adelphi, MD 20783

Commandant
Army War College
ATTN: Library
Carlisle Barracks, PA 17013

Commandant
Industrial College of the Armed Forces
Ft. Leslie J. McNair
ATTN: Document Control
Washington, DC 20315

Commandant
National War College
Ft. Leslie J. McNair
ATTN: Class. Rec. Library
Washington, DC 20315

Directorate of Safety Headquarters
Eastern Space and Missile Center
Patrick Air Force Base
ATTN: L. Ullian (SEM)
Florida 32925

SAMTEC/ROSF
ATTN: Colin Gardner
Vandenberg AFB, CA 93437

Commander
Air Force Weapons Laboratory
ATTN: Lt. N. Clemens (DYVS)
Kirtland Air Force Base, NM 87117

Air University Library
ATTN: Documents Section
Maxwell Air Force Base, AL 26112

40

NSWC TR 80-417

Copies

Institute for Defense Analysis
400 Army-Navy Drive
ATTN: Library
Arlington, VA 22202

Chairman
Department of Defense Explosives
Safety Board
Room 856-C Hoffman Bldg. 1
2461 Eisenhower Avenue
ATTN: R. Perkins
R. Scott
T. Zaker
Alexandria, VA 22331

Director
Defense Nuclear Agency
ATTN: Technical Library
Washington, DC 20305

Commander
Field Command
Defense Nuclear Agency
ATTN: FCTA
Kirtland Air Force Base, NM 87115

Defense Technical Information Center
Cameron Station
Alexandria, VA 22314

Library of Congress
ATTN: Gift and Exchange Division
Washington, DC 20540

Thiokol/Wasatch Division
P. O. Box 524
ATTN: Technical Library
Brigham City, Utah 84302

Martin Marietta Corp.
Michoud Operations
ATTN: B. Elam
New Orleans, Louisiana

Rockwell International Space Division
12214 Lakewood Blvd.
ATTN: Technical Library
Downey, CA 90241

Battelle Memorial Institute
505 King Avenue
ATTN: E. Rice
Columbus, OH 43201

Denver Research Institute
Mechanical Sciences and
Environmental Engineering
University of Denver
ATTN: J. Wisotski
Denver, CO 80210

Falcon Research
ATTN: D. Parks
Denver, CO 80210

General American Transportation
Corporation
General American Research Div.
7449 North Natchez Avenue
ATTN: Technical Library
Niles, IL 60648

General Electric Company - TEMPO
816 State Street
ATTN: W. Chan/DASIAC
Santa Barbara, CA 93102

Hercules Incorporated
Box 98
ATTN: D. Richardson
Magna, UT 84044

IIT Research Institute
10 West 35th Street
ATTN: Technical Library
Chicago, IL 60616

Kaman Sciences Corp.
P. O. Box 7463
Colorado Springs, CO 80907

Los Alamos Scientific Laboratory
P. O. Box 1663
ATTN: LASL Library
Los Alamos, NM 87544

12

NSWC TR 80-4T7

New Mexico Institute of Mining
and Technology
TERA
ATTN: M. L. Kempton
J. P. McLain
Socorro, NM 87801

Pacific Technology
P. O. Box 148
Del Mar, CA 92016

Physics International Company
2700 Merced Street
ATTN: Technical Library
San Leandro, CA 94577

R and D. Associates
P. O. Box 3580
ATTN: Technical Library
Santa Monica, CA 90403

Sandia Laboratories
P. O. Box 5800
ATTN: Library
J. Reed
L. Vortman
Albuquerque, NM 87115

Sandia Laboratories
Livermore Laboratory
P. O. Box 969
Livermore, CA 94550

Director
Scripps Institution of Oceanography
La Jolla, CA 92037

Shock Hydrodynamics Incorporated
15010 Ventura Boulevard
ATTN: Technical Library
Sherman Oaks, CA 91403

Southwest Research Institute
8500 Culebra Road
ATTN: W. Baker
San Antonio, TX 78206

Systems, Science and Software
P. O. Box 1620
La Jolla, CA 92037

Teledyne Energy Systems
110 W. Timonium Road
ATTN: T. Olsen
Lutherville, MD 21093

University of California
Lawrence Livermore Laboratory
ATTN: Technical Library
Livermore, CA 94550

URS Corporation
155 Bonet Road
ATTN: Document Control
San Mateo, CA 94402

Director
Woods Hole Oceanographic Institute
Woods Hole, MA 02543

J. H. Wiggins Corporation
1650 S. Pacific Coast Highway
ATTN: J. Baeker
Redonodo Beach, CA 90277